Tryptophan metabolism in *Aspergillus fumigatus*:
Impacts on virulence and toxin synthesis.

by

Tsokyi Choera

A dissertation submitted in partial fulfillment of
The requirements for the degree of

Doctor of Philosophy
(Microbiology)

at the
UNIVERSITY OF WISCONSIN-MADISON
2018

Date of final oral examination: **July 19th, 2018.**

The dissertation is approved by the following members of the Final Oral Committee:

Nancy Keller, Professor, Medical Microbiology & Immunology & Bacteriology
Jae-Hyuk, Yu, Professor, Bacteriology
Jon Woods, Professor, Medical Microbiology and Immunology
Jenny Gumperz, Professor, Medical Microbiology and Immunology
Loren Denlinger, Professor, Allergy, Pulmonary and Critical Care Medicine

Thesis Abstract

Aspergillus fumigatus is the most prevalent filamentous fungal pathogen of humans, causing either severe Allergic Bronchopulmonary Aspergillosis (ABPA) or often-fatal Invasive Pulmonary Aspergillosis (IPA) in individuals with hyper or hypo immune deficiencies, respectively. Disease is primarily initiated upon the inhalation of the ubiquitous airborne conidia – the initial inoculum produced by *A. fumigatus* – which are complete developmental units with an ability to exploit diverse environments, ranging from agricultural composts to animal lungs. Upon infection, conidia initially rely on their own metabolic processes for survival in the host's lungs, a nutritionally limiting environment. One such nutritional limitation is the availability of aromatic amino acids (AAAs) as animals lack the enzymes to synthesize tryptophan and phenylalanine and only produce tyrosine from dietary phenylalanine. However, *A. fumigatus* produces all three AAAs through the shikimate-chorismate pathway, where they play a critical role in fungal growth and development and in yielding many downstream metabolites. The downstream metabolites of tryptophan in *A. fumigatus* include the immunomodulatory kynurenine derived from indoleamine 2,3-dioxygenase (IDO) and toxins such as fumiquinazolines and fumigaclavine. The kynurenine pathway of *A. fumigatus* also leads to the *de novo* synthesis of nicotinamide adenine dinucleotide (NAD+), a cofactor required in redox reactions notably as an electron acceptor. In this thesis I present my investigation of the many branches of tryptophan metabolism of *A. fumigatus*. In Chapter 2, I explore how the tryptophan biosynthetic pathway can be manipulated to increase the *A. fumigatus* toxins that incorporate tryptophan and discuss the potential roles for therapeutics in targeting the enzymes of the anabolic pathway in Chapter 1. In Chapter 3, I investigate the role of the fungal tryptophan catabolic enzyme Ido and describe the metabolic crosstalk between the host and the pathogen, specifically focusing on kynurenines, in regulating

inflammation, while controlling *A. fumigatus* infections. In Chapter 4, I introduce how tryptophan as an *A. fumigatus* growth substrate alters fungal growth and metabolism, impacting fitness, and virulence in an invasive aspergillosis murine model and present evidence to suggest the mechanism to be through enhancement of fungal respiration via the mitochondria.

Acknowledgements

Throughout my scientific career, I feel fortunate to have interacted with many intellectually vibrant people who are passionately engaged in trying to gain a better understanding of the world they inhabit. My scientific path has taken me from studying transgenic tomatoes and understanding their resistance to fungal infection, to studying a human fungal pathogen and understanding it's metabolism and the infectivity of the asexual spore. Therefore, I would like to express gratitude in the interactions I have had; this includes undergraduates whom I taught, graduate students whom I learned from and with, and professors and staff whom I learned from. I have also learned many life lessons from my family that have impacted my scientific reasoning on the bench.

I must specifically thank Dr. Nancy P. Keller for giving me the independence, yet necessary support and advice to understand fungal metabolism and its impact on pathogenesis. It's been an honor to have worked with and learned from you over the past five years. Additionally, my thesis committee members: Dr. Jenny Gumperz, Dr. Jon Woods, Dr. JaeHyuk Yu, and Dr. Loren Denlinger deserves great thanks for dedicating their time in providing their valuable insights and critical feedback on my work.

Many thanks all the MDTP and MMI staff, particularly Cathy Davis Gray, for all the hard work behind the scenes and making sure I fulfill the program requirements.

It truly took a village to raise me through the PhD experience and I am extremely thankful to many. To His Holiness the 14th Dalai Lama of Tibet, for inspiring the wealth of education for the benefit of society. To my undergraduate mentor, Dr. Ann Powell for exposing me the fundamentals about molecular biology and for encouraging my interest in studying a human pathogen.

To the Powell/Allen lab graduate student mentors and colleagues, thank you for checking in on my graduate school career. To the Keller lab colleagues, thank you for your support over many

w(h)ine-nights, library, and terrace trips. Thank you for making graduate school more than just the science; this goes out to my MDTP friends as well.

I am eternally grateful to my family and friends who have been nothing but supportive as I've worked to attain my PhD. To Agu Sonam and Aunty Lhaga, thank you for making Madison feel like home and for countless tupperwares of comfort food. To Aunty Dorsh and Uncle Tashi, thank you for encouraging me to pursue a PhD outside of California; this experience has been challenging, yet enriching. To Chemi, adventuring since Evelyn Ave. days and looking forward to many more ahead. To Acha Tseyang, Tashi, Sonam, and Cho Wangden thank you for being one of my biggest support networks, for enduring long phone calls, being my tour guides, travel buddies, and cheerleaders throughout my life. To Khando and Jigmay, Asu is excited to be involved in your lives again; thank you for being reminders of life outside the lab.

Finally, to my Pala and Amala, Chime Wangchuk and Choedon Choera, who sacrificed their access to the little privileges of their life for ours, who used analogies of the great Milarepa, or simply called to remind me to take vitamins. This thesis is a reflection of perseverance engrained into my refugee mindset at an early age. Thank you for sharing your story of struggle as you escaped across the vast Himalayas on foot into India, where you accepted the challenges of adopting a new country and thrived against many communicable diseases. Thank you for enduring these hardships, establishing a comfortable life, and then uprooting once again as you immigrated to California for our betterment. Your struggle is what has inspired my interest in microbial pathogenesis, and your story of perseverance is one of the main reasons I have been able to earn a PhD. Thank you for the unconditional love and unwavering support in my endeavor to pursue a PhD. Love you all.

Table of Contents

CHAPTER 1

A multi-faceted role of tryptophan metabolism and indoleamine 2,3-dioxygenase activity in *Aspergillus fumigatus* - host interactions.

Originally published as:

Choera T, Zelante T, Romani L, Keller NP (2018). A multi-faceted role of tryptophan metabolism and indoleamine 2,3-dioxygenase activity in *Aspergillus fumigatus* - host interactions. **Frontiers in Immunology**-Microbial Immunology. Jan 22;8:1996. doi: 10.3389/fimmu.2017.01996. eCollection 2017.

Modifications have been made to increase legibility in the current format and to the references for consistency in this thesis.

1.1 Introduction

Aspergillus fumigatus is a saprophytic fungus that has a worldwide distribution. The asexual spores (called conidia) are ubiquitous and individuals inhale hundreds of spores daily. While most inhaled conidia are cleared by individuals with a healthy immune system, *A. fumigatus* can act as an opportunistic human pathogen in individuals with altered immune functions. Disease presentation can vary on the status of the host's immune system; *A. fumigatus* can cause Allergic Bronchopulmonary Aspergillosis (ABPA), a severe allergenic response, in the hyper-immune, or the fatal invasive growth Invasive Pulmonary Aspergillosis (IPA) in the hypo-immune, or in individuals with other susceptibilities such as patients unable to mount the necessary oxidative defenses such as in individuals with Chronic Granulomatous Disease (CGD) (1).

The manifestation of disease is dependent not only on the host's immune status but also fungal factors including strain heterogeneity (2). *Aspergillus fumigatus* growth in the mammalian lung, following survival of resident pulmonary defenses, requires the fungus to adapt to a hypoxic and nutritionally scarce environment. *Aspergillus* mutants unable to synthesize primary metabolites necessary for growth are generally impaired in virulence. For example, deletion of *cpcA*, a transcription factor that globally modulates amino acid biosynthesis in the fungus led to a less virulent phenotype in a murine model of IPA (3). Additional studies have shown that mutants in sulfur utilization (4), uracil/uridine synthesis (5), zinc uptake, iron acquisition and many more (6, 7) are also decreased in virulence.

To complicate disease progression further, there is an alarming rise in antifungal resistance strains of *A. fumigatus* (8, 9). Therefore, an understanding of *A. fumigatus* and host metabolic pathways is important in identifying nutrient limitations. One critical metabolic pathway is the biosynthesis of aromatic amino acids (AAAs, tryptophan, phenylalanine, and tyrosine), which are required not

only for growth of *A. fumigatus* but are also precursors for several toxins (Table 1). The host relies on dietary sources for all AAAs while *A. fumigatus* synthesizes all three. However, the host and *A. fumigatus* both possess AAA catabolic enzymes. In particular, one key enzyme important in immune homeostasis is indole 2,3 dioxygenase (IDO), which converts tryptophan (Trp) to kynurenine and related metabolites in both organisms. Historically, host IDOs activity has been described as an effective antimicrobial control for pathogens that are natural Trp auxotrophs such as *Staphylococcus aureus, Chlamydia spp.,* and *Toxoplasma gondii,* presumably by Trp starvation (10). However, *A. fumigatus* can synthesize its own Trp and thus the Trp starvation may not be an effective pathogen control for those microbes able to synthesize their own Trp pools. Although, IDOs also play additional roles in host defenses through modifying kynurenine levels and subsequent cytokine responses as described below. In this review, we will summarize the recent studies describing the anabolic and the catabolic pathways of Trp metabolism, the implications for therapeutics, and the host-pathogen interaction.

1.2 Tryptophan synthesis and potential therapeutic targeting

Chorismic acid derived from the shikimic acid pathway is a key intermediate in producing Trp, phenylalanine (Phe), and tyrosine (Tyr) in microorganisms including *A. fumigatus* (Fig. 1). Trp and Phe are classified as essential amino acids, whereas mammals acquire them from diet, whereas Tyr is synthesized via the hydroxylation of Phe (11, 12). The absence of the aromatic amino acid biosynthetic enzymes and the low bioavailability of Trp in humans makes the Trp biosynthetic enzymes attractive targets for antifungals (13).

1.2.1 Fungal tryptophan anabolic pathway

Aromatic amino acid synthesis has been extensively studied in *S. cerevisiae* and provides the basis for the functional characterization of orthologous enzymes in filamentous fungi (11, 12, 14-16).

The shikimic acid pathway is a 7-enzymatic step reaction that initiates with two substrates, phosphoenolpyruvate (PEP) and erythrose-4-phosphate (E4P), which are intermediates of glycolysis and pentose phosphate pathways, respectively (17) (Fig. 1). The first step of the shikimic acid pathway is catalyzed by 3-Deoxy-D-arabinoheptulosonate 7-phosphate (DAHP) synthase to convert PEP and E4P to DAHP. In *S. cerevisiae* and *A. nidulans*, there are two DAHP synthases, Aro3 and Aro4, which are allosterically inhibited by phenylalanine and tyrosine, respectively (12). Steps 2-6 in filamentous fungi such as *A. nidulans* and *A. fumigatus* are completed by the pentafunctional enzyme AroM, or Aro1 in the model organism *S. cerevisiae* (18). The shikimate pathway culminates in the production of chorismic acid synthesized by the enzyme chorismate synthase (AroB) from 5-enolpyruvylshikimate-3-phosphate (EPSP) (19).

The synthesis of Trp from chorismate is initiated by an anthranilate synthase (AS), which converts chorismate to anthranilate, followed by three enzymatic steps as presented in Figure 1 with the respective functions outlined in Table 2. Anthranilate synthase(s) in *S. cerevisiae* have been characterized and it consists of two subunits: anthranilate synthase subunit I (AAS-I), which binds chorismate and is subject to feedback inhibition by Trp and anthranilate synthase subunit II (AAS-II) which is a glutamine amidotransferase (20). The *A. nidulans trpC*, an AAS-II encoding gene, was characterized in 1977 (21) and found exchangeable with an *A. fumigatus trpC* in 1994 (22). Wang et al. (16) recently characterized *trpE*, the AAS-I encoding gene in *A. fumigatus*. Wang et al. (16) explored the functions of two putative AAS-Is termed *trpE* and *icsA* by creating null mutants. The deletion of *trpE* led to a Trp auxotrophic strain, whereas the deletion of *icsA* did not. To ensure that *icsA* did not serve a redundant role for Trp synthesis, the group overexpressed *icsA* in a *trpE* deletion and showed that the overexpression of *icsA* does not reverse the Trp auxotrophy concluding that TrpE is the only anthranilate synthase in *A. fumigatus*. Interestingly,

the group showed that IcsA is an active enzyme in *A. fumigatus* as the precursor-chorismate pool is altered in the absence or overproduction of IcsA, however, the product is not known (16). Sasse et al. also confirmed that deletion of *trpE* (they termed *trpA*) results in an *A. fumigatus* Trp auxotrophy (19).

1.2.2 The shikimate pathway as potential antifungal targets

Currently, there are four major classes of antifungals: azoles and amphotericin B targeting ergosterol, 5-fluorocytosine targeting DNA synthesis, and echinocandins targeting cell wall synthesis. These antifungals either exhibit high toxicity to the mammalian cell (particularly amphotericin B and 5-fluorocytosine) or lose efficacy due to the emergence of drug resistant strains (azoles and echinocandins) (8). With *A. fumigatus* being a eukaryotic pathogen and sharing many proteins with mammalian hosts, there are limitations to developing effective and safe antifungals and therefore a great need for treatments that are fungal specific. Since Trp is a human-essential amino acid and the enzymes in the biosynthesis are fungal specific, several studies have suggested utilizing and finding drugs to target the enzymes of this pathway (23-26).

Targeting essential amino acid pathways have already shown potential for new classes of antifungals. Several groups have explored inhibitors of genes or enzymes involved in methionine biosynthesis. Azoxybacillin, a compound isolated from *B. cereus* targets methionine biosynthesis by interfering with expression of homoserine transacetylase and sulfite reductase encoding genes (27-29). Whereas azoxybacillin displayed a broad spectrum antifungal activity *in vitro*, *in vivo* activity was low possibly due to bioavailability in the host (27). R1-331, a natural product from *Streptomyces akiyoshiensis*, is an effective inhibitor of homoserine dehydrogenase involved in both methionine and threonine biosynthesis (30, 31). Yamaguchi et al. show that R1-331 was

active against medically important fungi such as *Candida albicans* and *Cryptoccocus neoformans* and proved to be effective in the treatment of systemic murine candidiasis (30, 32).

Compounds targeting AAA pathways are limited with the most famous being the herbicide Roundup, where the active ingredient glyphosate inhibits EPSP synthase, one of the first enzymes initiating the shikimate pathway (33) (Fig. 1). Glyphosate has shown to inhibit growth of several fungi including *Candida maltose* (34), *Pneumocystis (35),* and *Cryptococcus neoformans* where glyphosate delayed fungal melanization *in vitro* and *in vivo* and prolonged mice survival during infection (36). Another inhibitor of AAA pathway is a fluorinated anthranilate moiety, 6-FABA, which targets the TrpE enzyme and showed bactericidal activity when used on *Mycobacterium tuberculosis* (37). The studies of these inhibitors suggest that the Trp biosynthetic pathway could be fruitful in future antifungal drug design.

The value of AAA pathways as drug targets is supported by the findings that AAA auxotrophic mutants are less virulent in animal infection models. Sasse et al. explored the possibility of these pathways as potential drug target by testing the virulence of several AAA auxotrophic mutants in a murine IPA model (19). This study demonstrated that AroM (Fig. 1) was required for *A. fumigatus* viability. The group also constructed a conditional AroB repression strain that was attenuated virulence. Both a Trp auxotroph (TrpE mutant) and Tyr/Phe auxotroph (AroC mutant) were severely attenuated in virulence for pulmonary infection. Interestingly, the group also unveiled a putative difference in AAA distribution within the host by conducting a systemic infection showing that in a bloodstream infection the TrpE and the AroC mutants although less virulent, can establish some infection (19). Taken together, these results suggest that inhibitors of AAA biosynthetic pathways can potentially be used against *A. fumigatus* as a standalone treatment in a localized pulmonary infection or as an additive treatment in a systemic infection. The result

of the bloodstream infection observed by Sasse et al. also suggests that there are mechanisms for the fungus to sense Trp in its environment and utilize it. In *S. cerevisiae* the tryptophan specific permease, Tat2, is required for tryptophan uptake in yeast (38) and its closest homolog in *A. fumigatus* (Afu7g04290) is upregulated during fungal encounters with neutrophils (39)and dendritic cells (40). In *A. nidulans*, the G-protein coupled receptor (Gpr) H may be responsible for sensing Trp and glucose and GprH is conserved in *A. fumigatus (41, 42)*. Perhaps, for a systemic infection, inhibition of specific permeases or development of a GprH antagonist would be useful in reducing infections by *Aspergillus*.

1.3 Catabolic tryptophan metabolites in fungi

Although the anabolic Trp pathway is absent in mammals, the common catabolic pathways exist in the mammalian host with possession of the same enzymes as *A. fumigatus* (Fig. 2). Through the expression of Trp degradation enzymes, immune cells are both controlling inflammation and combating microbial infection. In addition to Trp degradation pathways conserved with animals, *Aspergillus fumigatus* can also direct Trp pools to secondary metabolites that may impact host health and response (Table 1).

1.3.1 Fungal tryptophan catabolism

There are three putative pathways (Fig. 2 and Table 2) for the degradation of Trp in *A. fumigatus*. The kynurenine branch is catalyzed by IDOs that convert Trp into formylkynurenine. In *A. fumigatus*, there are 3 putative *ido* genes: *idoA*, *idoB*, and *idoC*, the orthologs of *A. oryzae ido*α, *ido*β, and *ido*γ, respectively (43). Enzymatic studies of *Aspergillus oryzae* IDO enzymes suggest two of the three enzymes, IDOα, and IDOβ, may participate in Trp degradation as they have a higher affinity of its substrate. However, the recent study by Wang et al., suggested IDOb might be the more dominant enzyme than IDOa as determined by gene expression of *A. fumigatus* grown

on Trp amended media (16). Additionally, *idoC* gene expression was slightly induced by the addition of Trp, but the authors note that IDOc had a closer relationship to bacterial IDOs than to fungal IDOs (16, 43). In *S. cerevisiae*, formylkynurenine is further oxidized to the immunomodulatory product kynurenine by a kynurenine formamidase denoted as Bna7, which has been described in *A. nidulans* and is predicted to be involved in NAD (+), biosynthesis (44). The kynurenine branch in fungi is involved in the de novo biosynthesis of NAD (+), a coenzyme that is required for oxidation-reduction reactions (45).

Tryptophan can also be metabolized via the indole pyruvate pathway, initiated through the transamination of Trp by aromatic aminotransferases (termed Aro8 and Aro9 in *S. cerevisiae*) (Iraqui et al., 1998). These aromatic aminotransferases are also involved in the synthesis of Phe and Tyr in *S. cerevisiae*, and their orthologs are present in *A. fumigatus* (16). In *S. cerevisiae*, the deletion of both Aro8 and Aro9 results in Phe and Tyr auxotrophies (12, 46, 47). In *Candida* spp., where filamentation and pigment production play a role in virulence, the products of these enzymes have been described to influence both phenotypes. The deletion of *aro*8 in *C. glabrata* results in a reduced pigment production and leads to an increased sensitivity to hydrogen peroxide (15). The *aro8* and *aro9* mutants of *C. albicans* results in a decreased conversion of Trp to indole acetaldehyde, which is formed via decarboxylation of indole pyruvate. Filamentation of *C. albicans* increased with the exposure to indole acetaldehyde (48).

Indole acetaldehyde can also be produced via the third putative product of Trp degradation: tryptamine. Tryptamine is most famously known as the active compound in psilocybin and for its similarity to serotonins (49). Although the production of tryptamine has yet to be described in *A. fumigatus*, the downstream product of the tryptamine and indole pyruvate pathway, indole acetic acid has been described in several *Aspergillus* spp. including *A. fumigatus* (50, 51). Downstream

metabolism of kynurenine, indole pyruvate, and tryptamine has not been explored further, but *A. fumigatus* does possess putative enzymes for the re-synthesis of anthranilate, the precursor to Trp (as denoted in Fig. 1 and 2).

1.3.2 Aromatic Amino Acid incorporation in *Aspergillus* toxins

Many filamentous fungi, including *A. fumigatus,* produce bioactive small molecules that can have detrimental impacts on human health. Subsets of these toxins are small peptides synthesized by non-ribosomal peptide synthetases (NRPS). Several pathogenic *Aspergillus* species synthesize AAA derived peptides including gliotoxin (**Phe** and serine) (52), fumiquinazoline (**Trp**, **Anthranilate** and Alanine) (53), fumigaclavine (**Trp**) (54), fumitremorgin (**Trp** and Proline) (55), hexadehydroastechrome (**Trp** and Alanine) (56), fumisoquin (**Tyr**, Serine and Methionine) (57), DPP-IV inhibitor WYK-1 (**Trp**, **Tyr** and Leucine) (58), cyclopiazonic acid (**Trp**) (59) and benzomalvin (**Phe** and **Anthranilate**)(60). Table 1 summarizes the known aromatic amino acid derived secondary metabolites of *A. fumigatus* and their effect on the host.

Although, fumiquinazolines have yet to be assessed for virulence in an animal model, they are known to have cytotoxic properties(53). Fumigaclavines have been described to have immunosuppressive properties in several studies including the suppression of antifungal cytokines such as TNFα, IL-17, and IFN-γ (61). Fumitremorgin, verruculogen, and tryprostatin – all related products of the fumitremorgin pathway – induce tremorgenic activity in mice and act on the central nervous system (55, 62-64). Mutants in the hexadehydroastechrome pathway (Yin et al., 2013) and gliotoxin (56, 65) pathways have altered virulence in murine IPA models. Decreased virulence of the *gliP* mutant (GliP is the NRPS required for gliotoxin synthesis) is dependent on host immune status (reviewed in (6)). Overexpression of *hasA* encoding the hexadehydroastechrome transcription factor and thus leading to increased hexadehydroastechrome production, was more

virulent than wild type *A. fumigatus* in a neutropenic model of IPA (56). Although the exact mechanism underlying the increased virulence of the OE::*hasA* strain is unknown, iron homeostasis and cross talk between metabolic pathways may contribute to the increased virulence of OE::*hasA* (66). These studies highlight the potential contribution of AAA derived toxins in virulence of *A. fumigatus*.

1.4 Host tryptophan catabolism via IDO

The function of host IDO during mammalian infection was originally thought to center on the anti-proliferative effects of pathogenic microorganism via deprivation of Trp exerted by the host. IDO is up-regulated by interferon gamma (IFNγ) and depletes Trp (the least abundant essential amino acid) to inhibit pathogen expansion (67, 68), as demonstrated in the constraint of chlamydial growth (69). Numerous studies have since implicated IDO activity as important in fungal infections and have reported the relative outcomes of IDO expression on disease progression (Table 3). Accumulating data continues to support that IDO participates in the host–pathogen interaction in human epithelial cells; therefore, the co-evolution of host and microbe Trp metabolism has been investigated (70). The current consensus is that IDO activation is pivotal in regulating inflammatory processes directly via Trp depletion and indirectly via the IDO-mediated release of Trp catabolic secondary metabolites (namely, kynurenines).

Dietary Trp is catabolized by two different IDO protein isoforms, IDO1 and IDO2 that are expressed by immune cells, and TDO (Trp 2,3-dioxygenase) that is mainly expressed in the liver. Cells involved in the innate processes of the anti-microbial defense, such as dendritic cells (DCs), neutrophils and macrophages express IDO1 upon microbial encounter mainly *via* toll-like receptor (TLRs) stimulation. How fungi specifically induce IDO expression is not known, however induction by other pathogens is associated with pathogen associated molecular patterns, including

lipopolysaccharides (LPS) and CpG oligodeoxynucleotides (CpG-ODN) (71-74), underlining a role for kynurenine metabolism in microbial-induced inflammatory processes.

1.4.1 IDO – mediated tolerance: impacts on antimicrobial responses

Evolutionary studies have shown that the host immune defense against microbes is characterized by three different mechanisms: avoidance, resistance and tolerance (75). Modules of immunity provide resistance to limit pathogen burden and tolerance and host damage caused by the immune reaction *per se*. However, the inflammatory reaction, although largely considered beneficial for its antimicrobial functions, may also contribute to pathogenicity. Thus, rescue from infection pathology may not only depend on microbial colonization (and inactivation of resistance mechanisms) but also on the resolution of tissue inflammatory pathology through tolerogenic responses to pathogens (76).

Studies using a mouse model of mucosal or invasive *Candida albicans* infection found that systemic inhibition of IDO *in vivo* reduced gastrointestinal inflammation and unexpectedly, elevated the levels of fungal colonization compared to control mice (77). Notably, tolerogenic responses towards *C. albicans* were abrogated when IDO was antagonized *in vivo,* as shown in various models of inflammatory disorders (78, 79). As with *C. albicans*, IDO and kynurenine production during *A. fumigatus* infection contributes to fungal pathogen eradication and the regulation of an unacceptable level of tissue damage(80). Indeed, IDO can increase kynurenine host levels to induce adaptive Treg expansion whilst limiting Th17 polarization (79, 81). In this context, the Th17 pathway, which down-regulates Trp catabolism, may instead favor pathology and better explain the paradoxical correlation between fungal infection and chronic inflammation (82).

Another example of this paradox was demonstrated in the context of Chronic Granulomatous Disease (CGD), in which a NADPH oxidase defect results in reduced host production of antimicrobial ROS and extreme susceptibility to *Aspergillus* infections (1, 81). Although human studies have excluded a role for IDO in CGD (83), further investigations into the IDO pathway are warranted as such studies have failed to demonstrate functional IDO activity at sites of chronic inflammation. Measures of IDO functional activity during IPA have, however, been made in mouse models, and implicate defective IDO activity as a key mediator of chronic inflammation in CGD (81). An exaggerated Th17 pulmonary response was associated with reduced fungal clearance in mouse models of CGD that develop IPA. Here, reduced IDO function was directly related to NADPH/ROS deficiency, as ROS is essential for IDO catalytic activity in mammals (84). ROS deficiency as a result of reduced NADPH function, significantly enhanced IL-17 inflammation and fungal germination in the lung, thus further reducing neutrophil-mediated antimicrobial activities (81).

Since regulation of homeostasis and peripheral tolerance are extremely important in prevention of invasive Aspergillosis or allergy to *Aspergillus* antigens (80, 85), the role of IDO has been extensively studied in this model of fungal infection(86-88). These studies highlight the induction of the IDO metabolic pathway at different site of fungal colonization as keratinocytes or lung as well as the important anti-inflammatory activity of IDO in the tissue microenvironment (86, 88-90).

1.4.2 Aryl hydrocarbon receptor (Ahr) activation by IDO metabolites in mammals: biological consequences.

The AhR is a ligand-activated transcription factor first identified for its role during embryonic development and induction of xenobiotic metabolizing enzymes as a response to environmental

toxins, such as dioxin (91). More recently, AhR has been shown to play a critical role in immunity by acting as an immune modulator during fungal infection (92). The connection between the AhR and the immune response lies in part in the endogenous Ahr ligands, which comprise many Trp metabolites, including kynurenine (93). Microbial Trp-derived metabolites can activate the AhR, leading to adjustments in the immune response that may hinder disease development (94). The AhR-IDO axis has been recently demonstrated in fungal infection, highlighting a role for IDO-derived metabolites to trigger AhR target genes (92, 95). For example, one AhR target gene, *Il22*, has been widely studied in the context of fungal/microbial infections (94, 96-98). AhR activation by IDO metabolites can also mediate the expansion of peripheral Treg with anti-inflammatory properties. Using IDO-deficient mice, increased pulmonary disease caused by *Paracoccidioides brasiliensis* was associated with decreased Treg expansion and reduced AhR protein expression (92). In murine models of IPA, distinct Treg populations capable of mediating anti-inflammatory effects expand following exposure to *Aspergillus* conidia (80). Late in infection, tolerogenic adaptive Treg (with shared phenotypic identity with the Treg controlling autoimmune diseases or diabetes) produce IL-10 and TGFβ, inhibit Th2 cells and prevent an allergic reaction to *Aspergillus* (80).

1.5 Conclusion

The interplay of Trp metabolic pathways and fungal/host interactions is intriguing with many unanswered questions of the exact nature of crosstalk of shared metabolites and consequences of activation of Trp degradative pathways. In *Aspergillus* infections in particular not only does the pathogen synthesize and degrade Trp but it also can utilize this amino acid (and its precursor anthranilate or the other two AAAs Tyr and Phe) to yield several potentially damaging toxins (Table 1). Also, as both host and *Aspergillus* share catabolic IDO pathways, it is unclear which

organism may generate immunomodulatory Trp degradation products and if they respond to each other's products (e.g. kynurenine). Development of *A. fumigatus* IDO mutants for investigation of disease development can yield valuable information on this front. The research on the expression host IDOs exhibit the importance of an extremely coordinated immune response to mount the right inflammatory response for clearance of spores. However, while an increased IDO expression in the host can control inflammation, the suppression of the IDO-regulated antifungal Th17 responses can favor fungal growth. In this context, it will be critical to explore the entire IDO-mediated innate response, including the specific T cell regulatory subsets affected by IDO activity.

Although the Trp catabolic pathway is shared between host and pathogen, the anabolic pathway is unique to *A. fumigatus.* The antifungals currently used in treatment are becoming increasingly ineffective with emerging drug resistant strains; therefore, drugs targeting essential fungal specific pathways are needed. A proposal for fungal treatment has been highlighted through the studies of essential amino acids. As AAA mutants are auxotrophs and decreased in virulence (16, 19), investigations of drugs targeting these pathway enzymes could lead to novel antifungal compounds. Indeed, a few compounds have exhibited some efficacy in targeting Trp metabolic pathways in *M. tuberculosis* and several fungi and efforts to identify additional inhibitors are warranted.

1.6 Acknowledgements

We would like to thank support from Dalai Lama Trust MSN178745 to TC, The Italian Grant "Programma per Giovani Ricercatori - Rita Levi Montalcini 2013" to TZ, and NIH 5R01AI065728-10 to NPK. The authors report no conflicts of interest.

1.8 Figures and Tables

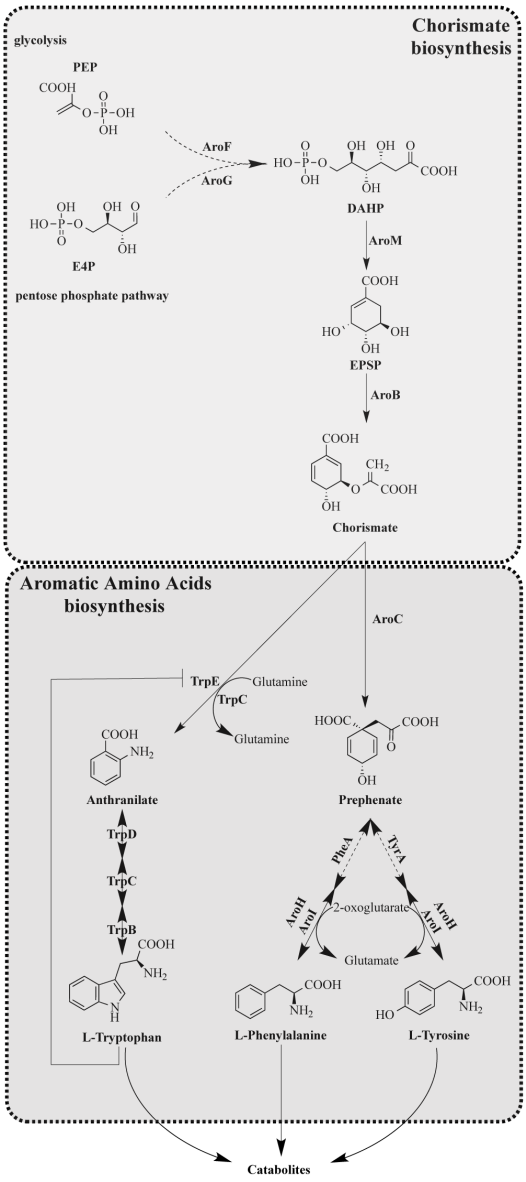

Figure 1. Tryptophan Anabolism of *A. fumigatus.*

Solid arrows indicate characterized reaction as being present in *A. fumigatus* with product detected. Dashed arrows indicate uncharacterized reactions, however putative orthologs are present in *A. fumigatus.*

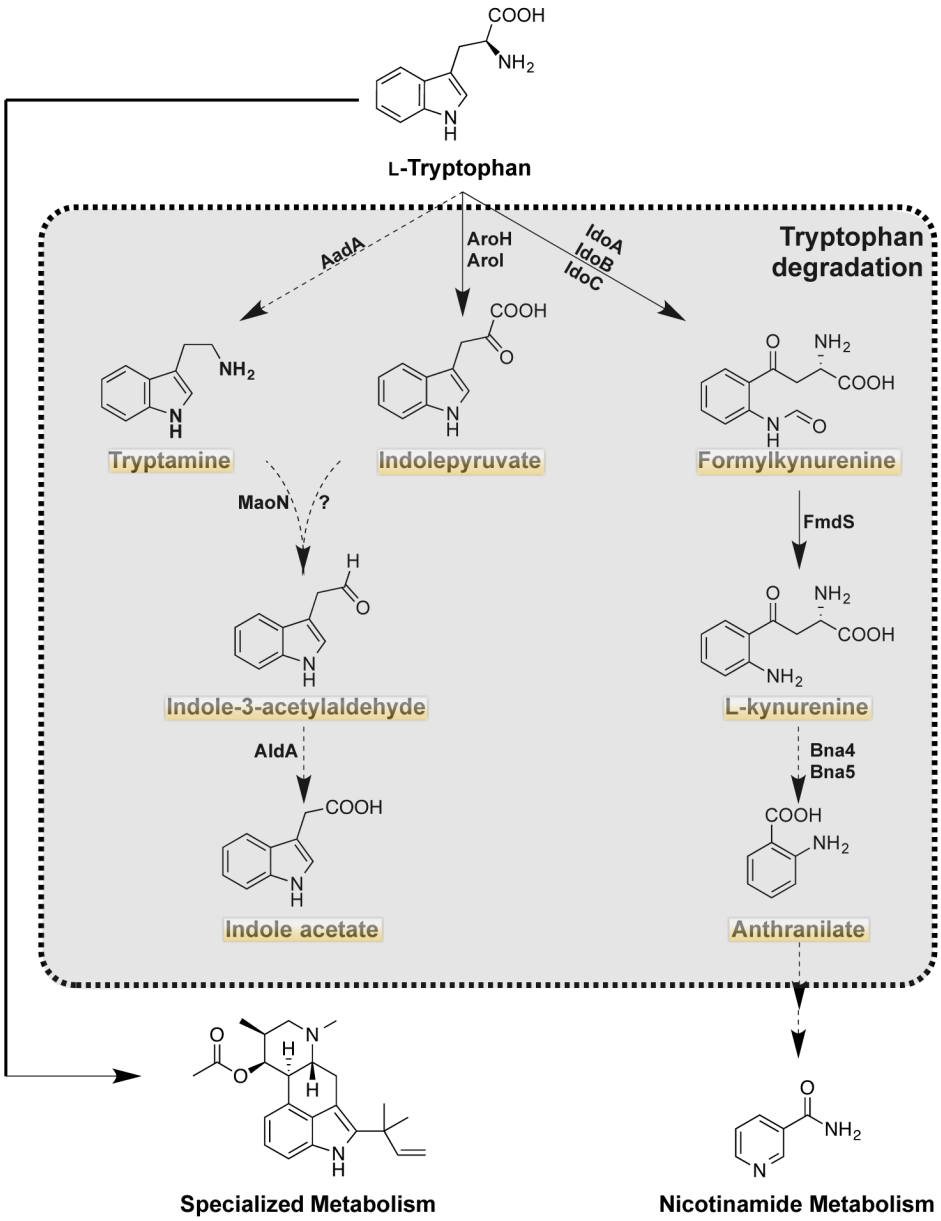

Figure 2. Tryptophan Catabolism of *A. fumigatus.*

Highlighted products are putatively produced in the mammalian host as the orthologous enzymes are present in the host (http://www.genome.jp/kegg). Solid arrows indicate characterized reaction as being present in *A. fumigatus* with product detected. Dashed arrows indicate uncharacterized reactions, however putative orthologs are present in *A. fumigatus.*

Table 1. *Aspergillus fumigatus* non-ribosomal peptides containing aromatic amino acids in their peptide structure.

Toxin	Aromatic Amino Acid[a]	Interaction with host[c-j]
Fumigaclavine C[c]	Tryptophan	Downregulation of Th1 cytokines including TNF-α, IL-1β, and IL-17A. Induction of host cell apoptosis Decrease activation of caspase-1
Fumiquizoline C[d]	Anthranilate Tryptophan	Cytotoxic
Fumisoquin[e]	Tyrosine	Nothing reported
Fumitremorgin[f] Tryprostatin A[g] Verruculogen[h]	Tryptophan	Neurotoxic and produces tremors in mice Tryprostatin causes the inhibition of microtubule assembly Verruculogen causes modification of the electrophysiological properties of HNEC [b]
Gliotoxin[i]	Phenylalanine	Virulent in a steroid murine model of IPA[b] Induction of host cell apoptosis and causes epithelial cell damage Inhibition of phagocytosis and oxidative bursts
Hexadehydroastechrome[j]	Tryptophan	Overexpression resulted in a significantly higher virulence in a neutropenic murine model of IPA[b]

[a] Only the aromatic amino acid is designated. Other amino acids are also in the structure of these metabolites
[b] Abbreviations: IPA, Invasive pulmonary aspergillosis; HNEC, human nasal epithelial cells
[c-j] Biosynthesis and host interactions based from the following sources: [c](61, 99); [d](53); [e](57); [f](64, 100); [g](101); [h](102, 103); [i](6, 65); [j](56, 66)

Table 2. *Aspergillus fumigatus* tryptophan metabolism genes and putative protein function**.**

Protein	Ortholog in *S. cerevisiae*	Gene name in *A. fumigatus*	Protein Function[a]	Ortholog in mammals
Chorismate biosynthesis				
AroF	Aro3	Afu1g02110	DAHP[b] synthase	-
AroG	Aro4	Afu7g04070		
AroM	Aro1	Afu1g13740	EPSP[b] synthase	-
AroB	Aro2	Afu1g06940	Chorismate synthase	-
AAA biosynthesis				
TrpE	Trp2	Afu6g12580	Anthranilate synthase	-
TrpC	Trp3	Afu1g13090		
TrpD	Trp4	Afu4g11980	Anthranilate Phosphoribosyltransferase	-
TrpC	Trp1	Afu1g13090	Phosphoribosylanthranilate isomerase	-
TrpB	Trp5	Afu2g13250	Tryptophan synthase	-
IcsA	-	Afu6g12110	Isochorismate synthase	-
AroC	Aro7	Afu5g13130	Chorismate mutase	-
PheA	Pha2	Afu5g05690	Prephenate dehydratase	-
TyrA	Tyr1	Afu2g10450	Prephenate dehydrogenase	-
AroH	Aro8	Afu2g13630	Aromatic amino acid transaminase	-
AroI	Aro9	Afu5g02290		
Tryptophan Degradation				
IdoA	Bna2	Afu3g14250	Indoleamine 2,3-dioxygenases	IDO1
IdoB	Bna2	Afu4g09830		IDO2
IdoC	Bna2	Afu7g02010		TDO[b]
FmdS	Bna7	Afu1g09960	Kynurenine Formamidase	AFMID[b]
Bna4	Bna4	Afu6g07340	Kynureninase	
Bna5	Bna5	Afu4g09840		KYNU[b]
AroH	Aro8	Afu2g13630	Aromatic amino acid transaminase	LAAO[b]
AroI	Aro9	Afu5g02290		
AadA	-	Afu3g02240	Tryptophan carboxylase	AADC[b]
MaoN	-	Afu3g00100	Monoamine oxidase	MAOA[b]
AldA	Ald4 Ald5	Afu2g00720 Afu7g01000 Afu6g11430	Aldehyde dehydrogenase	ALDH

[a] Prediction of protein function based on AspGD (http://www.aspgd.org/) and KEGG (http://www.genome.jp/kegg/kegg2.html)

[b] Abbreviation: DAHP synthase, 3-Deoxy-D-arabinoheptulosonate 7-phosphate (DAHP) synthase; EPSP synthase, enolpyruvylshikimate-3-phosphate synthase; AFMID, arylformamidase; KYNU, Kynureninase; LAAO, L-amino-acid oxidase; AADC, aromatic-L-amino-acid decarboxylase, MAOA, monoamine oxidase; ALDH2, aldehyde dehydrogenase family.

Table 3. Summary of studies where IDO enzyme activity was found to be implicated in fungal infections.

Fungus	Mouse model	IDO	Outcome	Reference
Candida albicans	Gastrointestinal inf.	Upregulation	Protection of the host against fungus	(104)
Candida albicans	Gastrointestinal inf.	Upregulation	Protection of the host against fungus	(77)
Candida albicans	Gastrointestinal inf.	Upregulation	Protection of the host against fungus	(71)
Candida albicans	*In vitro*	Downregulation	Not done	(105)
Aspergillus fumigatus	Keratitis	Upregulation	Protection of the host against fungus	(89)
Aspergillus fumigatus	Allergy	Overexpression	Protection of the host against fungus	(88)
Aspergillus fumigatus	IPA	Upregulation	Protection of the host against fungus	(86)
Aspergillus fumigatus	IPA in CGD mice	Upregulation	Protection of the host against fungus	(81)
Aspergillus fumigatus	IPA in CF mice	Upregulation	Protection of the host against fungus	(90)
Paracoccidioides brasiliensis	Pulmonary infection	Upregulation	Protection of the host against fungus	(92)
Paracoccidioides brasiliensis	Pulmonary infection	Upregulation	Protection of the host against fungus	(106)
Paracoccidioides brasiliensis	Pulmonary infection	Upregulation	Protection of the host against fungus	(107)
Histoplasma capsulatum	Pulmonary infection	Downregulation	Protection of the host against fungus	(108)
Histoplasma capsulatum	Pulmonary infection	Upregulation	Protection of the host against fungus	(109)

1.9 References

1. Segal BH, Romani LR. Invasive aspergillosis in chronic granulomatous disease. Medical Mycology. 2009;47(s1):S282-S90.
2. Keller NP. Heterogeneity confounds establishment of "a" model microbial strain. MBio. 2017;8(1).
3. Krappmann S, Bignell EM, Reichard U, Rogers T, Haynes K, Braus GH. The *Aspergillus fumigatus* transcriptional activator CpcA contributes significantly to the virulence of this fungal pathogen. Mol Microbiol. 2004;52(3):785-99.
4. Amich J, Dumig M, O'Keeffe G, Binder J, Doyle S, Beilhack A, et al. Exploration of sulfur assimilation of *Aspergillus fumigatus* reveals biosynthesis of sulfur-containing amino acids as a virulence determinant. Infect Immun. 2016;84(4):917-29.
5. D'Enfert C, Diaquin M, Delit A, Wuscher N, Debeaupuis JP, Huerre M, et al. Attenuated virulence of uridine-uracil auxotrophs of *Aspergillus fumigatus*. Infect Immun. 1996;64(10):4401-5.
6. Dagenais TR, Keller NP. Pathogenesis of *Aspergillus fumigatus* in invasive aspergillosis. Clin Microbiol Rev. 2009;22(3):447-65.
7. Rhodes JC. *Aspergillus fumigatus*: growth and virulence. Med Mycol. 2006;44 Suppl 1:S77-81.
8. Perlin DS, Rautemaa-Richardson R, Alastruey-Izquierdo A. The global problem of antifungal resistance: prevalence, mechanisms, and management. Lancet Infect Dis. 2017.
9. Sanglard D. Emerging threats in antifungal-resistant fungal pathogens. Front Med (Lausanne). 2016;3:11.
10. MacKenzie CR, Heseler K, Muller A, Daubener W. Role of indoleamine 2,3-dioxygenase in antimicrobial defence and immuno-regulation: tryptophan depletion versus production of toxic kynurenines. Curr Drug Metab. 2007;8(3):237-44.
11. Lingens F. Regulation of aromatic amino acid biosynthesis in microorganisms. Acta Microbiol Acad Sci Hung. 1976;23(2):161-6.
12. Braus GH. Aromatic amino acid biosynthesis in the yeast *Saccharomyces cerevisiae*: a model system for the regulation of a eukaryotic biosynthetic pathway. Microbiol Rev. 1991;55(3):349-70.
13. Tagliamonte A, Gessa R, Biggio G, Vargiu L, Gessa GL. Daily changes of free serum tryptophan in humans. Life Sci. 1974;14(2):349-54.
14. Pereira SA, Livi GP. Aromatic amino-acid biosynthesis in *Candida albicans*: identification of the ARO4 gene encoding a second DAHP synthase. Curr Genet. 1996;29(5):441-5.
15. Brunke S, Seider K, Almeida RS, Heyken A, Fleck CB, Brock M, et al. *Candida glabrata* tryptophan-based pigment production via the Ehrlich pathway. Molecular microbiology. 2010;76(1):25-47.
16. Wang PM, Choera T, Wiemann P, Pisithkul T, Amador-Noguez D, Keller NP. TrpE feedback mutants reveal roadblocks and conduits toward increasing secondary metabolism in *Aspergillus fumigatus*. Fungal Genet Biol. 2016;89:102-13.

17. Hawkins AR, Lamb HK, Moore JD, Charles IG, Roberts CF. The pre-chorismate (shikimate) and quinate pathways in filamentous fungi: theoretical and practical aspects. J Gen Microbiol. 1993;139(12):2891-9.
18. Duncan K, Edwards RM, Coggins JR. The pentafunctional AroM enzyme of *Saccharomyces cerevisiae* is a mosaic of monofunctional domains. Biochem J. 1987;246(2):375-86.
19. Sasse A, Hamer SN, Amich J, Binder J, Krappmann S. Mutant characterization and *in vivo* conditional repression identify aromatic amino acid biosynthesis to be essential for *Aspergillus fumigatus* virulence. Virulence. 2016;7(1):56-62.
20. Graf R, Mehmann B, Braus GH. Analysis of feedback-resistant anthranilate synthases from *Saccharomyces cerevisiae*. J Bacteriol. 1993;175(4):1061-8.
21. Kafer E. The anthranilate synthetase enzyme complex and the trifunctional *trpC* gene of *Aspergillus*. Can J Genet Cytol. 1977;19(4):723-38.
22. Borgia PT, Dodge CL, Eagleton LE, Adams TH. Bidirectional gene transfer between *Aspergillus fumigatus* and *Aspergillus nidulans*. FEMS Microbiol Lett. 1994;122(3):227-31.
23. Ianiri G, Idnurm A. Essential gene discovery in the basidiomycete *Cryptococcus neoformans* for antifungal drug target prioritization. MBio. 2015;6(2).
24. Blanco B, Prado V, Lence E, Otero JM, Garcia-Doval C, van Raaij MJ, et al. *Mycobacterium tuberculosis* shikimate kinase inhibitors: design and simulation studies of the catalytic turnover. J Am Chem Soc. 2013;135(33):12366-76.
25. Hu W, Sillaots S, Lemieux S, Davison J, Kauffman S, Breton A, et al. Essential gene identification and drug target prioritization in *Aspergillus fumigatus*. PLoS Pathog. 2007;3(3):e24.
26. Kaltdorf M, Srivastava M, Gupta SK, Liang C, Binder J, Dietl AM, et al. Systematic identification of anti-fungal drug targets by a metabolic network approach. Front Mol Biosci. 2016;3:22.
27. Aoki Y, Yamamoto M, Hosseini-Mazinani SM, Koshikawa N, Sugimoto K, Arisawa M. Antifungal azoxybacilin exhibits activity by inhibiting gene expression of sulfite reductase. Antimicrob Agents Chemother. 1996;40(1):127-32.
28. Aoki Y, Kamiyama T, Fujii T, Yamamoto M, Ohwada J, Arisawa M. Design of an antifungal methionine inhibitor not antagonized by methionine. Biol Pharm Bull. 1995;18(9):1267-71.
29. Aoki Y, Kondoh M, Nakamura M, Fujii T, Yamazaki T, Shimada H, et al. A new methionine antagonist that has antifungal activity: mode of action. J Antibiot (Tokyo). 1994;47(8):909-16.
30. Yamaguchi M, Yamaki H, Shinoda T, Tago Y, Suzuki H, Nishimura T, et al. The mode of antifungal action of (S)2-amino-4-oxo-5-hydroxypentanoic acid, RI-331. J Antibiot (Tokyo). 1990;43(4):411-6.
31. Jacques SL, Ejim LJ, Wright GD. Homoserine dehydrogenase from *Saccharomyces cerevisiae*: kinetic mechanism and stereochemistry of hydride transfer. Biochim Biophys Acta. 2001;1544(1-2):42-54.

32. Yamaki H, Yamaguchi M, Nishimura T, Shinoda T, Yamaguchi H. Unique mechanism of action of an antifungal antibiotic RI-331. Drugs Exp Clin Res. 1988;14(7):467-72.
33. Tan S, Evans R, Singh B. Herbicidal inhibitors of amino acid biosynthesis and herbicide-tolerant crops. Amino Acids. 2006;30(2):195-204.
34. Bode RM, Christian ; Birnbaum, Dieter. Mode of action of glyphosate in *Candida maltosa*. Archives of Microbiology. 1984;140(1):83-5.
35. Chin KW, M.A. ; Kaneshiro, E.S. Glyphosate reduces organism viability and inhibits growth *in vitro* of *Pneumocystis*. Journal of Eukary Microbiol. 1999;46(5):139S-41S.
36. Fernandes JD, Martho K, Tofik V, Vallim MA, Pascon RC. The role of amino acid permease and tryptophan biosynthesis in *Cryptococcus neoformans* survival. PLoS One. 2015;10(7):e0132369.
37. Abdel-Rahman HM, El-Koussi NA, Hassan HY. Fluorinated 1,2,4-Triazolo[1,5-a]pyrimidine-6-carboxylic acid derivatives as antimycobacterial agents. Arch Pharm (Weinheim). 2009;342(2):94-9.
38. Forsberg H, Gilstring CF, Zargari A, Martinez P, Ljungdahl PO. The role of the yeast plasma membrane SPS nutrient sensor in the metabolic response to extracellular amino acids. Molecular microbiology. 2001;42(1):215-28.
39. Sugui JA, Kim HS, Zarember KA, Chang YC, Gallin JI, Nierman WC, et al. Genes differentially expressed in conidia and hyphae of *Aspergillus fumigatus* upon exposure to human neutrophils. PLoS One. 2008;3(7):e2655.
40. Morton CO, Varga JJ, Hornbach A, Mezger M, Sennefelder H, Kneitz S, et al. The temporal dynamics of differential gene expression in *Aspergillus fumigatus* interacting with human immature dendritic cells *in vitro*. PLoS One. 2011;6(1):e16016.
41. Brown NA, Dos Reis TF, Ries LN, Caldana C, Mah JH, Yu JH, et al. G-protein coupled receptor-mediated nutrient sensing and developmental control in *Aspergillus nidulans*. Molecular microbiology. 2015;98(3):420-39.
42. Grice CM, Bertuzzi M, Bignell EM. Receptor-mediated signaling in *Aspergillus fumigatus*. Front Microbiol. 2013;4:26.
43. Yuasa HJ, Ball HJ. The evolution of three types of indoleamine 2,3 dioxygenases in fungi with distinct molecular and biochemical characteristics. Gene. 2012;504(1):64-74.
44. Fraser JA, Davis MA, Hynes MJ. The formamidase gene of *Aspergillus nidulans*: regulation by nitrogen metabolite repression and transcriptional interference by an overlapping upstream gene. Genetics. 2001;157(1):119-31.
45. Ohashi K, Kawai S, Murata K. Secretion of quinolinic acid, an intermediate in the kynurenine pathway, for utilization in NAD+ biosynthesis in the yeast *Saccharomyces cerevisiae*. Eukaryot Cell. 2013;12(5):648-53.
46. Bulfer SL, Brunzelle JS, Trievel RC. Crystal structure of *Saccharomyces cerevisiae* Aro8, a putative alpha-aminoadipate aminotransferase. Protein Sci. 2013;22(10):1417-24.

47. Urrestarazu A, Vissers S, Iraqui I, Grenson M. Phenylalanine- and tyrosine-auxotrophic mutants of *Saccharomyces cerevisiae* impaired in transamination. Mol Gen Genet. 1998;257(2):230-7.
48. Rao RP, Hunter A, Kashpur O, Normanly J. Aberrant synthesis of indole-3-acetic acid in *Saccharomyces cerevisiae* triggers morphogenic transition, a virulence trait of pathogenic fungi. Genetics. 2010;185(1):211-20.
49. Tylš F, Páleníček T, Horáček J. Psilocybin – Summary of knowledge and new perspectives. European Neuropsychopharmacology. 2014;24(3):342-56.
50. Bilkay IK, S ; Aksoz, N. Indole-3-acetic acid and gibberellic acid production in *Aspergillus niger*. Turk J Biol. 2010;34:313-8.
51. Pattaeva MR, Bakhtiyor. Growth and phytohormones production by thermophilic *Aspergillus fumigatus* 2 and thermotolerant *Aspergillus terreus* 8 strains in salt stress. British Journal of Applied Science & Technology,. 2015;8(3):305-12.
52. Macdonald JC, Slater GP. Biosynthesis of gliotoxin and mycelianamide. Can J Biochem. 1975;53(4):475-8.
53. Lim FY, Ames B, Walsh CT, Keller NP. Co-ordination between BrlA regulation and secretion of the oxidoreductase FmqD directs selective accumulation of fumiquinazoline C to conidial tissues in *Aspergillus fumigatus*. Cell Microbiol. 2014;16(8):1267-83.
54. Mulinti P, Allen NA, Coyle CM, Gravelat FN, Sheppard DC, Panaccione DG. Accumulation of ergot alkaloids during conidiophore development in *Aspergillus fumigatus*. Curr Microbiol. 2014;68(1):1-5.
55. Yamazaki M, Suzuki S. Toxicology of tremorgenic mycotoxins, fumitremorgin A and B. Dev Toxicol Environ Sci. 1986;12:273-82.
56. Yin WB, Baccile JA, Bok JW, Chen Y, Keller NP, Schroeder FC. A nonribosomal peptide synthetase-derived iron(III) complex from the pathogenic fungus *Aspergillus fumigatus*. J Am Chem Soc. 2013;135(6):2064-7.
57. Baccile JA, Spraker JE, Le HH, Brandenburger E, Gomez C, Bok JW, et al. Plant-like biosynthesis of isoquinoline alkaloids in *Aspergillus fumigatus*. Nat Chem Biol. 2016;12(6):419-24.
58. Imamura K, Tsuyama Y, Hirata T, Shiraishi S, Sakamoto K, Yamada O, et al. Identification of a gene involved in the synthesis of a dipeptidyl peptidase IV inhibitor in *Aspergillus oryzae*. Appl Environ Microbiol. 2012;78(19):6996-7002.
59. Liu X, Walsh CT. Cyclopiazonic acid biosynthesis in *Aspergillus* sp.: characterization of a reductase-like R* domain in cyclopiazonate synthetase that forms and releases cyclo-acetoacetyl-L-tryptophan. Biochemistry. 2009;48(36):8746-57.
60. Clevenger KD, Bok JW, Ye R, Miley GP, Verdan MH, Velk T, et al. A scalable platform to identify fungal secondary metabolites and their gene clusters. Nat Chem Biol. 2017;13(8):895-901.

61. Guo W, Hu S, Elgehama A, Shao F, Ren R, Liu W, et al. Fumigaclavine C ameliorates dextran sulfate sodium-induced murine experimental colitis via NLRP3 inflammasome inhibition. J Pharmacol Sci. 2015;129(2):101-6.
62. Yamazaki M, Fujimoto H, Kawasaki T. Chemistry of tremorogenic metabolites. Fumitremorgin A from *Aspergillus fumigatus*. Chem Pharm Bull (Tokyo). 1980;28(1):245-54.
63. Cole RJ. Fungal tremorogens. Prikl Biokhim Mikrobiol. 1993;29(1):44-50.
64. Suzuki S, Kikkawa K, Yamazaki M. Abnormal behavioral effects elicited by a neurotropic mycotoxin, fumitremorgin A in mice. J Pharmacobiodyn. 1984;7(12):935-42.
65. Sugui JA, Pardo J, Chang YC, Zarember KA, Nardone G, Galvez EM, et al. Gliotoxin is a virulence factor of *Aspergillus fumigatus*: *gliP* deletion attenuates virulence in mice immunosuppressed with hydrocortisone. Eukaryot Cell. 2007;6(9):1562-9.
66. Wiemann P, Lechner BE, Baccile JA, Velk TA, Yin WB, Bok JW, et al. Perturbations in small molecule synthesis uncovers an iron-responsive secondary metabolite network in *Aspergillus fumigatus*. Front Microbiol. 2014;5:530.
67. Zelante T, Fallarino F, Bistoni F, Puccetti P, Romani L. Indoleamine 2,3-dioxygenase in infection: the paradox of an evasive strategy that benefits the host. Microbes Infect. 2009;11(1):133-41.
68. Colangelo EJ. Cervicocranium and the aviator's protective helmet. Aviat Space Environ Med. 1975;46(10):1263-4.
69. Thomas SM, Garrity LF, Brandt CR, Schobert CS, Feng GS, Taylor MW, et al. IFN-gamma-mediated antimicrobial response. Indoleamine 2,3-dioxygenase-deficient mutant host cells no longer inhibit intracellular *Chlamydia* spp. or *Toxoplasma* growth. J Immunol. 1993;150(12):5529-34.
70. Aldajani WA, Salazar F, Sewell HF, Knox A, Ghaemmaghami AM. Expression and regulation of immune-modulatory enzyme indoleamine 2,3-dioxygenase (IDO) by human airway epithelial cells and its effect on T cell activation. Oncotarget. 2016;7(36):57606-17.
71. Bonifazi P, Zelante T, D'Angelo C, De Luca A, Moretti S, Bozza S, et al. Balancing inflammation and tolerance *in vivo* through dendritic cells by the commensal *Candida albicans*. Mucosal Immunol. 2009;2(4):362-74.
72. Jung ID, Lee C-M, Jeong Y-I, Lee JS, Park WS, Han J, et al. Differential regulation of indoleamine 2,3-dioxygenase by lipopolysaccharide and interferon gamma in murine bone marrow derived dendritic cells. FEBS Letters. 2007;581(7):1449-56.
73. Gorski JP, Howard JB. Effect of methylamine on the structure and function of the fourth component of human complement, C4. J Biol Chem. 1980;255(21):10025-8.
74. Fallarino F, Volpi C, Zelante T, Vacca C, Calvitti M, Fioretti MC, et al. IDO mediates TLR9-driven protection from experimental autoimmune diabetes J Immunol. 2009;183(10):6303-12.
75. Rivas FV, Chervonsky AV, Medzhitov R. ART and immunology. Trends in Immunology. 2014;35(10):451.

76. Soares MP, Gozzelino R, Weis S. Tissue damage control in disease tolerance. Trends in Immunology. 2014;35(10):483-94.
77. Bozza S, Fallarino F, Pitzurra L, Zelante T, Montagnoli C, Bellocchio S, et al. A crucial role for tryptophan catabolism at the host/*Candida albicans* Interface. J Immunol. 2005;174(5):2910-8.
78. Romani L. Cell mediated immunity to fungi: a reassessment. Med Mycol. 2008;46(6):515-29.
79. Zelante T, Bozza S, De Luca A, D'Angelo C, Bonifazi P, Moretti S, et al. Th17 cells in the setting of *Aspergillus* infection and pathology. Med Mycol. 2009;47 Suppl 1:S162-9.
80. Montagnoli C, Fallarino F, Gaziano R, Bozza S, Bellocchio S, Zelante T, et al. Immunity and tolerance to *Aspergillus* involve functionally distinct regulatory T cells and tryptophan catabolism. J Immunol. 2006;176(3):1712-23.
81. Romani L, Fallarino F, De Luca A, Montagnoli C, D'Angelo C, Zelante T, et al. Defective tryptophan catabolism underlies inflammation in mouse chronic granulomatous disease. Nature. 2008;451(7175):211-5.
82. De Luca A, Pariano M, Cellini B, Costantini C, Villella VR, Jose SS, et al. The IL-17F/IL-17RC axis promotes respiratory allergy in the proximal airways. Cell Rep. 2017;20(7):1667-80.
83. De Ravin SS, Zarember KA, Long-Priel D, Chan KC, Fox SD, Gallin JI, et al. Tryptophan/kynurenine metabolism in human leukocytes is independent of superoxide and is fully maintained in chronic granulomatous disease. Blood. 2010;116(10):1755-60.
84. Macchiarulo A, Camaioni E, Nuti R, Pellicciari R. Highlights at the gate of tryptophan catabolism: a review on the mechanisms of activation and regulation of indoleamine 2,3-dioxygenase (IDO), a novel target in cancer disease. Amino Acids. 2009;37(2):219-29.
85. Zelante T, De Luca A, Bonifazi P, Montagnoli C, Bozza S, Moretti S, et al. IL-23 and the Th17 pathway promote inflammation and impair antifungal immune resistance. European Journal of Immunology. 2007;37(10):2695-706.
86. de Luca A, Bozza S, Zelante T, Zagarella S, D'Angelo C, Perruccio K, et al. Non-hematopoietic cells contribute to protective tolerance to *Aspergillus fumigatus* via a TRIF pathway converging on IDO. Cell Mol Immunol. 2010;7(6):459-70.
87. Jiang N, Zhao GQ, Lin J, Hu LT, Che CY, Li C, et al. Expression of indoleamine 2,3-dioxygenase in a murine model of *Aspergillus fumigatus* keratitis. Int J Ophthalmol. 2016;9(4):491-6.
88. Paveglio SA, Allard J, Foster Hodgkins SR, Ather JL, Bevelander M, Campbell JM, et al. Airway epithelial indoleamine 2,3-dioxygenase inhibits CD4+ T cells during *Aspergillus fumigatus* antigen exposure. Am J Respir Cell Mol Biol. 2011;44(1):11-23.
89. Jiang N, Zhao G, Lin J, Hu L, Che C, Li C, et al. Indoleamine 2,3-Dioxygenase is involved in the inflammation response of corneal epithelial cells to *Aspergillus fumigatus* infections. PLoS One. 2015;10(9):e0137423.

90. Iannitti RG, Carvalho A, Cunha C, De Luca A, Giovannini G, Casagrande A, et al. Th17/Treg imbalance in murine cystic fibrosis is linked to indoleamine 2,3-dioxygenase deficiency but corrected by kynurenines. Am J Respir Crit Care Med. 2013;187(6):609-20.
91. Mackowiak B, Wang H. Mechanisms of xenobiotic receptor activation: Direct vs. indirect. Biochimica et Biophysica Acta (BBA) - Gene Regulatory Mechanisms. 2016;1859(9):1130-40.
92. Araujo EF, Feriotti C, Galdino NAL, Preite NW, Calich VLG, Loures FV. The IDO-AhR axis controls Th17/Treg immunity in a pulmonary model of fungal infection Front Immunol. 2017;8:880.
93. Hubbard TD, Murray IA, Perdew GH. Indole and tryptophan metabolism: endogenous and dietary routes to Ah receptor activation. Drug Metabolism and Disposition. 2015;43(10):1522-35.
94. Zelante T, Iannitti RG, Cunha C, De Luca A, Giovannini G, Pieraccini G, et al. Tryptophan catabolites from microbiota engage aryl hydrocarbon receptor and balance mucosal reactivity via interleukin-22. Immunity. 2013;39(2):372-85.
95. Bessede A, Gargaro M, Pallotta MT, Matino D, Servillo G, Brunacci C, et al. Aryl hydrocarbon receptor control of a disease tolerance defence pathway. Nature. 2014;511(7508):184-90.
96. Goupil M, Cousineau-Cote V, Aumont F, Senechal S, Gaboury L, Hanna Z, et al. Defective IL-17- and IL-22-dependent mucosal host response to *Candida albicans* determines susceptibility to oral candidiasis in mice expressing the HIV-1 transgene. BMC Immunol. 2014;15:49.
97. Xu X, Weiss ID, Zhang HH, Singh SP, Wynn TA, Wilson MS, et al. Conventional NK cells can produce IL-22 and promote host defense in *Klebsiella pneumoniae* pneumonia. J Immunol. 2014;192(4):1778-86.
98. Guo X, Qiu J, Tu T, Yang X, Deng L, Anders RA, et al. Induction of innate lymphoid cell-derived interleukin-22 by the transcription factor STAT3 mediates protection against intestinal infection. Immunity. 2014;40(1):25-39.
99. Zhu YX, Yao LY, Jiao RH, Lu YH, Tan RX. Enhanced production of Fumigaclavine C in liquid culture of *Aspergillus fumigatus* under a two-stage process. Bioresour Technol. 2014;152:162-8.
100. Frisvad JC, Larsen TO. Extrolites of *Aspergillus fumigatus* and other pathogenic species in *Aspergillus* section fumigati. Front Microbiol. 2015;6:1485.
101. Usui T, Kondoh M, Cui CB, Mayumi T, Osada H. Tryprostatin A, a specific and novel inhibitor of microtubule assembly. Biochem J. 1998;333 (Pt 3):543-8.
102. Feng Y, Holte D, Zoller J, Umemiya S, Simke LR, Baran PS. Total synthesis of Verruculogen and Fumitremorgin A enabled by ligand-controlled C-H borylation. J Am Chem Soc. 2015;137(32):10160-3.
103. Khoufache K, Puel O, Loiseau N, Delaforge M, Rivollet D, Coste A, et al. Verruculogen associated with *Aspergillus fumigatus* hyphae and conidia modifies the electrophysiological properties of human nasal epithelial cells. BMC Microbiol. 2007;7:5.

104. De Luca A, Montagnoli C, Zelante T, Bonifazi P, Bozza S, Moretti S, et al. Functional yet balanced reactivity to *Candida albicans* requires TRIF, MyD88, and IDO-dependent inhibition of Rorc. J Immunol. 2007;179(9):5999-6008.
105. Cheng SC, van de Veerdonk F, Smeekens S, Joosten LA, van der Meer JW, Kullberg BJ, et al. *Candida albicans* dampens host defense by downregulating IL-17 production. J Immunol. 2010;185(4):2450-7.
106. Araujo EF, Medeiros DH, Galdino NA, Condino-Neto A, Calich VL, Loures FV. Tolerogenic plasmacytoid dendritic cells control *Paracoccidioides brasiliensis* infection by inducting regulatory T cells in an IDO-dependent manner. . PLoS Pathog. 2016;12(12):e1006115.
107. Araujo EF, Loures FV, Bazan SB, Feriotti C, Pina A, Schanoski AS, et al. Indoleamine 2,3-dioxygenase controls fungal loads and immunity in Paracoccidioidomicosis but is more important to susceptible than resistant hosts. PLoS Negl Trop Dis. 2014;8(11):e3330.
108. Hage CA, Horan DJ, Durkin M, Connolly P, Desta Z, Skaar TC, et al. Histoplasma capsulatum preferentially induces IDO in the lung. Med Mycol. 2013;51(3):270-9.
109. George MM, Subramanian Vignesh K, Landero Figueroa JA, Caruso JA, Deepe GS, Jr. Zinc induces dendritic cell tolerogenic phenotype and skews regulatory T Cell-Th17 balance. J Immunol. 2016;197(5):1864-76.

CHAPTER 2

TrpE feedback mutants reveal roadblocks and conduits towards increasing secondary metabolism in *Aspergillus fumigatus*

Originally published as:

Wang, PM‡, Choera, T‡, Wiemann P, Pisithkul T, Amador-Noguez D, Keller NP. TrpE feedback mutants reveal roadblocks and conduits towards increasing secondary metabolism in *Aspergillus fumigatus*. **Fungal Genet Biol.** 2016 Apr; 89:102-113. ‡ These authors contributed equally to this work.

Modifications have been made to increase legibility in the current format.

My contribution was the characterization of the all the TrpE mutant strains, including the growth, physiology and metabolite profiling.

2.1 Abstract

Small peptides formed from non-ribosomal peptide synthetases (NRPS) are bioactive molecules produced by many fungi including the genus Aspergillus. A subset of NRPS utilizes tryptophan and its precursor, the non-proteinogenic amino acid anthranilate, in synthesis of various metabolites such as *A. fumigatus* fumiquinazolines (Fqs) produced by the fmq gene cluster. The *A. fumigatus* genome contains two putative anthranilate synthases - a key enzyme in conversion of anthranilic acid to tryptophan - one beside the fmq cluster and one in a region of co-linearity with other Aspergillus spp. Only the gene found in the co-linear region, *trpE*, was involved in tryptophan biosynthesis. We found that site-specific mutations of the TrpE feedback domain resulted in significantly increased production of anthranilate, tryptophan, p-aminobenzoate and fumiquinazolines FqF and FqC. Supplementation with tryptophan restored metabolism to near wild type levels in the feedback mutants and suggested that synthesis of the tryptophan degradation product kynurenine could negatively impact Fq synthesis. The second putative anthranilate synthase gene next to the fmq cluster was termed *icsA* for its considerable identity to isochorismate synthases in bacteria. Although *icsA* had no impact on *A. fumigatus* Fq production, deletion and over-expression of *icsA* increased and decreased respectively aromatic amino acid levels suggesting that IcsA can draw from the cellular chorismate pool.

2.2 Introduction

The Kingdom Fungi constitutes an unparalleled genomic resource of natural product (also called secondary metabolite) pathways with many fungi containing up to 70 secondary metabolite gene clusters in their genome (1). Although some natural products – both harmful and beneficial – are produced in copious quantities under laboratory growth conditions, most are produced either in small quantities or not at all. Numerous efforts have recently been aimed at inducing production of these lowly expressed metabolites, primarily through over-expression of the secondary metabolite cluster genes in endogenous and/or exogenous host systems (2).

Not all over expression efforts have resulted in success. Many reasons could account for these failures, ranging from toxicity of the products to the host system, unknown post-transcriptional regulations, requirement of other genes not in the cluster, and lack of sufficient primary metabolite pools. All-natural products originate from various primary metabolites. Polyketides are derived from acyl coenzyme A (CoA) and malonyl-CoA units, terpenes from isoprene units and non-ribosomal peptides from proteinogenic and non-proteinogenic amino acids (3). Non-ribosomal peptides are synthesized by non-ribosomal peptide synthetases (NRPS), which consist minimally of A (adenylation), PCP (peptide carrier protein), C (condensation) and releasing domains. The A domain determines which amino acid is incorporated into the growing chain. For example, *Aspergillus fumigatus* FmqA is a three A domain NRPS incorporating anthranilate, L-tryptophan and L-alanine into the precursor peptide fumiquinazoline F (FqF) (4). FqF is further processed by additional enzymes to the end metabolite FqC (Fig. 1). As a considerable subset of fungal NRPS utilize both anthranilate and L-tryptophan in production of valuable alkaloid peptides (5), we became interested in the potential contribution of modulating tryptophan biosynthesis to increase production of alkaloid peptides using fumiquinazolines (Fqs) as the targeted metabolites.

Figure 2 presents the known and predicted *A. fumigatus* enzymes involved in aromatic amino acid metabolism. Chorismate is a common intermediate for the aromatic amino acids anthranilate, L-tryptophan, L-phenylalanine and L-tyrosine in yeast (6). L-tryptophan is derived from chorismate by five enzymatic steps encoded by four genes in *A. fumigatus* (Fig. 2 and Table 1). Anthranilate synthase (AS) [EC 4.1.3.27] catalyzes the production of anthranilate from chorismate in the L-tryptophan biosynthesis branch. ASs have been characterized in bacteria (7-9), in plants (10-12) and in *Saccharomyces cerevisiae* (6, 13). In yeast, AS consists of two subunits (AAS-I and AAS-II) that are necessary to yield anthranilate from chorismate by addition of an amino group from L-glutamine (13). AAS-I is responsible for chorismate binding, and AAS-II is a glutamine amidotransferase that catalyzes the transfer of the amino group (13). A tryptophan feedback loop specified by amino acids in the AAS-I subunit (12, 13) makes AS the rate-limiting enzyme in L-tryptophan synthesis. Feedback inhibition resistant forms of this enzyme – allowing for increased tryptophan pools – have been associated with increases in several plant natural products including the alkaloid lochnericine in transgenic hairy root cultures of the periwinkle Catharanthus roseus (14) and indole alkaloids in rice (15). In Aspergillus spp., the AAS-II encoding gene, *trpC*, was first characterized in A. nidulans in 1977 (16) but, until now, *trpE* encoding AAS-I has only been defined by predicted enzymatic activity.

Here, we show that AAS-I feedback mutants in *A. fumigatus* enhance Fq production. The *A. fumigatus* genome contains two putative AAS-I proteins, one beside the fmq cluster and one in a region of co-linearity with other Aspergillus spp. Over-expression of the fmq-cluster-associated gene (*icsA*/Afu6g12110) could not complement the tryptophan auxotrophy of the *trpE* (Afu6g12580) deletion mutant and had no significant difference on Fq production. However, over-expression of *icsA* resulted in significantly decreased anthranilate, L-tryptophan, L-phenylalanine,

and L-tyrosine levels, suggesting that IcsA metabolizes chorismate into a yet unknown product in *A. fumigatus*. Phylogenetic analysis showed it to be closely related to bacterial isochorismate synthases. The second gene, *trpE* (Afu6g12580), encoded the canonical AAS-I required for L-tryptophan production. Creation of synthetic feedback resistant alleles of TrpE resulted in strains that produced approximately 1.5-fold more FqF and FqC and displayed a 120+ fold increase in intracellular levels of anthranilate and up to 3+ fold more tryptophan than the control strain on minimal medium. Supplementation with L-tryptophan eliminated any gain in Fq production and in fact lowered production in the single site feedback mutant, potentially through increases in the L-tryptophan degradation product L-kynurenine.

2.3 Materials and Methods

2.3.1 Strains and medium

Strains used or created in this study are listed in Table 2. The genetic background of the primary strain used in this study is *A. fumigatus* AF293 (17). All strains were maintained as glycerol stocks at -80 °C, and activated on solid glucose minimal media (GMM) at 37 °C (18). Growth media was supplemented with 1.26 g/L uridine and 0.56 g/L uracil for pyrG auxotrophs, 1 g/L L-arginine for argB auxotrophs, and 1 g/L L-tryptophan for *trpE* auxotrophs.

2.3.2 Genetic manipulation

Fungal DNA extraction, gel electrophoresis, restriction enzyme digestion, Southern blotting, hybridization and probe preparation were performed according to standard methods (19). For DNA isolation, *A. fumigatus* strains were grown for 24 h at 37 °C in steady state liquid GMM, supplemented as needed for auxotrophs. DNA isolation was performed as described by Sambrook and Russell (19). Gene deletion mutants in this study were constructed by targeted integration of the deletion cassette through transformation (20, 21). The deletion cassettes were constructed using

a double-joint fusion PCR (DJ-PCR) approach (20, 21). *A. fumigatus* protoplast generation and transformation were carried out as previously described (20, 21). The plasmids used in this work are listed in Table S1 and all primers are listed in Table S2.

An *A. fumigatus trpE* (Afu6g12580) disruption cassette consisted of the following: 1 kb DNA fragment upstream of the *trpE* start codon (primers DAf6g12580F1 and DAf6g12580R1), a 2.7 kb selectable auxotrophic marker, *A. fumigatus* argB, cloned from plasmid pJMP4 (22) (primers GF A. Fumi argB F and GF A. Fumi argB R), and 1 kb DNA fragment downstream of the *trpE* stop codon (primers DAf6g12580F2 and DAf6g12580R2). The deletion construct was transformed into AF293.6 (pyrG1, argB1). Transformants were screened for arginine prototroph in media supplemented with $_{L}$-tryptophan for *trpE* auxotrophs, uridine and uracil for pyrG auxotrophs. Transformants obtained were verified by PCR using primers PM-F6g12580F and PM-F6g12580R, and Southern analysis using a *trpE* probe SB1 (primers DAf6g12580F1 and DAf6g12580R2) (Fig. S1). TPMW6.2 (Δ*trpE*, pyrG1-) was chosen for further experiments.

In order to complement the Δ*trpE* mutant with a wild-type and feedback insensitive *trpE* copies, the plasmids pPMW1 ($trpE^{C}$), pPMW2 ($trpE^{S77L}$) and pPMW3($trpE^{S66R,S77L}$) were constructed using in vivo yeast recombination (23) of 4 linear DNA fragments consisting of (1) the gpdA(p) promoter obtained by PCR from plasmid pJMP9.1 (24) (with primers PM-yAup-gpdA F and PM-yAup-gpdA R), (2) a AscI-linearized 2μ-based yeast-Escherichia coli shuttle plasmid pYH-yA-riboA (Palmer, J.M. and Keller, unpublished), (3) the first half of wild-type or a Ser66Arg-mutated *trpE* gene (obtained by PCR from *A. fumigatus* wild-type genomic DNA with primers PM-F6g12580F and PM-S66-afu6g12580R for $trpE^{C}$; and with primers PM-F6g12580F and PM-R66M-afu6g12580R for the S66R-mutation) and (4) the second half of wild-type or a Ser77Leu-mutated *trpE* gene (obtained by PCR from *A. fumigatus* wild-type genomic DNA with primers

PM-S77 Afu6g12580F and PM-riboB-Afu6g12580R for *trpE*^{C}; and with primers PM-L77M Afu6g12580F and PM-riboB-Afu6g12580R for the S77L-mutation), respectively. The above fragments contained 20-35 bp overlapping bases to the correct flanking fragments for in vivo yeast recombination to create the plasmids. All of the plasmids described above were verified by restriction digest profiles and sequencing, and then digested with AvrII and SacII to release the appropriate gpdA(p)-*trpE* fragment to be ligated into the AvrII/SacII sites of pJMP9.1 (24). The resulting plasmids pPMW4(OE::*trpE*^{C}), pPMW5 (OE::*trpE*^{S77L}), pPMW6(OE::*trpE*^{S66R,S77L}) and the parent plasmid pJMP9.1 were transformed into the auxotrophic Δ*trpE* mutant TPMW6.2 (Δ*trpE*, pyrG1) to yield mutants TPMW8.9 (*trpE*^{C}), TPMW9.5(*trpE*^{S77L}), TPMW10.9 (*trpE*^{S66R,S77L}) and TPMW12.4 (Δ*trpE*), respectively. These mutants were selected for tryptophan and pyrimidine prototrophy in media supplemented with $_{L}$-tryptophan for *trpE* auxotrophs, in case site-mutation strain cannot produce $_{L}$-tryptophan for growth. PCR screening (primers PM-F6g12580F and PM-F6g12580R) and Southern analysis were applied to obtain single-gene-copy replacement transformants, using probe SB2 (primer pair PM-F6g12580F/DAf6g12580R2) (Fig. S2A). Over-expression of *trpE* was verified via Northern analysis for *trpE*^{C}, *trpE*^{S77L}, and *trpE*^{S66R,S77L} compared to the complemented parental strain TJW55.2 (Fig. S2B)

icsA (Afu6g12110) was disrupted and over-expressed both in AF293.1 (pyrG1) and TPMW6.2 (Δ*trpE*, pyrG1) using a pyrG marker cassette. To construct the *icsA* deletion cassette, two 1 kb fragments flanking the ORF were amplified from AF293 genomic DNA using the primer pair DAfu6gF1/ DAfu6gR1 and DAfu6gF2/ DAfu6gR2, respectively (Table S2). The selection marker, A. parasiticus pyrG, was PCR amplified from plasmid pJW24 (25) using the primer pair ParapyrGF/ParapyrGR (Table S2). To construct an *icsA* over-expression strain at its locus, its native promoter was replaced with the constitutive promoter, gpdA(p), amplified from plasmid

pJMP9.1 using the primer pair OEpyrGgpdF/OEpyrGgpdR. The two 1 kb fragments for the *icsA* over-expression cassette were amplified from AF293 genomic DNA using the primer pair DAfu6gF1/OEAfu6gR1 and OEAfu6gF2/DAfu6gR2, respectively (Table S2). Transformants were selected for pyrimidine prototrophy in media without any supplements and amended with L-tryptophan in case TPMW6.2 was used as the parental strain. Transformants were further screened by PCR (primer pair diAfu6gF1/diAfu6gR1 for Δ*icsA* mutants, OEdiAfu6gF/OEdiAfu6gR for OE::*icsA* mutants) and Southern analysis using probe SB3 (primer pair DAfu6gF1/DAfu6gR2) (Fig. S3). The obtained mutants were named TPMW1.13 (Δ*icsA*), TPMW1.70 (OE::*icsA*), TPMW7.14 (Δ*trpE* Δ*icsA*), and TPMW11.18 (Δ*trpE* OE::*icsA*). Over-expression of *icsA* was verified via Northern analysis for TPMW1.70 compared to the complemented parental strain TJW55.2, and the *icsA* deletion strain TPMW1.13 (Fig. S4).

2.3.3 Phylogenetic analysis

For phylogenetic analysis, reviewed and curated sequences from the Swiss-Prot database (www.uniprot.org) of proteins containing a chorismate binding domain (isochorismate synthase, anthranilate synthase and p-aminobenzoate synthase) were retrieved and aligned using ClustalW (MegAlign, DNAStar, Madison, WI, USA) together with the protein sequences of Afu6g12110/IcsA, Afu6g04820/PabaA, and Afu6g12580/TrpE (www.aspergillus.org) (26). From the alignment, the chorismate binding domains were extracted based on the canonical chorismate binding domain from the Conserved Domain Database (CDD) (www.ncbi.nlm.nih.gov). Phylogenetic analysis of the chorismate binding domains was performed using MAFFT (http://mafft.cbrc.jp/alignment/software/) (27) and (http://www.microbesonline.org/fasttree/) (28). Results were visualized using FigTree (http://tree.bio.ed.ac.uk/software/figtree/) collapsing branches with bootstrap values below 70% support value. For phylogenetic analysis of the

indoleamine 2,3-dioxygenase (Ido) proteins, sequences from Aspergillus and Fusarium species were obtained from the National Center for Biotechnology Information (NCBI) by performing a protein blast search using the *S. cerevisiae* Bna2p sequence as query. Sequences were processed and visualized including Ido sequences previously analyzed by Yuasa and Ball (29-31) as described for the chorismate binding domain proteins above.

2.3.4 Physiology experiments

Colony diameters of strains were measured after 3 days of growth at 37 °C on solidified GMM and GMM supplemented with 5 mM $_{L}$-tryptophan, respectively. Strains were point-inoculated onto the media at 10^4 conidia total (in 5 µL). Conidial production studies were performed on solid GMM and tryptophan plates. For each plate, a 10 mL top layer of cool but molten agar that contained 10^7 spores of each strain, respectively, was added. Strains were cultured at 37 °C for 24 h. A core of 1.5 cm diameter was removed from the plates and homogenized in 2 mL 0.01% Tween 80 to release the spores. Spores were counted on a hemocytometer. Three replicates were used for each assay and statistical significance was calculated with by analysis of variance (ANOVA) using Prism 6 software (Graph Pad).

2.3.5 Primary metabolites extraction and analysis

A. fumigatus strains were inoculated into 50 mL of liquid GMM and GMM supplemented with 5mM $_{L}$-tryptophan, respectively, at 10^7 conidia per mL and cultured at 25 °C and 250 rpm for 84 h in triplicates. Fungal tissue was collected by rapid filtration using miracloth and immediately frozen in liquid nitrogen. About 0.1 g of fungal tissue was transferred to a 15 mL conical vial containing 3 mL extraction solvent (2/2/1 (v/v/v) acetonitrile/methanol/water) cooled on dry ice. After homogenization and centrifugation, 2 mL of supernatant was filtered using a 0.45 µm PTFE Mini-UniPrep filter vial (Agilent). The supernatant of these hyphal metabolites were used for

metabolite analysis. For metabolite measurement, samples were dried under N_2 and resuspended in LC-MS grade water (Sigma-Aldrich). Samples were analyzed using an HPLC-MS system consisting of a Dionex UPHLC coupled by electrospray ionization (ESI; negative mode) to a hybrid quadrupole-high-resolution mass spectrometer (Q Exactive orbitrap, Thermo Scientific) operated in full scan mode. Liquid chromatography separation was achieved using an ACQUITY UPLC® BEH C18 (2.1 x 100 mm column, 1.7 μm particle size, Waters). Solvent A was 97:3 water:methanol with 10 mM tributylamine and 10 mM acetic acid, pH 8.2; solvent B was methanol. The gradient was: 0 min, 5% B; 1.5 min, 5% B, 11.5 min, 95% B; 12.5 min, 95% B; 13 min, 5% B; 14.5 min, 5% B. Autosampler and column temperatures were 4 °C and 25 °C, respectively. Metabolite peaks were identified by their exact mass and matching retention time to those of pure standards (Sigma-Aldrich).

2.3.6 RNA extraction and northern analysis

For northern expression analysis of *trpE* and *icsA* in *A. fumigatus* wild-type AF293 at different time point, wild-type strain AF293 was grown in liquid glucose minimal media (GMM) (replacing nitrate with 20mM glutamine as nitrogen source) at 37 °C and 250 rpm for 24 h. Then mycelia were collected, transferred into solid GMM and grown in duplicates for the indicated time at 29 °C. To verify over-expression of *icsA* via northern blot, TPMW1.13 (Δ*icsA*), TPMW1.70 (OE::*icsA*) and the complemented strain TJW55.2 were grown in liquid GMM at 37 °C and 250 rpm for 24 h. For northern analysis, strains TPMW8.9 ($trpE^{C}$), TPMW9.5 ($trpE^{S77L}$), TPMW10.9 ($trpE^{S66R,S77L}$) and the complemented control strain TJW55.2 were inoculated into 50 mL of liquid GMM containing 20mM glutamine as nitrogen source as indicated in the text according to Schrettl et al. (32). Strains were grown for 24 h at 37 °C, 250 rpm with an initial spore concentration of 10^6 conidia per mL. Mycelia were harvested by filtration through Miracloth (Calbiochem) and 2 g of

mycelia were transferred into 50 mL of liquid GMM and GMM supplemented with 5mM L-tryptophan, respectively. Strains were grown in duplicates for 1 h at 29 °C and 250 rpm. Mycelia were harvested by filtration through Miracloth. Total RNA was extracted with Trizol reagent (Invitrogen) from freeze-dried mycelia, according to the manufacturer's protocol. Northern analysis was performed as described by Sambrook and Russell (19). Northern analysis for *trpE* used *trpE* probe SB1 (primers DAf6g12580F1 and DAf6g12580R2), for *icsA* used *icsA* probe SB3 (primer pair DAfu6gF1/DAfu6gR2). Other probes for northern analysis were constructed using primers listed in Table S2 and labeled with dCTP αP^{32}.

2.3.7 Secondary metabolite extraction and chromatography

Secondary metabolites of strains were extracted after 6 days of growth at 29 °C on solidified GMM and GMM supplemented with 5 mM L-tryptophan, respectively. Strains were point-inoculated onto the media at 10^4 conidia total (in 5 µL). Agar cores (1.5 cm in diameter) were prepared in triplicate for each strain cultured. Three cores from each plate were extracted with 2.5 mL of ethyl acetate. The solvent was evaporated and suspended in 500 µL 19.5/79.5/1 (v/v/v) acetonitrile/water/formic acid. Subsequently, the samples were filtered using a 0.45 µm PTFE Mini-UniPrep filter vial (Agilent) and 50 µL of the filtrate analyzed by high-performance liquid chromatography (HPLC) (Perkin Elmer) coupled to a photo diode array (PDA) as described by Wiemann et al. (33). Fq quantification was performed as described by Ames and Walsh (5).

2.4 Results

2.4.1 The *A. fumigatus* genome contains a canonical anthranilate synthase and a putative isochorismate synthase.

When characterizing the fmq cluster (4, 34), a putative anthranilate synthase subunit I (AAS-I), Afu6g12110, was found 8.3 kb downstream of the fmq gene cluster (Fig. 1A). Considering the

requirement for both L-tryptophan and anthranilate for Fq synthesis (Fig. 1B), it seemed reasonable that Afu6g12110 could be involved in synthesis of both amino acids. Further analysis of the genome, however, revealed a canonical AAS-I, Afu6g12580, which was present in region of co-linearity in all sequenced Aspergillus species. In contrast genes displaying significant homology to Afu6g12110 were only detected in a subset of Aspergillus species located at dispersed genomic locations (http://www.aspergillusgenome.org). A comparison of the two proteins indicated they shared 30% identity (E value=$6x10^{-23}$), primarily along the conserved chorismate binding domain. As a first step toward determining the function of the two potential anthranilate synthases in *A. fumigatus*, a phylogenetic tree was created. Our results show that Afu6g12580, is closely related to characterized AAS-I of fungi including A. nidulans, Neurospora crassa, and *S. cerevisiae* (Fig. 3) and thus was named TrpE following terminology used in A. nidulans. By contrast, the protein sequence of Afu6g12110 was most closely related to bacterial isochorismate synthases (Fig. 3) and named IcsA for isochorismate synthase. Notably IcsA lacked the feedback inhibition domain found in TrpE and all known AAS-I (Fig. 4A) but contained a chorismate binding domain also found in PabaA (Afu6g04820). Under culture conditions with nitrate as sole nitrogen source, *trpE* but not *icsA* was strongly expressed (Fig. 4B).

To determine if these proteins were required for tryptophan biosynthesis, we deleted and over-expressed both genes in the *A. fumigatus* AF293 genetic background. Southern analysis and Northern analysis of transformants for each gene identified correct gene replacement and over-expression constructs for both genes (Figs. S1-4). One representative deletion mutant for each gene, TPMW12.4 (Δ*trpE*) and TPMW1.13 (Δ*icsA*), one representative over-expression (OE) strain, TPMW8.9 (*trpE*^{C}) and TPMW1.70 (OE::*icsA*), as well as the double mutants TPMW7.14 (Δ*trpE* Δ*icsA*) and TPMW11.18 (Δ*trpE* OE::*icsA*) were chosen for further studies (Table 2). The

Δ*trpE* mutant could not grow unless supplemented with L-tryptophan. Complementation of Δ*trpE* with a *trpE* allele restored wild-type-like growth (Fig. 5A). In contrast neither the Δ*icsA* nor the OE::*icsA* strains exhibited a phenotypical difference to the respective control strains on any media examined in this study (Fig. 5A and Fig. S5). Furthermore, the OE::*icsA* allele could not complement the tryptophan auxotrophy of Δ*trpE* (Fig. 5A) thus suggesting that *icsA* played no major role in tryptophan or anthranilate biosynthesis.

2.4.2 TrpE feedback mutants exhibit increased production of anthranilate and fumiquinazolines FqF and FqC and IcsA mutants alter amino acid pools

To create feedback insensitive mutants in *A. fumigatus*, we first aligned the TrpE sequence with known AAS-I proteins and readily located the amino acids involved in feedback inhibition (Fig. 5B). Two mutant alleles were created, one was designed to change serine residue 77 to leucine (S77L), and the other was designed to additionally change serine residue 66 to arginine (S66R). These residues were chosen as they have been shown essential for tryptophan feedback inhibition in yeast (13) and some plants (11, 35). Transformation of the Δ*trpE* strain with a wild-type and these two mutant *trpE* alleles, respectively, yielded three strains TPMW8.9 ($trpE^{C}$), TPMW9.5 ($trpE^{S77L}$) and TPMW10.9 ($trpE^{S66R,S77L}$) for comparison of aromatic acid metabolism and Fq synthesis (Fig. S2).

Although there were no significant differences in growth or sporulation among the three strains on either GMM or GMM supplemented with 5 mM L-tryptophan (Fig. 5C), we observed a large intracellular buildup of anthranilate (ca. 120 fold vs. control strain $trpE^{C}$) in the feedback mutant $trpE^{S77L}$ grown on GMM medium (Fig. 6A). The substantial increase in intracellular anthranilate was consistent with the loss of tryptophan feedback in this enzyme, which resulted in the increased biosynthesis of the related intermediates. In agreement with this, we also observed increased

tryptophan levels (4 fold) in the *trpE*^{S77L} mutant. Surprisingly, we also found that p-aminobenzoate (7 fold) and to a small extent phenylalanine (1.4 fold) were increased in this mutant. The *trpE*^{S66R,S77L} feedback mutant displayed smaller but still significant increased levels of anthranilate (ca. 13 fold) and p-aminobenzoate (5.5 fold). Examination of Fq production in these three strains showed that FqC and FqF production was significantly increased by 1.3-1.8 fold in both feedback mutants grown on GMM medium (Fig. 6A).

We then assessed the metabolome of the *icsA* mutants. Although there was no significant impact of either mutant on Fq production, deletion of *icsA* resulted in a significant increase in phenylalanine and tyrosine levels (as well as alanine) whereas OE::*icsA* exhibited significantly decreased anthranilate, L-tryptophan, L-phenylalanine, and L-tyrosine levels (Fig. 6B). Together this data suggested that IcsA metabolizes chorismate into a yet unknown metabolite thereby making the common substrate less available for TrpE and AroC, respectively (Fig. 2).

To assess if the TrpE feedback mutants could be pushed to further increase Fq production, media was supplemented with L-tryptophan. We found this treatment primarily restored metabolite levels of the feedback mutants to those of wild type. There were no differences between wild type and the *trpE*^{S66R,S77L} mutant (Fig. 6C). The *trpE*^{S77L} mutant still accumulated significantly more anthranilate, p-aminobenzoate and phenylalanine than wild type but at much less fold than in GMM medium. Furthermore, in contrast to results on GMM, this mutant produced less FqC and FqF than wild type (Fig. 6C). Finally, two tryptophan degradation products, L-kynurenine and indolepyruvate were detected in all three strains grown on tryptophan medium. The single site mutant produced significantly more L-kynurenine than either the wild type or the double site mutant, possibly suggesting that increases in L-kynurenine production could be related to decreases in Fq production (Fig. 6C).

2.4.3 Transcriptional profiling of tryptophan metabolism genes

To help interpret the changes in primary and secondary metabolite synthesis on GMM and GMM supplemented with L-tryptophan, we next examined a transcriptional profile of L-tryptophan metabolic genes in both GMM and GMM medium supplemented with L-tryptophan for the two feedback mutants (*trpE*^{S77L} and *trpE*^{S66R,S77L}) and complemented control *trpE*^{C} (Fig. 7). Genes were identified through blast analysis using characterized genes from tryptophan metabolic enzymes in *S. cerevisiae* and KEGG L-tryptophan metabolism (http://www.genome.jp/kegg/pathway.html) to identify putative genes and encoded proteins illustrated in Fig. 2 and Table 1.

Chorismate is a common precursor for metabolic pathways leading to the formation of L-tryptophan, p-aminobenzoate, salicylate and L-phenylalanine/L-tyrosine in microbes and plants (6, 36, 37). Four putative enzymes, encoded by pabaA, aroC, *icsA*, and *trpE*/*trpC* (Fig. 2, Table 1), theoretically could compete for and utilize chorismate as a substrate to catalyze the committed step of the respective pathways to produce p-aminobenzoate, L-phenylalanine/L-tyrosine, isochorismate, and L-tryptophan in *A. fumigatus* (Fig. 2). Although we did not detect isochorimate in our analysis, over-expression of *icsA* decreased anthranilate, L-tryptophan, L-phenylalanine, and L-tyrosine levels suggesting that IcsA can reduce the cellular chorismate pool (Fig. 6B). Furthermore, our metabolic data (Fig. 6) supported the activities of the other enzymes and suggested that pabaA and aroC may be up-regulated in the feedback-domain site mutants grown on GMM medium. However, this was not borne out at the transcriptional level as there were no differences in pabaA or aroC expression between the wild type and feedback mutants in either GMM or L-tryptophan supplemented medium (Fig. 7). In fact, there were no differences in gene expression between these three strains for any of the genes assessed.

Tryptophan supplementation, however, did impact gene expression. Two putative L-tryptophan degradation genes, aroH and idoB were highly up-regulated in all three strains (Fig. 7). aroH (Afu2g13630) encodes a putative aromatic aminotransferase involved in transamination of L-tryptophan to generate indolepyruvate and idoB (Afu4g09830) encodes a putative indoleamine 2,3-dioxygenase which could be involved in dioxygenation of L-tryptophan as the first step to produce L-kynurenine. This matched well with production of these two products by *A. fumigatus* grown on L-tryptophan supplemented medium (Fig. 6B). Two other genes, Afu3g14250 and Afu7g02010, also encode putative indoleamine 2,3-dioxygenases with Afu7g02010 weakly expressed under these conditions. Based on the phylogenetic analysis of indoleamine 2,3-dioxygenases (Fig. S6), we name these genes idoA (Afu3g14250), idoB (Afu4g09830), and idoC (Afu7g02010). L-tryptophan supplementation also affected *trpC* expression (increased) and trpB (decreased) but had no impact on expression of cpcA, encoding the ortholog of Gcn4p in yeast, the transcription factor globally modulating Aspergillus spp. amino acid biosynthesis (38).

2.5 Discussion

Aspergillus fumigatus is an opportunistic human pathogen renowned for its secondary metabolites that are thought to contribute to disease development (39). The fumiquinazolines are signature metabolites of *A. fumigatus* and comprise a family of cytotoxic peptidyl alkaloids, which have received considerable interest due to their complex biochemistry, antitumor properties and cellular localization (4, 34, 40) but until now, nothing is known of the effect of primary metabolism on their biosynthesis. Here our efforts focused on the effect of manipulating tryptophan biosynthesis on Fq production.

Anthranilate is a non-proteinogenic aryl β-amino acid generated from enzymatic amination of chorismate by anthranilate synthases (ASs), and serves as the framework for the indole ring of the

amino acid L-tryptophan (5). Along with L-tryptophan, anthranilate is incorporated into several fungal peptidyl alkaloids including Fq, the benzodiazepine dione, ardeemin and asperlicin (5, 41). AS consists of two subunits, anthranilate synthase subunit I (AAS-I) termed TrpE as described here, and AAS-II termed TrpC (16), respectively in Aspergillus species. We found *trpE* was present in a region of co-linearity in all sequenced Aspergillus spp. while a second protein, IcsA, encoded by a gene near the fmq cluster and with considerable homology to TrpE was more closely related to bacterial isochorismate synthases and lacked the tryptophan feedback domain found in TrpE and all known AAS-I (Figs. 3 and 4A). The Δ*trpE* mutant required exogenous L-tryptophan for growth and could not be rescued by OE::*icsA*. However, over-expression of *icsA* decreased anthranilate, L-tryptophan, L-phenylalanine, and L-tyrosine levels suggesting that IcsA can draw from the cellular chorismate pool (Fig. 6B). A protein alignment of the *A. fumigatus* IcsA and TrpE with characterized bacterial ASS-I and isochorismate synthases revealed that important residues that changed enzymatic activity of the Salmonella typhimorium ASS-I from producing anthranilate to isochorismate (42) are identical to the *A. fumigatus* IcsA, suggesting that it likely is responsible for isochorismate formation although we did not identify this metabolite in our study. Identification of the putative IcsA metabolic product will be a future task.

The bacterium Pseudomonas aeruginosa possesses two ASs, TrpEG and PhnAB (7). Although only the former and not the latter is required for L-tryptophan biosynthesis in P. aeruginosa, over-expression of phnAB can rescue a *trpE*G deletion. A third protein harboring a chorismate binding domain is bifunctional PchA in P. aeruginosa (Fig. 3) and was shown to be involved in isochorismate and subsequently salicylic acid production, that is incorporated into the bacterium's siderophores, mediating iron uptake (43). Based on the chorismate binding domains, IcsA from *A. fumigatus* is closely related to MbtI from Mycobacterium tuberculosis (Fig. 3), that is also

responsible for salicylic acid formation (44). *Escherichia coli* harbors two enzymes, EntC and MenF, that are responsible for isochorismate production (45), that also group with IcsA in our analysis (Fig. 3). Bioinformatic analysis shows some but not all Aspergilli contain putative IcsA homologs, all missing the feedback domain and often located near secondary metabolite clusters. Although fungal siderophores do not contain salicylic acid or isochorismate (46), *A. fumigatus* was shown to produce at least one other amino acid-derived small molecule with iron binding abilities (33, 47). What the role, if any, IcsA-like proteins play in fungal physiology has yet to be elucidated. The importance of the feedback regulation of AS in the control of metabolic flow in L-tryptophan production and secondary metabolites has been demonstrated in many plants expressing feedback-resistant AS genes (11, 12, 14, 15, 48-50). Here, inactivation of the putative feedback domain in TrpE of *A. fumigatus* also had a significant effect on aromatic amino acid metabolism and Fq production with the single mutation strain *trpE*^{S77L} consistently having a greater impact on metabolism than the double site mutant. It was only this mutant which showed a significant increase in L-tryptophan pools, similar to reports of increased L-tryptophan pools in feedback mutants in plants (12, 14, 49, 50). This same strain also showed modest but significant increases in one of the two other aromatic amino acids, L-phenylalanine (Fig. 6A). As Fqs contain L-alanine, L-tryptophan, and anthranilate, the decreased L-alanine was consistent with the increased Fqs. However, both feedback mutants showed large increases in anthranilate and p-aminobenzoate that possibly diverted precursor pools from fumiquinazolines as reflected by the modest increases in FqF and FqC when grown on minimal medium (Fig. 6A). p-aminobenzoate is synthesized by PabaA and PabaB (Fig. 2 and Table 1) in Aspergillus spp. and strains with inactivation of either gene require p-aminobenzoate for growth (51-53). Possibly less efficient versions of these enzymes could reduce p-aminobenzoate accumulation and enhance Fq synthesis. Studies in E. coli

and Arabidopsis thaliana have shown that the p-aminobenzoate synthase complex is not inhibited by tryptophan, but by 2-fluorochorismate and methotrexate, respectively (54-56). Whether or not these or analogous inhibitors could direct metabolite flux towards Fq biosynthesis in *A. fumigatus* could be explored in future studies.

An interesting finding was that supplementation with tryptophan restored metabolite levels in the TrpE feedback mutants to those near the control strain. This suggests that there is an additional regulatory control mechanism(s) for tryptophan synthesis other than anthranilate synthase that is controlled differentially by externally added tryptophan and tryptophan produced by *A. fumigatus* itself. Intracellular amino acid pools are stored in vacuoles (57) and their accessibility will differ from supplementation from external sources. Our data allude to different intra- and extracellular amino tryptophan sensing mechanisms in *A. fumigatus*, supporting a hypothesis of distinct nitrogen sensing mechanisms in other filamentous fungi (58, 59). Our expression profiling data suggests that several tryptophan degradation pathways could be important in this regard (Fig. 7). The decrease of FqF and FqC in the TrpE single feedback mutant grown on L-tryptophan amended medium may be reflective of not only differential regulatory mechanisms and diversion of chorismate to p-aminobenzoate and L-phenylalanine but also to the increase in the degradation product L-kynurenine (Fig. 6C).

L-kynurenine is produced by indoleamine 2,3-dioxygenase (Ido) activity. Whereas *S. cerevisiae* has a single Ido gene (BNA2) (60), *A. fumigatus*, like many other filamentous Ascomycetes, possesses three putative Ido genes, idoA (Afu3g14250), idoB (Afu4g09830) and idoC (Afu7g02010) (Fig. 2 and Table 1) in its genome (31). One of them, idoB, was highly induced and a second, idoC, slightly induced by external L-tryptophan (Fig. 7). Enzymatic studies of A. oryzae Ido enzymes suggest two of the three enzymes, Idoα and Idoβ, may participate in tryptophan

degradation (29). The Idoα showed higher activity and lower K_m values (higher affinity for substrates), similar to the enzymatic properties of Bna2p in *S. cerevisiae* (29, 30). However, idoA, the homolog of A. oryzae idoα, was not induced by tryptophan under our conditions (Fig. 7). Instead idoB, the homolog of A. oryzae idoβ was most highly induced by L-tryptophan. The third Ido in A. oryzae, Idoγ, had a closer relationship to bacterial Idos than fungal Idos (Fig. S6) and showed very high K_m values (low affinity for substrates) and low catalytic efficiencies for L-tryptophan (30). idoC, the homolog of idoγ, was slightly induced by L-tryptophan. Our data suggests that *A. fumigatus* idoB is mostly likely to contribute to L-kynurenine production.

L-tryptophan can also be metabolized via the indolepyruvate pathway. AroH (termed Aro8 in *S. cerevisiae* (61) is a key enzyme in the transamination of L-tryptophan to generate indolepyruvate and aroH was highly induced by L-tryptophan feeding. Similar to *S. cerevisiae*, AroH could also participates in L-phenylalanine and L-tyrosine synthesis in *A. fumigatus* (Fig. 2) and therefore could direct metabolite pools to L-phenylalanine and L-tyrosine as well as towards L-tryptophan degradation. Thus it is likely that both AroH and IdoB activities could divert pathways from fumiquinazoline synthesis, a hypothesis we will explore in future studies.

In summary, we have genetically characterized two putative *A. fumigatus* chorismate binding proteins, TrpE and IcsA. TrpE was required for L-tryptophan production and its deletion results in tryptophan auxotroph, and over-expression of the fmq-cluster-associated gene (*icsA*/Afu6g12110) could not complement the tryptophan auxotroph of deletion *trpE* mutant or significantly change the Fq production. However, deletion and over-expression of *icsA* resulted in significantly changed anthranilate, L-tryptophan, L-phenylalanine, and L-tyrosine levels, suggesting that IcsA metabolizes chorismate into a yet unknown product in *A. fumigatus*. Synthetic feedback resistant alleles of TrpE had a significant effect in aromatic amino acid metabolism, resulting in anthranilate

and L-tryptophan accumulation and modest increases in Fq synthesis on minimal growth medium. Inhibition of tryptophan-feedback effect in TrpE eliminated a roadblock during anthranilate biosynthesis, as a conduit to increase the anthranilate and tryptophan related secondary metabolism in *A. fumigatus*.

2.6 Acknowledgements

P.M.W. was supported by grant from the National Natural Science Foundation of China NSFC No. 41406141 and NIH (R01 AI065728) to N.P.K.

2.7 Tables

Table 1. *Aspergillus fumigatus* tryptophan metabolism genes and putative protein function

Alias	Protein	Ortholog in *S. cerevisiae*	GenBank accession	EC number	Protein function[a]
Tryptophan biosynthesis					
Afu1g13740	AroM	Aro1	XM_747651	2.7.1.71	Shikimate kinase
Afu1g13740	AroM	Aro1		2.5.1.19	EPSP[b] synthase
Afu1g06940	AroB	Aro2	XM_745350	4.2.3.5	Chorismate synthase
Afu6g12580	TrpE	Trp2	XM_746043	4.1.3.27	Anthranilate synthase
Afu1g13090	TrpC	Trp3	XM_747586		
Afu4g11980	TrpD	Trp4	XM_746540	2.4.2.18	Anthranilate phosphoribosyltransferase
Afu1g13090	TrpC	Trp1	XM_747586	5.3.1.24	Phosphoribosylanthranilate isomerase
Afu1g13090	TrpC	Trp3	XM_747586	4.1.1.48	Indoyl-glycerolphosphate synthase
Afu2g13250	TrpB	Trp5	XM_750564	4.2.1.20	Tryptophan synthase
Chorismate branch					
Afu6g04820	PabaA	Abz1	XM_742503	2.6.1.85	ADC[b] synthetase
Afu2g01650	PabaB	Abz2	XM_744207	4.1.3.38	ADC[b] lyase
Afu6g12110	IcsA	-	XM_745997	5.4.4.2	Isochorismate synthase
Afu5g13130	AroC	Aro7	XM_748248	5.4.99.5	Chorismate mutase
Tryptophan degradation					
Afu2g13630	AroH	Aro8	XM_750603	2.6.1.27 2.6.1.57	Aromatic amino acid transaminase
Afu3g14250	IdoA	Bna2	XM_749108	1.13.11.52	Indoleamine 2,3-dioxygenases
Afu4g09830	IdoB	Bna2	XM_746750		
Afu7g02010	IdoC	Bna2	XM_741638		

[a] Prediction of protein function based on AspGD (http://www.aspgd.org/) and KEGG (http://www.genome.jp/kegg/)

[b] Abbreviation: EPSP synthase, enolpyruvylshikimate-3-phosphate synthase; ADC, 4-Amino-4-deoxychorismate.

Table 2. Fungal strains used in this study

Name	ID	Parental strain	Genotype	Reference
AF293			Wild-type	(17)
AF293.1		AF293	pyrG1	(17)
AF293.1 comp	TJW55.2	AF293.1	A.p.pyrG	(62)
Δ*icsA*	TPMW1.13	AF293.1	Δ*icsA*::A.p.pyrG	This study
OE::*icsA*	TPMW1.70	AF293.1	gpdA(p)::*icsA*::A.p.pyrG	This study
AF293.6		AF293.1	pyrG1; argB1	(63)
Δ*trpE* pyrG-	TPMW6.2	AF293.6	Δ*trpE*::argB; pyrG1	This study
Δ*trpE*	TPMW12.4	TPMW6.2	Δ*trpE*::argB; A.p.pyrG	This study
Δ*trpE* Δ*icsA*	TPMW7.14	TPMW6.2	Δ*trpE*::argB; Δ*icsA*::A.p.pyrG	This study
Δ*trpE* OE::*icsA*	TPMW11.18	TPMW6.2	Δ*trpE*::argB; gpdA(p)::*icsA*::A.p.pyrG	This study
$trpE^{C}$	TPMW8.9	TPMW6.2	gpdA(p)::$trpE^{C}$::A.p.pyrG; Δ*trpE*::argB	This study
$trpE^{S77L}$	TPMW9.5	TPMW6.2	gpdA(p)::$trpE^{S77L}$::A.p.pyrG; Δ*trpE*::argB	This study
$trpE^{S66R,S77L}$	TPMW10.9	TPMW6.2	gpdA(p)::$trpE^{S66R,S77L}$::A.p.pyrG; Δ*trpE*::argB	This study

2.8 Figures

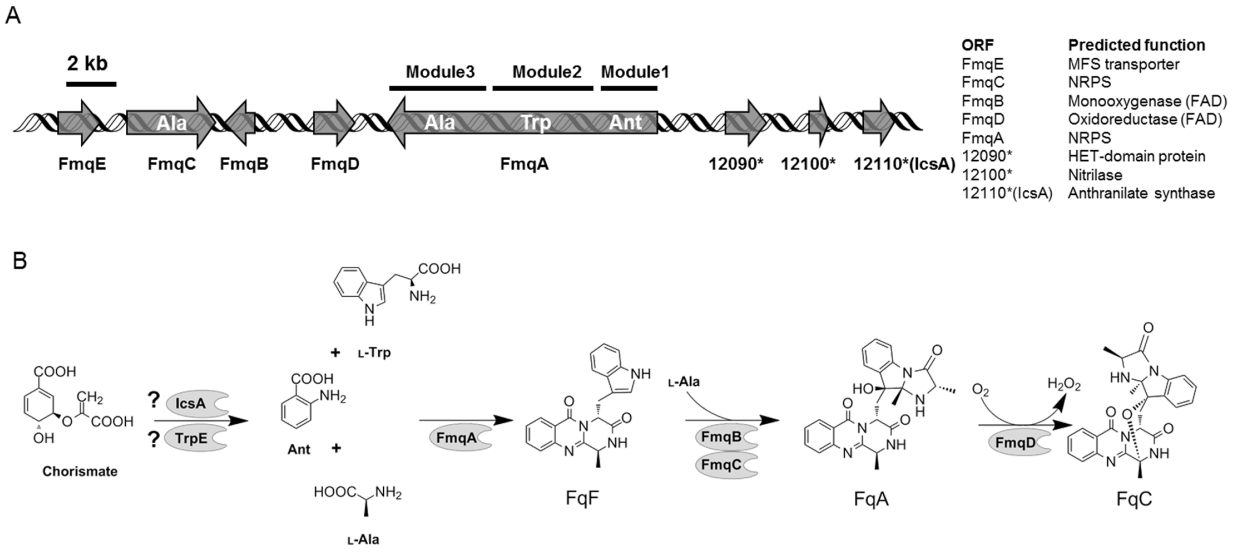

Figure 1. Fumiquinazoline biosynthesis in *A. fumigatus*. (Modified from that of Ames et al. (4) and Lim et al.(34))

(A) Fumiquinazoline gene cluster in *A. fumigatus* with nearby putative anthranilate synthase gene Afu6g12110 (*icsA*). * Abbreviation: 12090, Afu6g12090; 12100, Afu6g12100; 12110, Afu6g12110.
(B) Biosynthetic route of fumiquinazolines in *A. fumigatus*. Abbreviations: Ant, anthranilate; L-Trp, L-tryptophan; L-Ala, L-alanine; FqF, fumiquinazoline F; FqA, fumiquinazoline A; FqC, fumiquinazoline C.

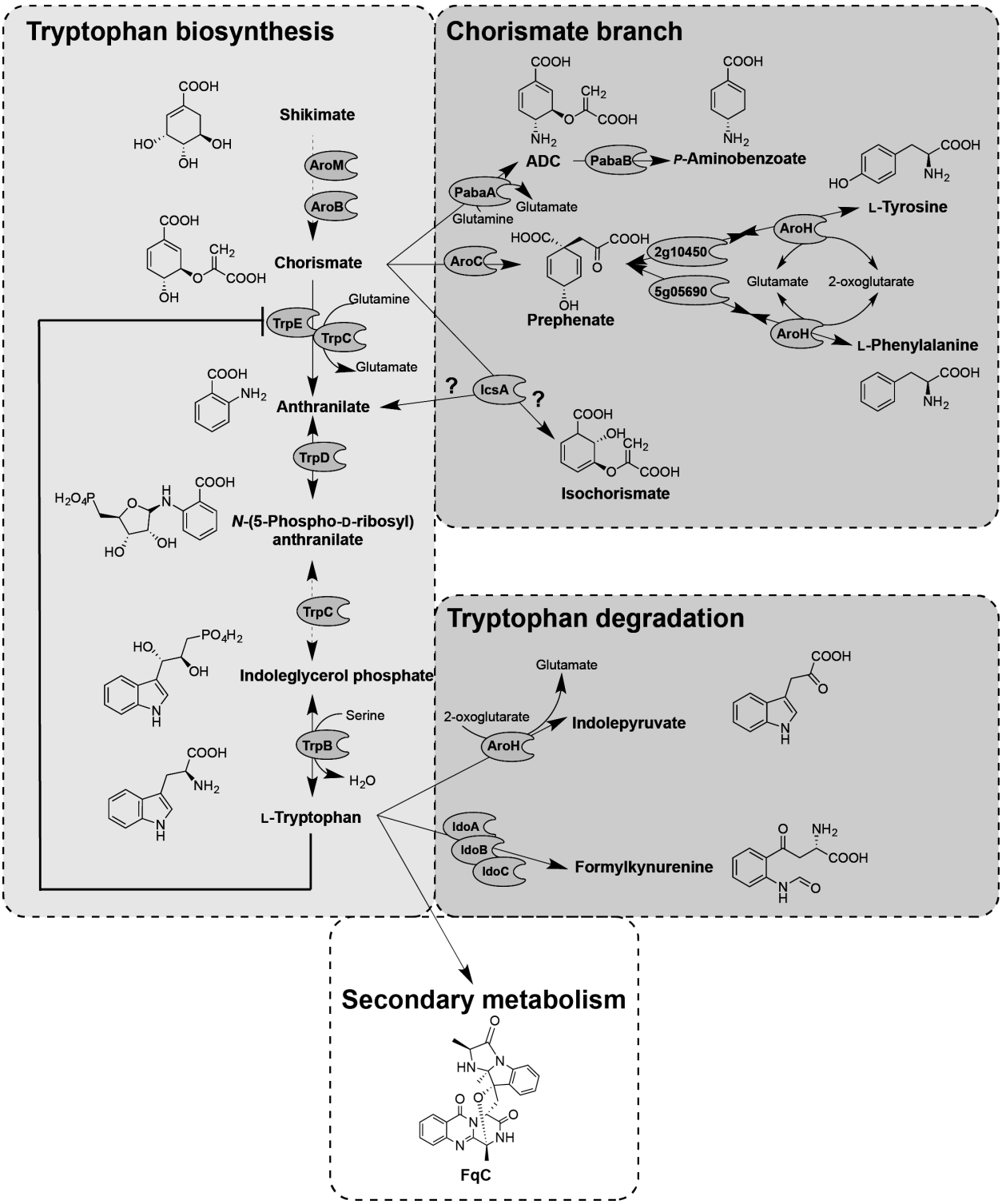

Figure 2. Schematic outline of the L-tryptophan metabolism and regulation of enzyme in *A. fumigatus*.

Enzymes are indicated by their gene designations: AroM (Afu1g13740), shikimate kinase (EC:2.7.1.71), EPSP synthase (EC:2.5.1.19); AroB (Afu1g06940), chorismate synthase

(EC:4.2.3.5); TrpC (Afu1g13090), TrpE (Afu6g12580), anthranilate synthase (EC:4.1.3.27); TrpD (Afu4g11980), anthranilate phosphoribosyltransferase (EC:2.4.2.18); TrpC (Afu1g13090), phosphoribosylanthranilate isomerase (EC:5.3.1.24), indole-3-glycerol-phosphate synthase (EC:4.1.1.48); TrpB (Afu2g13250), tryptophan synthase (EC:4.2.1.20); PabaA (Afu6g04820), ADC synthetase (EC:2.6.1.85); PabaB (Afu2g01650), ADC lyase (4.1.3.38); AroC (Afu5g13130), chorismate mutase (EC:5.4.99.5); 2g10450 (Afu2g10450), prephenate dehydrogenase (EC:1.3.1.13); 5g05690 (Afu5g05690), prephenate dehydratase (EC:4.2.1.51); AroH (Afu2g13630), aromatic aminotransferase (EC:2.6.1.27; 2.6.1.57; 2.6.1.58); IcsA (Afu6g12110), isochorismate synthetase (EC:5.4.4.2); IdoA (Afu3g14250), IdoB (Afu4g09830), IdoC (Afu7g02010), indoleamine 2,3-dioxygenase (EC:1.13.11.52). Abbreviations: EPSP, enolpyruvylshikimate-3-phosphate; ADC, 4-Amino-4-deoxychorismate.

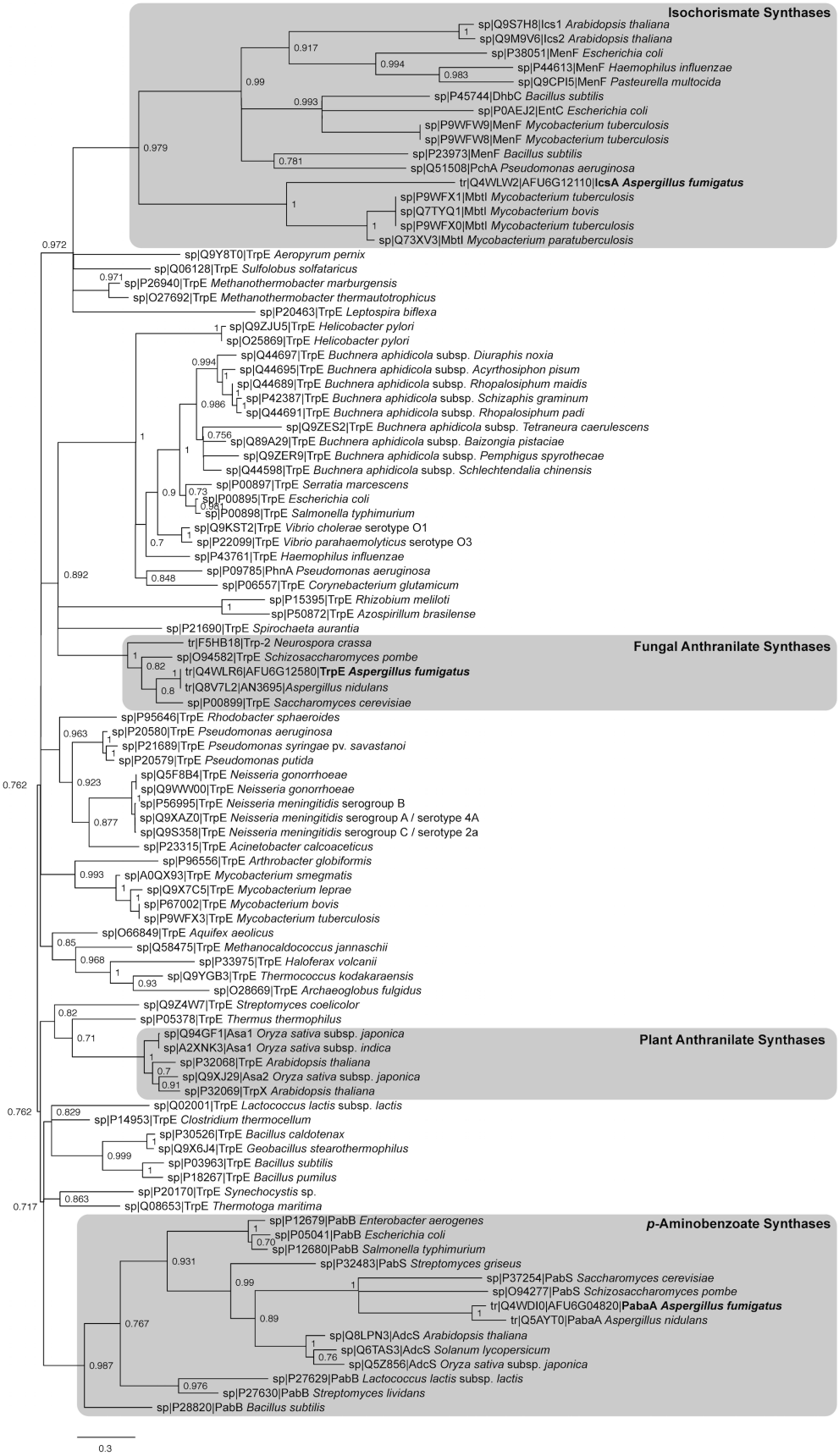
Isochorismate Synthases
sp|Q9S7H8|Ics1 Arabidopsis thaliana
sp|Q9M9V6|Ics2 Arabidopsis thaliana
sp|P38051|MenF Escherichia coli
sp|P44613|MenF Haemophilus influenzae
sp|Q9CPI5|MenF Pasteurella multocida
sp|P45744|DhbC Bacillus subtilis
sp|P0AEJ2|EntC Escherichia coli
sp|P9WFW9|MenF Mycobacterium tuberculosis
sp|P9WFW8|MenF Mycobacterium tuberculosis
sp|P23973|MenF Bacillus subtilis
sp|Q51508|PchA Pseudomonas aeruginosa
tr|Q4WLW2|AFU6G12110|IcsA Aspergillus fumigatus
sp|P9WFX1|MbtI Mycobacterium tuberculosis
sp|Q7TYQ1|MbtI Mycobacterium bovis
sp|P9WFX0|MbtI Mycobacterium tuberculosis
sp|Q73XV3|MbtI Mycobacterium paratuberculosis
sp|Q9Y8T0|TrpE Aeropyrum pernix
sp|Q06128|TrpE Sulfolobus solfataricus
sp|P26940|TrpE Methanothermobacter marburgensis
sp|O27692|TrpE Methanothermobacter thermautotrophicus
sp|P20463|TrpE Leptospira biflexa
sp|Q9ZJU5|TrpE Helicobacter pylori
sp|O25869|TrpE Helicobacter pylori
sp|Q44697|TrpE Buchnera aphidicola subsp. Diuraphis noxia
sp|Q44695|TrpE Buchnera aphidicola subsp. Acyrthosiphon pisum
sp|Q44689|TrpE Buchnera aphidicola subsp. Rhopalosiphum maidis
sp|P42387|TrpE Buchnera aphidicola subsp. Schizaphis graminum
sp|Q44691|TrpE Buchnera aphidicola subsp. Rhopalosiphum padi
sp|Q9ZES2|TrpE Buchnera aphidicola subsp. Tetraneura caerulescens
sp|Q89A29|TrpE Buchnera aphidicola subsp. Baizongia pistaciae
sp|Q9ZER9|TrpE Buchnera aphidicola subsp. Pemphigus spyrothecae
sp|Q44598|TrpE Buchnera aphidicola subsp. Schlechtendalia chinensis
sp|P00897|TrpE Serratia marcescens
sp|P00895|TrpE Escherichia coli
sp|P00898|TrpE Salmonella typhimurium
sp|Q9KST2|TrpE Vibrio cholerae serotype O1
sp|P22099|TrpE Vibrio parahaemolyticus serotype O3
sp|P43761|TrpE Haemophilus influenzae
sp|P09785|PhnA Pseudomonas aeruginosa
sp|P06557|TrpE Corynebacterium glutamicum
sp|P15395|TrpE Rhizobium meliloti
sp|P50872|TrpE Azospirillum brasilense
sp|P21690|TrpE Spirochaeta aurantia
Fungal Anthranilate Synthases
tr|F5HB18|Trp-2 Neurospora crassa
sp|O94582|TrpE Schizosaccharomyces pombe
tr|Q4WLR6|AFU6G12580|TrpE Aspergillus fumigatus
tr|Q8V7L2|AN3695|Aspergillus nidulans
sp|P00899|TrpE Saccharomyces cerevisiae
sp|P95646|TrpE Rhodobacter sphaeroides
sp|P20580|TrpE Pseudomonas aeruginosa
sp|P21689|TrpE Pseudomonas syringae pv. savastanoi
sp|P20579|TrpE Pseudomonas putida
sp|Q5F8B4|TrpE Neisseria gonorrhoeae
sp|Q9WW00|TrpE Neisseria gonorrhoeae
sp|P56995|TrpE Neisseria meningitidis serogroup B
sp|Q9XAZ0|TrpE Neisseria meningitidis serogroup A / serotype 4A
sp|Q9S358|TrpE Neisseria meningitidis serogroup C / serotype 2a
sp|P23315|TrpE Acinetobacter calcoaceticus
sp|P96556|TrpE Arthrobacter globiformis
sp|A0QX93|TrpE Mycobacterium smegmatis
sp|Q9X7C5|TrpE Mycobacterium leprae
sp|P67002|TrpE Mycobacterium bovis
sp|P9WFX3|TrpE Mycobacterium tuberculosis
sp|O66849|TrpE Aquifex aeolicus
sp|Q58475|TrpE Methanocaldococcus jannaschii
sp|P33975|TrpE Haloferax volcanii
sp|Q9YGB3|TrpE Thermococcus kodakaraensis
sp|O28669|TrpE Archaeoglobus fulgidus
sp|Q9Z4W7|TrpE Streptomyces coelicolor
sp|P05378|TrpE Thermus thermophilus
Plant Anthranilate Synthases
sp|Q94GF1|Asa1 Oryza sativa subsp. japonica
sp|A2XNK3|Asa1 Oryza sativa subsp. indica
sp|P32068|TrpE Arabidopsis thaliana
sp|Q9XJ29|Asa2 Oryza sativa subsp. japonica
sp|P32069|TrpX Arabidopsis thaliana
sp|Q02001|TrpE Lactococcus lactis subsp. lactis
sp|P14953|TrpE Clostridium thermocellum
sp|P30526|TrpE Bacillus caldotenax
sp|Q9X6J4|TrpE Geobacillus stearothermophilus
sp|P03963|TrpE Bacillus subtilis
sp|P18267|TrpE Bacillus pumilus
sp|P20170|TrpE Synechocystis sp.
sp|Q08653|TrpE Thermotoga maritima
p-Aminobenzoate Synthases
sp|P12679|PabB Enterobacter aerogenes
sp|P05041|PabB Escherichia coli
sp|P12680|PabB Salmonella typhimurium
sp|P32483|PabS Streptomyces griseus
sp|P37254|PabS Saccharomyces cerevisiae
sp|O94277|PabS Schizosaccharomyces pombe
tr|Q4WDI0|AFU6G04820|PabaA Aspergillus fumigatus
tr|Q5AYT0|PabaA Aspergillus nidulans
sp|Q8LPN3|AdcS Arabidopsis thaliana
sp|Q6TAS3|AdcS Solanum lycopersicum
sp|Q5Z856|AdcS Oryza sativa subsp. japonica
sp|P27629|PabB Lactococcus lactis subsp. lactis
sp|P27630|PabB Streptomyces lividans
sp|P28820|PabB Bacillus subtilis
0.3

Figure 3. Maximum likelihood phylogenetic analysis of chorismate-binding domains extracted from 99 characterized protein sequences.

Monophyletic leaves of relevant proteins are boxed in grey. *A. fumigatus* proteins are indicated in bold.

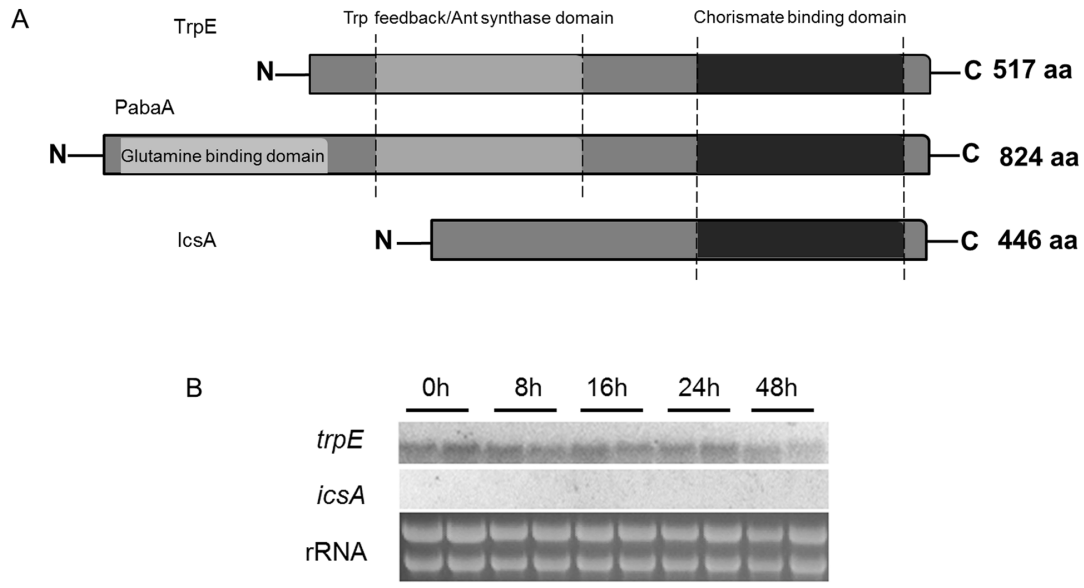

Figure 4. Domain architecture and expression analysis of chorismate-binding domain proteins in *A. fumigatus*.

(A) Domain comparison of *A. fumigatus* TrpE, PabaA and IcsA. Abbreviations: Ant, Anthranilate; Trp, Tryptophan.
(B) Northern expression analysis of *trpE* and *icsA* in *A. fumigatus* wild-type AF293. Ribosomal RNA was visualized by ethidium bromide staining as loading control. *A. fumigatus* strain AF293 was grown in liquid GMM containing 20mM glutamine as nitrogen source at 37 °C and 250 rpm for 24 h. Then mycelia were collected, transferred into solid GMM and grown in duplicates for the indicated time at 29 °C.

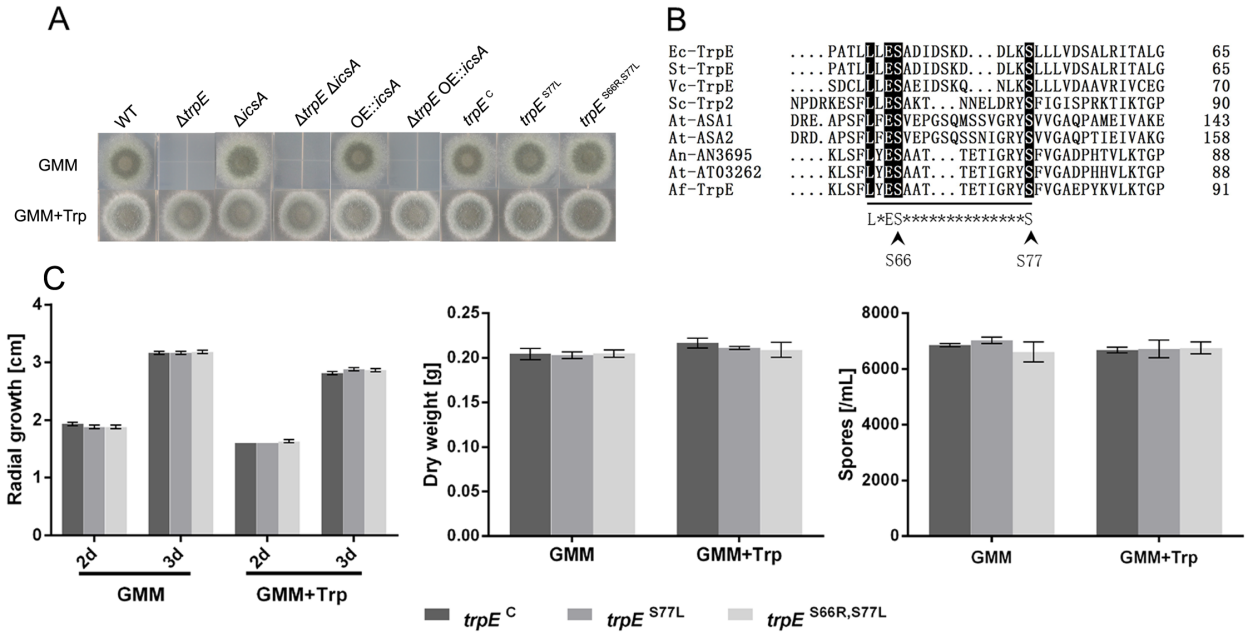

Figure 5. Physiological analysis of *A. fumigatus* mutants used in this study and the alignment of anthranilate synthases.

(A) Radial growth of the *A. fumigatus* wild-type strain (WT), Δ*trpE*, Δ*icsA*, double deletion mutant Δ*icsA*Δ*trpE*, *icsA* over-expression strain OE::*icsA*, double mutant Δ*trpE* OE::*icsA*, Δ*trpE* complemented strain $trpE^{C}$, and site mutants $trpE^{S77L}$ and $trpE^{S66R,S77L}$ and on solid GMM and GMM amended with 5mM L-tryptophan (Trp) medium at 37 °C.

(B) Alignment of the L*ES*$_n$S regions of anthranilate synthases from various organisms. The conserved motif is indicated on the bottom line. The sequences shown are: Ec-TrpE, *Escherichia coli* TrpE (CAA23666); St-TrpE, *Salmonella enterica* TrpE(WP_001194371); Vc-TrpE, *Vibrio cholerae* TrpE (WP_001030227); Sc-Trp2, *Saccharomyces cerevisiae* Trp2 (NP_011014); At-ASA1, *Arabidopsis thaliana* ASA1 (NP_001190231); At-ASA2, *Arabidopsis thaliana* ASA2 (NP_180530); An-AN3695, *Aspergillus nidulans* AN3695 (CBF75591); At-AT03262, *Aspergillus terreus* AT03262 (XP_001212440); Af-TrpE, *Aspergillus fumigatus* TrpE (XP_751136). Identical residues among the various proteins are indicated by dark shading, and respective amino acid residue numbers are shown at the C-termini. Arrows mark amino acids of Af-TrpE mutated in this study. (C) Quantification of radial growth on solid media GMM and GMM+5mM L-tryptophan (Trp) at 37 °C, dry weight of mycelia from culture in liquid medium GMM and GMM+5mM L-tryptophan (Trp) at 37 °C, and spore production on solid GMM and GMM+5mM L-tryptophan (Trp) at 37 °C. No phenotype was observed for tryptophan-feedback mutants $trpE^{S77L}$ and $trpE^{S66R,S77L}$ compared with $trpE^{C}$.

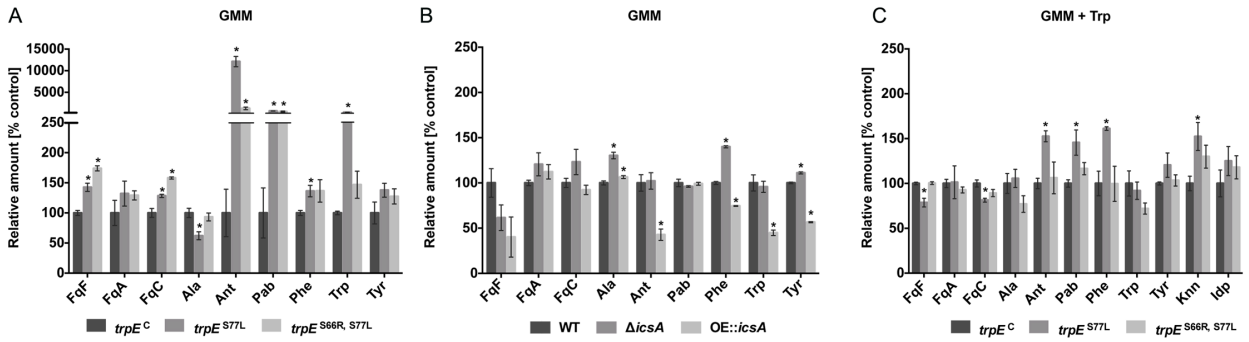

Figure 6. Primary metabolites and fumiquinazoline production in *A. fumigatus trpE* and *icsA* mutants.

(A) Comparison of primary metabolites and fumiquinazoline production in the complemented control strain *trpE*^{C} and the feedback site mutants *trpE*^{S77L} and *trpE*^{S66R,S77L} grown on GMM medium.
(B) Comparison of primary metabolites and fumiquinazoline production in wild-type control strain AF293.1 comp (TJW55.2) and *icsA* mutants grown on GMM medium.
(C) Comparison of primary metabolites and fumiquinazoline production in the complemented control strain *trpE*^{C} and the feedback site mutants *trpE*^{S77L} and *trpE*^{S66R,S77L} grown on GMM supplemented with 5mM L-tryptophan (Trp) medium.
The amounts of metabolites were normalized to the relative amount of the complemented control strain *trpE*^{C} (100%). Displayed are means ± SEM. Asterisk indicates $p < 0.05$ using an ANOVA test for statistical significance with Prism 6 software, comparing mutants to the control strain TJW55.2 or *trpE*^{C}.
Abbreviations: FqF, Fumiquinazoline F; FqC, Fumiquinazoline C; FqA, Fumiquinazoline A; Ala, L-alanine; Ant, Anthranilate; Pab, p-aminobenzoate; Phe, L-phenylalanine; Trp, L-tryptophan; Tyr, L-tyrosine; Knn, L-kynurenine ; Idp, Indolepyruvate.

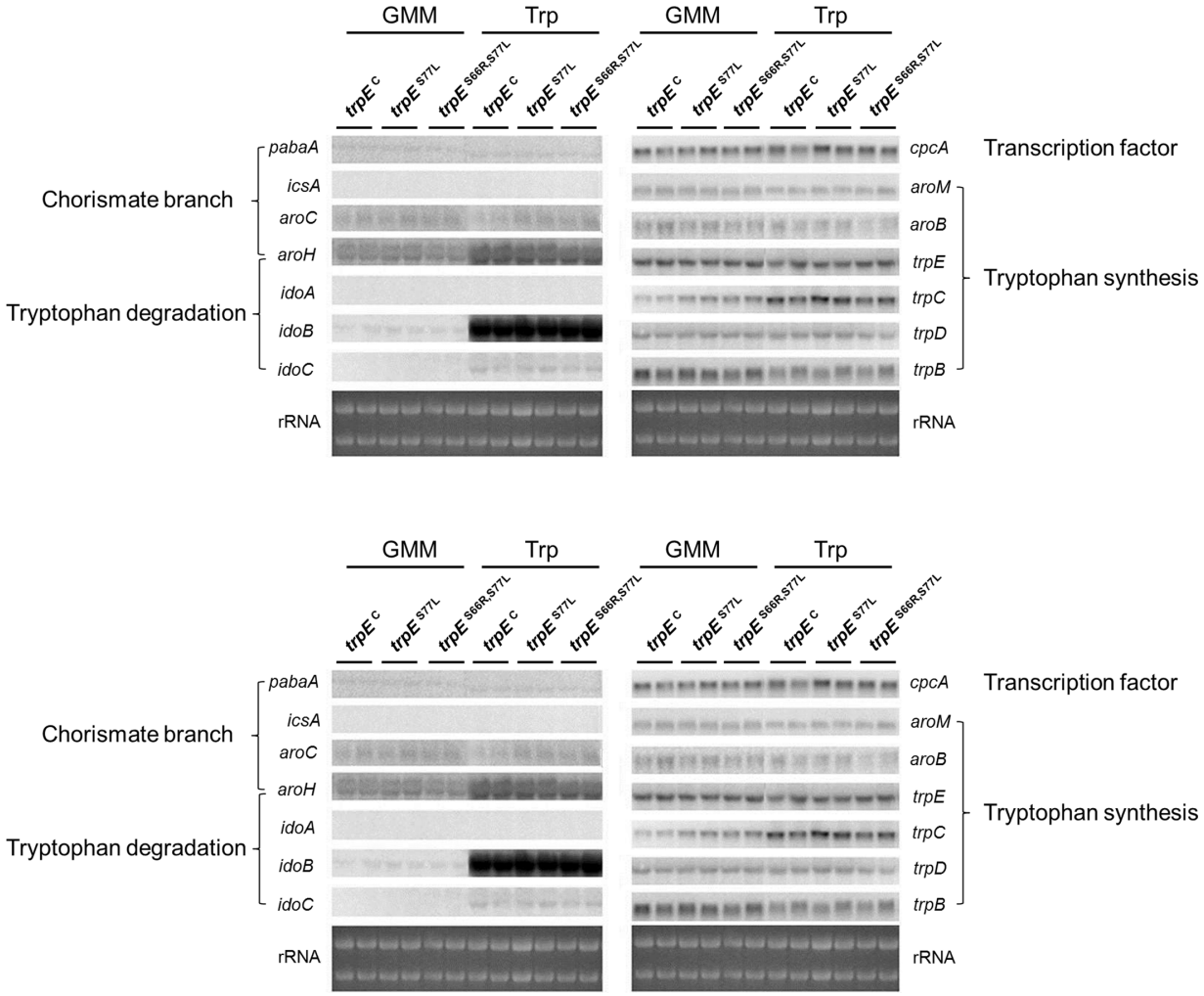

Figure 7. Northern expression analysis of genes related to tryptophan metabolism.
Northern expression analysis of indicated genes comparing the *A. fumigatus* Δ*trpE* complemented strain *trpE*^{C}, the *trpE* tryptophan-feedback mutant *trpE*^{S77L}, and *trpE*^{S66R,S77L}. Ribosomal RNA was visualized by ethidium bromide staining as loading control. The indicated strains were grown in liquid glucose minimal media (GMM) (replacing nitrate with 20 mM glutamine as sole nitrogen source) at 37 °C and 250 rpm for 24 h. After the initial incubation period, 2 g of mycelia were transferred into liquid GMM and GMM supplemented with 5mM L-tryptophan (Trp), respectively. The indicated strains were grown in duplicates for 1 h at 29 °C and 250 rpm.

Supplemental Figures and Tables

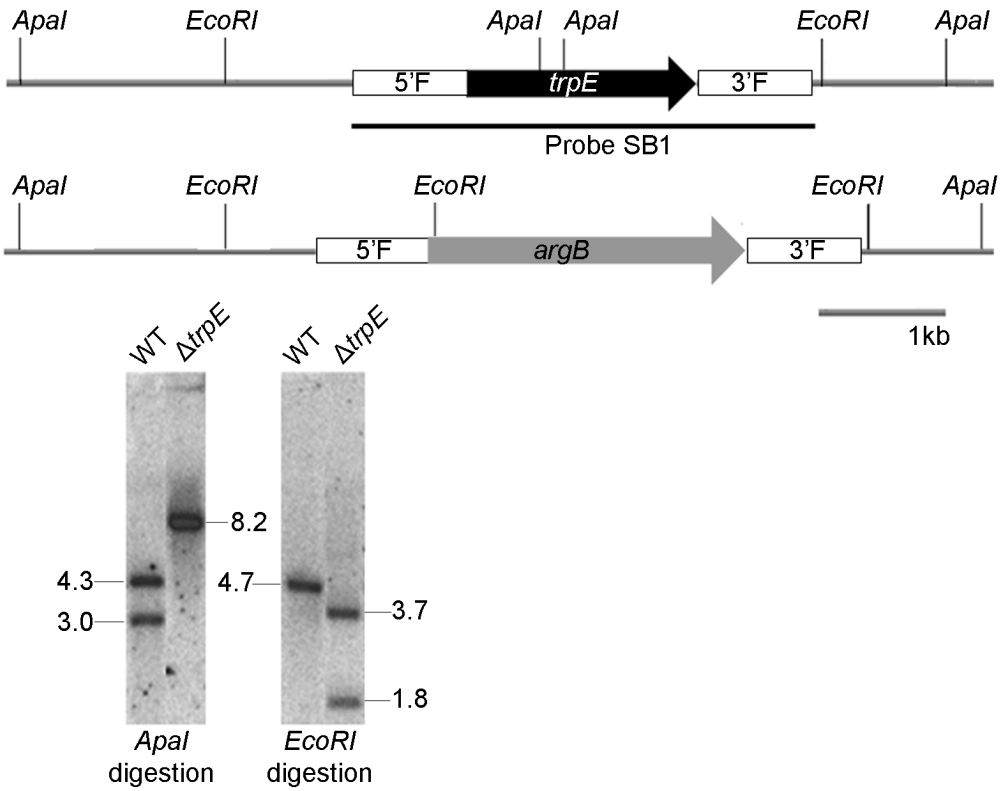

Figure S1. Southern analysis of Δ*trpE* mutant.

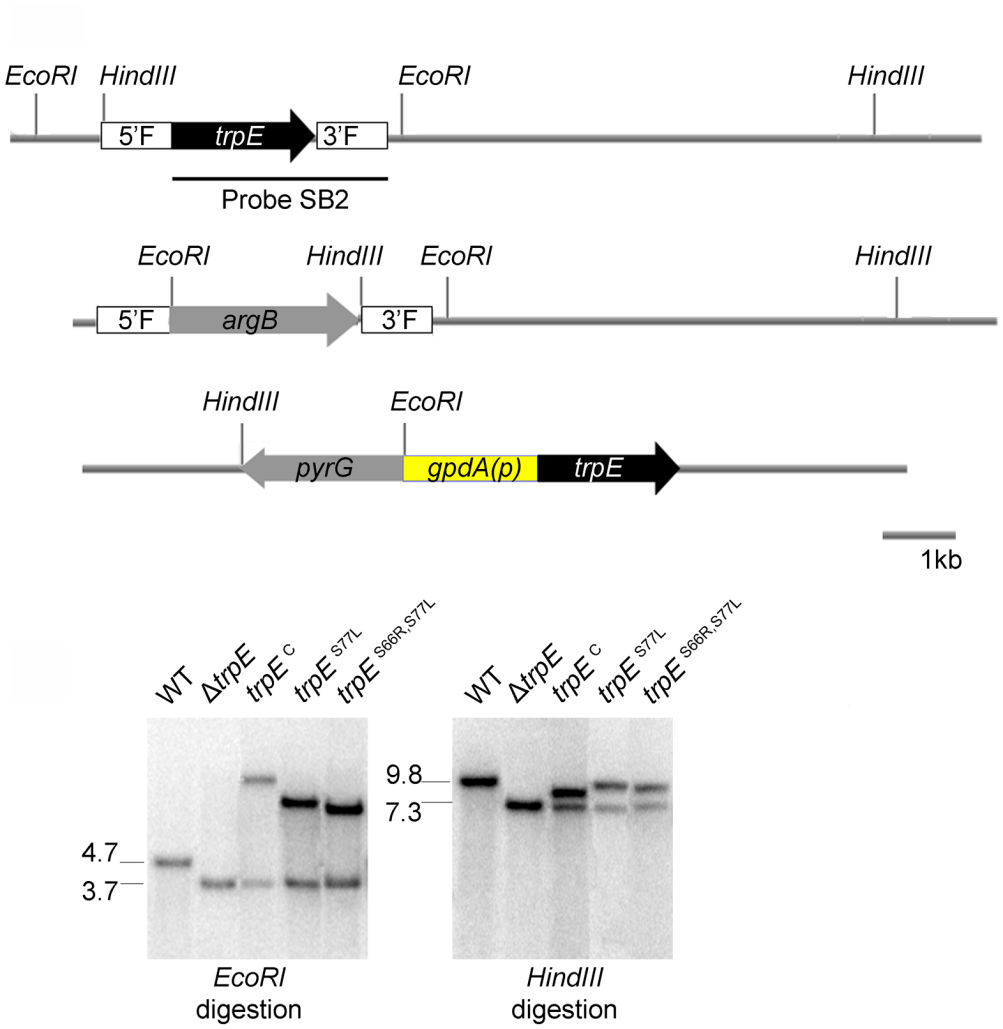

Figure S2. Southern (A) and northern analysis (B) of *trpE* complemented strain (*trpE*^{C}), and tryptophan-feedback mutants (*trpE*^{S77L}, *trpE*^{S66R,S77L}) (Probe cpcA as control).

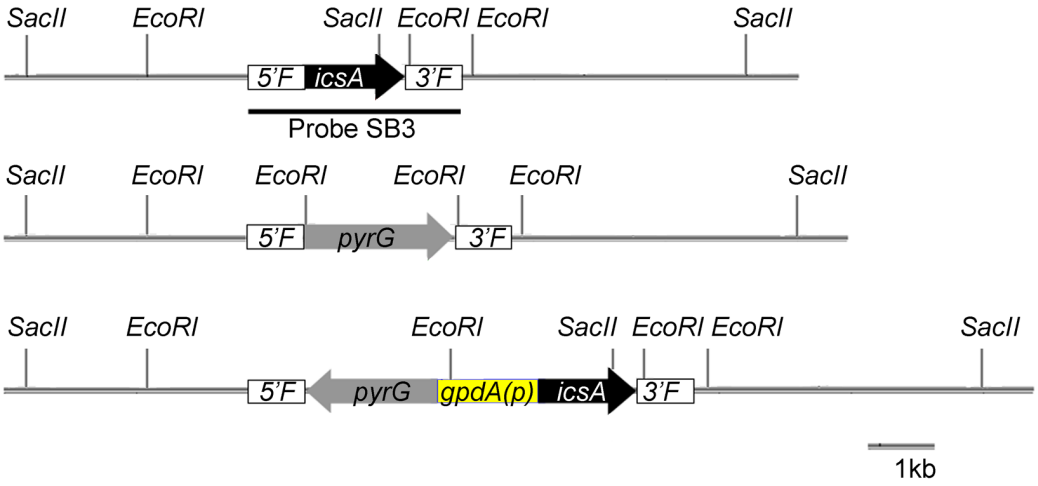
SacII
EcoRI
SacII
EcoRI
EcoRI
SacII
5'F
icsA
3'F
Probe SB3
SacII
EcoRI
EcoRI
EcoRI
EcoRI
SacII
5'F
pyrG
3'F
SacII
EcoRI
EcoRI
SacII
EcoRI
EcoRI
SacII
5'F
pyrG
gpdA(p)
icsA
3'F
1kb

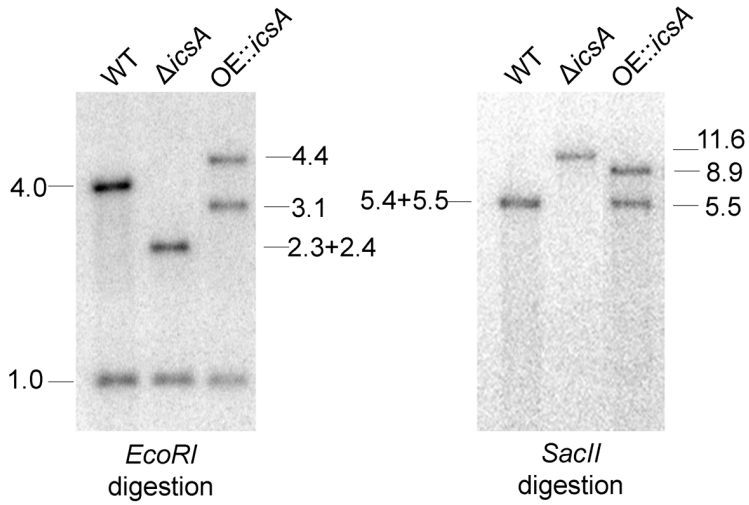
WT
ΔicsA
OE::icsA
4.0
1.0
4.4
3.1
2.3+2.4
EcoRI
digestion
WT
ΔicsA
OE::icsA
5.4+5.5
11.6
8.9
5.5
SacII
digestion

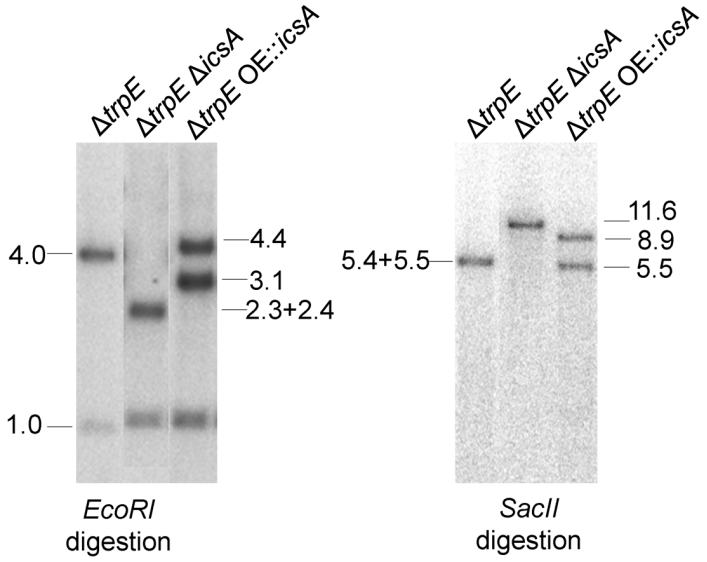
ΔtrpE
ΔtrpE ΔicsA
ΔtrpE OE::icsA
4.0
1.0
4.4
3.1
2.3+2.4
EcoRI
digestion
ΔtrpE
ΔtrpE ΔicsA
ΔtrpE OE::icsA
5.4+5.5
11.6
8.9
5.5
SacII
digestion

Figure S3. Southern analysis of *icsA* mutants.

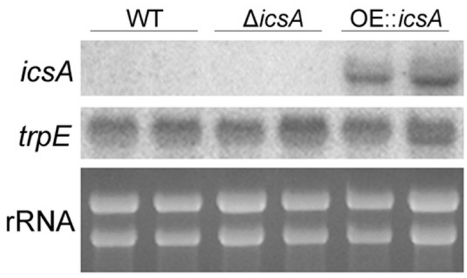

Figure S4. Northern expression analysis of *icsA* in wild-type strain AF293.1 comp TJW55.2 (WT) and *icsA* mutants, probe *trpE* as control (G).

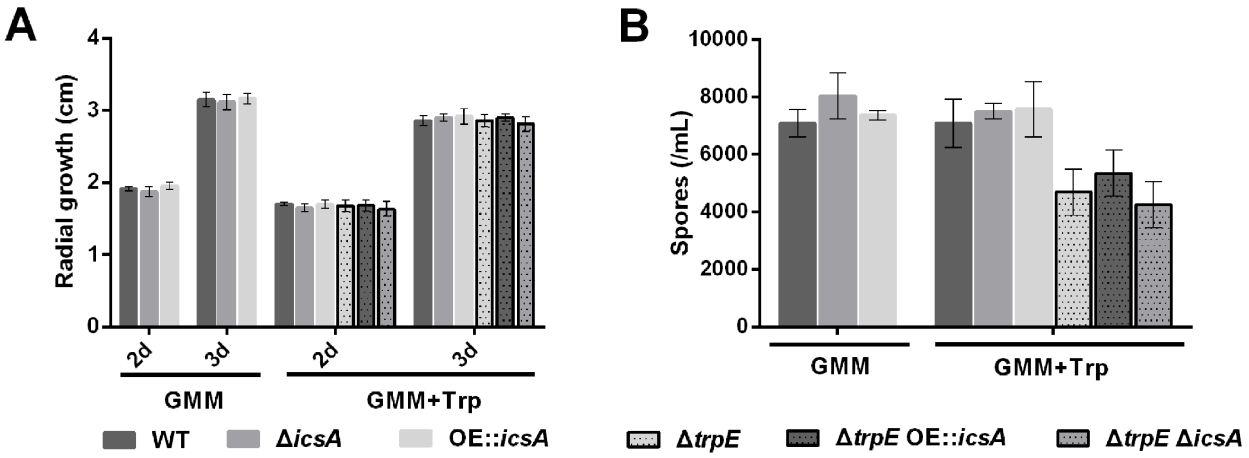

Figure S5. (A) Quantification of radial growth and (B) Spore production on solid GMM and GMM+5mM L-tryptophan (Trp) at 37 °C.

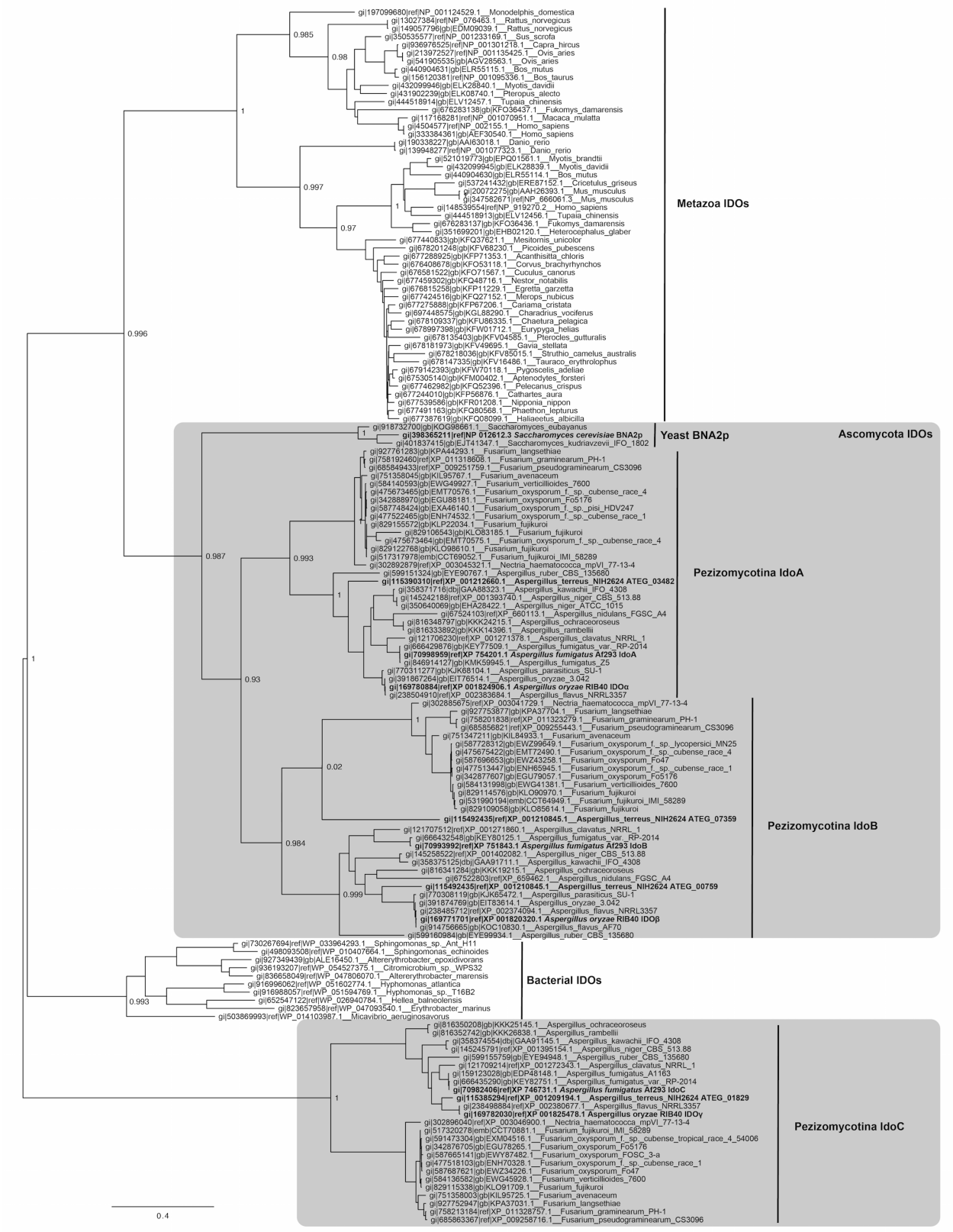

Figure S6 Maximum likelihood phylogenetic analysis of indole-2,3-dioxygenases.

Table S1. Plasmids used in this study

Name	Parental plasmid	Description	Reference
pJMP4		*A. fumigatus* argB	(22)
pJW24		A. parasiticus pyrG	(25)
pJMP9.1		A. parasiticus pyrG; A.nidulans gpdA(p)	(24)
pYH-yA-riboA		URA3; YA flanking;A.fumigatus riboB;Amp; 2μ	(Palmer, J.M. and Keller, unpublished)
pPMW1	pYH-yA-riboA	*trpE*^{C} in pYH-yA-riboA	This study
pPMW2	pYH-yA-riboA	*trpE*^{S77L} in pYH-yA-riboA	This study
pPMW3	pYH-yA-riboA	*trpE*^{S66R,S77L} in pYH-yA-riboA	This study
pPMW4	pJMP9.1	*trpE*^{C} in pJMP9.1	This study
pPMW5	pJMP9.1	*trpE*^{S77L} in pJMP9.1	This study
pPMW6	pJMP9.1	*trpE*^{S66R,S77L} in pJMP9.1	This study

Table S2. Primers used in this study

Name	Sequence (5' to 3')	Purpose
DAf6g12580F1	AAGAAAGCCAATCTTGCCAGTCG	5' Flank Δ*trpE*; probe SB1
DAf6g12580R1	AAATTTGTCTTGGATGCAGACCGCGTTCC CTCTCGGTGATAAGTCTAGTGAATTTGC	
DAf6g12580F2	ATCAAATGGATGTATGGGTCTCTCCTTCG GCTATTCAGAAATGGGATGACTATGACG	3' Flank Δ*trpE*; probe SB1 and SB2 for southern and northern blot for *trpE*
DAf6g12580R2	CAATAGGAGAACCAGAATTGAGG	
GF A.Fumi argB F	GAACGCGGTCTGCATCCAAG	argB cloning
GF A.Fumi argB R	GAAGGAGAGACCCATACATCC	
PM-yAup-gpdA F	GAAGTATATATCAGCGAACAACATCAAGC CGACCTAGGTACAGAAGTCCAATTGC	pPMW1-3 construction
PM-yAup-gpdA R	TGAACGGTATATACTCACAGACGGCGCCA TATGGTGATGTCTGCTCAAGCGGGGTAG	
PM-F6g12580F	ATGGCGCCGTCTGTGAGTATATACC	*trpE* cloning; Δ*trpE* transformant screening; probe SB2 for southern and northern blot for *trpE*
PM-F6g12580R	GCTCCATGCTCAGATATTTGTCC	
PM-S66-afu6g12580R	CCAATTGTCTCCGTAGTAGCCGCACTCTC ATACAGAAACGATAATTTCG	pPMW1 construction
PM-R66M-afu6g12580R	CCAATTGTCTCCGTAGTAGCCGCTCTCTCA TACAGAAACGATAATTTCG*	pPMW3 construction
PM-S77-Afu6g12580F	GCTACTACGGAGACAATTGGAAGATATAG TTTCGTCGGCGCAGGTACG	pPMW1 construction

PM-L77M-Afu6g12580F	GCTACTACGGAGACAATTGGAAGATATCTGTTCGTCGGCGCAGGTACG*	pPMW2-3 construction
PM-riboB-Afu6g12580R	GGGAGTCATCCATAACTCAGTCCGCGGATCCACTAGTCTCTCACGTCTCGTGGCGAACC	pPMW1-3 construction
DAfu6gF1	AGAGATTAGTCTGGCGTTGAGGC	5’ Flank Δ*icsA* and OE-*icsA*; probe SB3 for southern and northern blot for *icsA*
DAfu6gR1	CGATATCAAGCTATCGATACCTCGACTCGGAACTGAGTTCAGCTTGAAGAATGGAGGG	5’ Flank Δ*icsA*
DAfu6gF2	GTCGCTGCAGCCTCTCCGATTGTCGAATATGCTGGCCAACGATGGAAAAGAGGACAGC	3’ Flank Δ*icsA*
DAfu6gR2	ATCGGAAACGGGAAATACCTCC	3’ Flank Δ*icsA*; probe SB3 for southern and northern blot for *icsA*
diAfu6gF1	CTCCAAATATTCCATCCATGGG	Δ*icsA* transformant screening
diAfu6gR1	CTTTAATAGCGATTGACTCGGG	Δ*icsA* transformant screening and 3’ Flank OE-*icsA*
ParapyrGF	GAGTCGAGGTATCGATAGCTTG	pyrG cloning
ParapyrGR	ATTCGACAATCGGAGAGGCTGC	
OEAfu6gR1	CCAATTCGCCCTATAGTGAGTCGTATTACGGGAACTGAGTTCAGCTTGAAGAATGGAGGG	5’ Flank OE-*icsA*
OEpyrGgpdF	CGTAATACGACTCACTATAGGG	gpdA(p)-pyrG cloning
OEpyrGgpdR	GGTGATGTCTGCTCAAGCGGGGTAGC	
OEAfu6gF2	CAGCTACCCCGCTTGAGCAGACATCACCATGGCCCGCTTCGGACAGCAGATCATCCTCCC	3’ Flank OE-*icsA*
OEdiAfu6gF	ACTGTGGAAAAGGGAAAGGGG	OE-*icsA* transformant screening
OEdiAfu6gR	ATTATCCATCGAGTCCGAGCC	
cpcAF	ATGCCTGACTTCTTCGGTCTC	probe of northern blot for cpcA
cpcAR	AAGGGCCTTCCAGTACTGTTC	
pabaAF	GCGCCATTTATAGGCGATG	probe of northern blot for pabaA
pabaAR	TGTTCCGGAGAATCTAGTCTGG	
aroCF	TCCAAGGCGTTAGACCTGG	probe of northern blot for aroC
aroCR	CTCGACTTCCACCACCTTGGTC	

aroHF	GCAGTGATATGTTCAAGAGCCC	probe of northern blot for aroH
aroHR	GATGCTTCTGCCAATCGATCTC	
idoAF	ATGCTTCCTCCTATCCCCGCTC	probe of northern blot for idoA
idoAR	TCCCTCACTATCATCTGCCGTCC	
idoBF	GGTTTCTCCCTGATACCCTTCC	probe of northern blot for idoB
idoBR	TATTTGGCGGCAGCTTTTGTCG	
idoCF	TCCCTCCAACCTCTACCACAAC	probe of northern blot for idoC
idoCR	CCTCTGATCGCGCACCATTTCC	
aroMF	CGGACCCACGAAAATCAGCATC	probe of northern blot for aroM
aroMR	TTCTTCGCTAGAGATGGCGGCTG	
aroBF	GGGAGAATACTTTCGGGTC	probe of northern blot for aroB
aroBR	ATGCCGAACTCCGTTCCAG	
*trpC*F	GCGGTCTTTCGCAATGACG	probe of northern blot for *trpC*
*trpC*R	GAGGCAGGCCTTCATATAC	
trpDF	AAAGCTCGTGGGAAGAAGG	probe of northern blot for trpD
trpDR	GCAGAGCCAGAGAATGAAG	
trpBF	TGCCAGGTGCCAAGAACAG	probe of northern blot for trpB
trpBR	GGATCTGTGAAGGGAATGC	

2.9 References

1. Cacho RA, Tang Y, Chooi YH. Next-generation sequencing approach for connecting secondary metabolites to biosynthetic gene clusters in fungi. Frontiers in microbiology. 2014 4294208]; 5:[774 p.].
2. Anyaogu DC, Mortensen UH. Heterologous production of fungal secondary metabolites in Aspergilli. Frontiers in microbiology. 2015 4322707]; 6:[77 p.].
3. Keller NP, Turner G, Bennett JW. Fungal secondary metabolism - from biochemistry to genomics. Nature reviews Microbiology. 2005;3(12):937-47.
4. Ames BD, Liu X, Walsh CT. Enzymatic processing of fumiquinazoline F: a tandem oxidative-acylation strategy for the generation of multicyclic scaffolds in fungal indole alkaloid biosynthesis. Biochemistry. 2010;49(39):8564-76.
5. Ames BD, Walsh CT. Anthranilate-activating modules from fungal nonribosomal peptide assembly lines. Biochemistry. 2010;49(15):3351-65.
6. Braus GH. Aromatic amino acid biosynthesis in the yeast *Saccharomyces cerevisiae*: a model system for the regulation of a eukaryotic biosynthetic pathway. Microbiol Rev. 1991;55(3):349-70.
7. Palmer GC, Jorth PA, Whiteley M. The role of two Pseudomonas aeruginosa anthranilate synthases in tryptophan and quorum signal production. Microbiology. 2013;159(Pt 5):959-69.
8. Bae YM, Holmgren E, Crawford IP. Rhizobium meliloti anthranilate synthase gene: cloning, sequence, and expression in Escherichia coli. Journal of bacteriology. 1989;171(6):3471-8
9. Ito J, Cox EC, Yanofsky C. Anthranilate synthetase, an enzyme specified by the tryptophan operon of Escherichia coli: purification and characterization of component I. Journal of bacteriology. 1969;97(2):725-33.
10. Morino K, Matsuda F, Miyazawa H, Sukegawa A, Miyagawa H, Wakasa K. Metabolic profiling of tryptophan-overproducing rice calli that express a feedback-insensitive α subunit of anthranilate synthase. Plant and cell physiology. 2005;46(3):514-21.
11. Saika H, Oikawa A, Nakabayashi R, Matsuda F, Saito K, Toki S. Changes in primary and secondary metabolite levels in response to gene targeting-mediated site-directed mutagenesis of the anthranilate synthase gene in rice. Metabolites. 2012;2(4):1123-38.
12. Tozawa Y, Hasegawa H, Terakawa T, Wakasa K. Characterization of rice anthranilate synthase alpha-subunit genes OASA1 and OASA2. Tryptophan accumulation in transgenic rice expressing a feedback-insensitive mutant of OASA1. Plant physiology. 2001;126(4):1493-506.
13. Graf R, Mehmann B, Braus GH. Analysis of feedback-resistant anthranilate synthases from *Saccharomyces cerevisiae*. Journal of bacteriology. 1993;175(4):1061-8.
14. Hughes EH, Hong SB, Gibson SI, Shanks JV, San KY. Expression of a feedback-resistant anthranilate synthase in Catharanthus roseus hairy roots provides evidence for tight regulation of terpenoid indole alkaloid levels. Biotechnology and bioengineering. 2004;86(6):718-27.

15. Dubouzet JG, Matsuda F, Ishihara A, Miyagawa H, Wakasa K. Production of indole alkaloids by metabolic engineering of the tryptophan pathway in rice. Plant biotechnology journal. 2013;11(9):1103-11.
16. Käfer E. The anthranilate synthetase enzyme complex and the trifunctional *trpC* gene of Aspergillus. Canadian Journal of Genetics and Cytology. 1977;19(4):723-38.
17. Osherov N, Kontoyiannis DP, Romans A, May GS. Resistance to itraconazole in *Aspergillus nidulans* and *Aspergillus fumigatus* is conferred by extra copies of the A. nidulans P-450 14α-demethylase gene, pdmA. Journal of Antimicrobial Chemotherapy. 2001;48(1):75-81.
18. Shimizu K, Keller NP. Genetic involvement of a cAMP-dependent protein kinase in a G protein signaling pathway regulating morphological and chemical transitions in *Aspergillus nidulans*. Genetics. 2001;157(2):591-600.
19. Sambrook J, Russell D. Molecular cloning: a laboratory manual. Cold Spring Harbor, New York: Cold Spring Harbor Laboratory Press; 2001.
20. Szewczyk E, Nayak T, Oakley CE, Edgerton H, Xiong Y, Taheri-Talesh N, et al. Fusion PCR and gene targeting in *Aspergillus nidulans*. Nat Protoc. 2006;1(6):3111-20.
21. Lim FY, Sanchez JF, Wang CC, Keller NP. Toward awakening cryptic secondary metabolite gene clusters in filamentous fungi. Methods Enzymol. 2012;517:303-24.
22. Palmer JM, Bok JW, Lee S, Dagenais TR, Andes DR, Kontoyiannis DP, et al. Loss of CclA, required for histone 3 lysine 4 methylation, decreases growth but increases secondary metabolite production in *Aspergillus fumigatus*. PeerJ. 2013; 1:[e4 p.].
23. Yin WB, Chooi YH, Smith AR, Cacho RA, Hu Y, White TC, et al. Discovery of cryptic polyketide metabolites from dermatophytes using heterologous expression in *Aspergillus nidulans*. ACS synthetic biology. 2013;2(11):629-34.
24. Lim FY, Hou Y, Chen Y, Oh JH, Lee I, Bugni TS, et al. Genome-based cluster deletion reveals an endocrocin biosynthetic pathway in *Aspergillus fumigatus*. Applied and environmental microbiology. 2012;78(12):4117-25.
25. Calvo AM, Bok J, Brooks W, Keller NP. veA is required for toxin and sclerotial production in Aspergillus parasiticus. Applied and Environmental Microbiology. 2004;70(8):4733-9.
26. Cerqueira GC, Arnaud MB, Inglis DO, Skrzypek MS, Binkley G, Simison M, et al. The Aspergillus Genome Database: multispecies curation and incorporation of RNA-Seq data to improve structural gene annotations. Nucleic acids research. 2014;42;705-10.
27. Katoh K, Misawa K, Kuma K, Miyata T. MAFFT: a novel method for rapid multiple sequence alignment based on fast Fourier transform. Nucleic acids research. 2002;30(14):3059-66.
28. Price MN, Dehal PS, Arkin AP. FastTree: computing large minimum evolution trees with profiles instead of a distance matrix. Molecular biology and evolution. 2009;26(7):1641-50.
29. Yuasa HJ, Ball HJ. Molecular evolution and characterization of fungal indoleamine 2,3-dioxygenases. J Mol Evol. 2011;72(2):160-8.
30. Yuasa HJ, Ball HJ. The evolution of three types of indoleamine 2,3 dioxygenases in fungi with distinct molecular and biochemical characteristics. Gene. 2012;504(1):64-74.

31. Yuasa HJ, Ball HJ. Indoleamine 2, 3-dioxygenases with very low catalytic activity are well conserved across kingdoms: IDOs of Basidiomycota. Fungal Genetics and Biology. 2013;56:98-106.
32. Schrettl M, Kim HS, Eisendle M, Kragl C, Nierman WC, Heinekamp T, et al. SreA-mediated iron regulation in *Aspergillus fumigatus*. Molecular microbiology. 2008;70(1):27-43.
33. Wiemann P, Lechner BE, Baccile JA, Velk TA, Yin WB, Bok JW, et al. Perturbations in small molecule synthesis uncovers an iron-responsive secondary metabolite network in *Aspergillus fumigatus*. Frontiers in microbiology. 2014 4208449]; 5:[530 p.].
34. Lim FY, Ames B, Walsh CT, Keller NP. Co-ordination between BrlA regulation and secretion of the oxidoreductase FmqD directs selective accumulation of fumiquinazoline C to conidial tissues in *Aspergillus fumigatus*. Cellular microbiology. 2014;16(8):1267-83.
35. Kanno T, Komatsu A, Kasai K, Dubouzet JG, Sakurai M, Ikejiri-Kanno Y, et al. Structure-based in vitro engineering of the anthranilate synthase, a metabolic key enzyme in the plant tryptophan pathway. Plant physiology. 2005;138(4):2260-8.
36. Tzin V, Galili G. New insights into the shikimate and aromatic amino acids biosynthesis pathways in plants. Molecular Plant. 2010;3(6):956-72.
37. Maeda H, Dudareva N. The shikimate pathway and aromatic amino Acid biosynthesis in plants. Annual review of plant biology. 2012;63:73-105.
38. Krappmann S, Bignell EM, Reichard U, Rogers T, Haynes K, Braus GH. The *Aspergillus fumigatus* transcriptional activator CpcA contributes significantly to the virulence of this fungal pathogen. Mol Microbiol. 2004;52(3):785-99.
39. Bok JW, Balajee SA, Marr KA, Andes D, Nielsen KF, Frisvad JC, et al. LaeA, a regulator of morphogenetic fungal virulence factors. Eukaryotic cell. 2005;4(9):1574-82.
40. Han X, Xu X, Cui C, Gu Q. Alkaloidal compounds produced by a marine-derived fungus, *Aspergillus fumigatus* H1-04, and their antitumor activities. Chinese Journal of Medicinal Chemistry. 2007;17(4): 232–7.
41. Walsh CT, Haynes SW, Ames BD, Gao X, Tang Y. Short pathways to complexity generation: fungal peptidyl alkaloid multicyclic scaffolds from anthranilate building blocks. ACS chemical biology. 2013;8(7):1366-82.
42. Plach MG, Löffler P, Merkl R, Sterner R. Conversion of anthranilate synthase into isochorismate synthase: implications for the evolution of chorismate-utilizing enzymes. Angewandte Chemie-international Edition. 2015;54(38):11270-4.
43. Serino L, Reimmann C, Visca P, Beyeler M, Chiesa VD, Haas D. Biosynthesis of pyochelin and dihydroaeruginoic acid requires the iron-regulated pchDCBA operon in Pseudomonas aeruginosa. Journal of bacteriology. 1997;179(1):248-57.
44. Harrison AJ, Yu M, Gårdenborg T, Middleditch M, Ramsay RJ, Baker EN, et al. The structure of MbtI from Mycobacterium tuberculosis, the first enzyme in the biosynthesis of the siderophore mycobactin, reveals it to be a salicylate synthase. Journal of bacteriology. 2006;188(17):6081-91.

45. Buss K, Müller R, Dahm C, Gaitatzis N, Skrzypczak-Pietraszek E, Lohmann S, et al. Clustering of isochorismate synthase genes menF and entC and channeling of isochorismate in Escherichia coli. Biochimica Et Biophysica Acta-gene Structure and Expression. 2001;1522(3):151-7.
46. Haas H. Fungal siderophore metabolism with a focus on *Aspergillus fumigatus*. Natural product reports. 2014;31(10):1266-76.
47. Yin WB, Baccile JA, Bok JW, Chen Y, Keller NP, Schroeder FC. A nonribosomal peptide synthetase-derived iron(III) complex from the pathogenic fungus *Aspergillus fumigatus*. J Am Chem Soc. 2013;135(6):2064-7.
48. Hong S-B, Peebles CA, Shanks JV, San K-Y, Gibson SI. Expression of the Arabidopsis feedback-insensitive anthranilate synthase holoenzyme and tryptophan decarboxylase genes in Catharanthus roseus hairy roots. Journal of biotechnology. 2006;122(1):28-38.
49. Ishihara A, Asada Y, Takahashi Y, Yabe N, Komeda Y, Nishioka T, et al. Metabolic changes in Arabidopsis thaliana expressing the feedback-resistant anthranilate synthase α subunit gene OASA1D. Phytochemistry. 2006;67(21):2349-62.
50. Li J, Last RL. The Arabidopsis thaliana trp5 mutant has a feedback-resistant anthranilate synthase and elevated soluble tryptophan. Plant physiology. 1996;110(1):51-9.
51. Brown JS, Aufauvre-Brown A, Brown J, Jennings JM, Arst H, Holden DW. Signature-tagged and directed mutagenesis identify PABA synthetase as essential for *Aspergillus fumigatus* pathogenicity. Molecular microbiology. 2000;36(6):1371-80.
52. Mellado L, Calcagno-Pizarelli AM, Lockington RA, Cortese MS, Kelly JM, Arst HN, Jr., et al. A second component of the SltA-dependent cation tolerance pathway in *Aspergillus nidulans*. Fungal genetics and biology : FG & B. 2015;82:116-28.
53. Tang CM, Smith JM, Arst HN, Jr., Holden DW. Virulence studies of *Aspergillus nidulans* mutants requiring lysine or p-aminobenzoic acid in invasive pulmonary aspergillosis. Infection and immunity. 1994;62(12):5255-60.
54. Sahr T, Ravanel S, Basset G, Nichols BP, Hanson AD, Rebeille F. Folate synthesis in plants: purification, kinetic properties, and inhibition of aminodeoxychorismate synthase. The Biochemical journal. 2006;396(1):157-62.
55. Parsons JF, Jensen PY, Pachikara AS, Howard AJ, Eisenstein E, Ladner JE. Structure of Escherichia coli aminodeoxychorismate synthase: architectural conservation and diversity in chorismate-utilizing enzymes. Biochemistry. 2002;41(7):2198-208.
56. Bulloch EM, Jones MA, Parker EJ, Osborne AP, Stephens E, Davies GM, et al. Identification of 4-amino-4-deoxychorismate synthase as the molecular target for the antimicrobial action of (6 S)-6-fluoroshikimate. Journal of the American Chemical Society. 2004;126(32):9912-3.
57. Sekito T, Fujiki Y, Ohsumi Y, Kakinuma Y. Novel families of vacuolar amino acid transporters. IUBMB life. 2008;60(8):519-25.

58. Wagner D, Wiemann P, Huss K, Brandt U, Fleissner A, Tudzynski B. A sensing role of the glutamine synthetase in the nitrogen regulation network in Fusarium fujikuroi. PloS one [Internet]. 2013 3829961]; 8(11):[e80740 p.]
59. Wiemann P, Tudzynski B. The nitrogen regulation network and its impact on secondary metabolism and pathogenicity. In: Proctor DWBaRH, editor. Fusarium: Genomics, Molecular and Cellular Biology. Norwich, UK: Caister Academic Press; 2013. p. 111-42.
60. Panozzo C, Nawara M, Suski C, Kucharczyka R, Skoneczny M, Becam AM, et al. Aerobic and anaerobic NAD^+ metabolism in *Saccharomyces cerevisiae*. FEBS letters. 2002;517(1-3):97-102.
61. Iraqui I, Vissers S, Cartiaux M, Urrestarazu A. Characterisation of *Saccharomyces cerevisiae* ARO8 and ARO9 genes encoding aromatic aminotransferases I and II reveals a new aminotransferase subfamily. Mol Gen Genet. 1998;257(2):238-48.
62. Bok JW, Keller NP. LaeA, a regulator of secondary metabolism in Aspergillus spp. Eukaryotic cell. 2004;3(2):527-35.
63. Xue T, Nguyen CK, Romans A, Kontoyiannis DP, May GS. Isogenic auxotrophic mutant strains in the *Aspergillus fumigatus* genome reference strain AF293. Archives of microbiology. 2004;182(5):346-53.

CHAPTER 3

Fungal and mammalian IDOs cooperate in shaping the host response to infection

Tsokyi Choera[1]♯, Teresa Zelante[2]♯, Anne Beauvais[3], Giuseppe Pieraccini[4], Marco Pieroni[5], Claudia Galosi[1], Claudia Beato[6], Giuseppe Paolicelli[1], Antonella De Luca[1], Francesca Boscaro[4], Riccardo Romoli[4], Xin Liu[1], Adilia Warris[7], Francesca Fallarino[1], Monica Borghi[1], Marilena Pariano[1], Melissa Ida Palmieri[1], Gabriele Costantino[5], Mauro Calvitti[2], Vasilis Oikonomou[1], Marco Gargaro[1], Alicia Y. Wong[8], Louis Boon[9], Marcel den Hartog[9], Jean Paul Latgè[3], Puccetti Paolo[2], Xin Luo, Nancy P. Keller[1] and Luigina Romani[2]*.

♯ These authors contributed equally.

I designed and performed all the experiment related to the fungal side including the generation and the characterization of *A. fumigatus* Ido and Aro mutants, physiology, and measurement of fungal intracellular metabolites. I also contributed to the design of some of the in vivo experiments.

3.1 Abstract

Indoleamine 2,3-dioxygenases (IDOs) – belonging in the heme dioxygenase family and degrading L-tryptophan – are responsible for the *de novo* synthesis of nicotinamide adenine dinucleotide (NAD^+). As such, they are expressed by a variety of invertebrate and vertebrate species, including fungi, able to synthesize enzymatically active forms of Idos. In mammals, IDO1 has remarkably evolved to expand its functions, so to become a prominent homeostatic regulator, capable of modulating infection and immunity in multiple ways, including local tryptophan deprivation, production of biologically active tryptophan catabolites, and non-enzymatic cell-signaling activity. Whether Idos in fungi have pleiotropic functions that might impact on host reactivity has been unclear. We found that *Aspergillus fumigatus* possesses three distinct *IDO* genes – *idoA*, *idoB*, and *idoC* – that were transcriptionally expressed under conditions of tryptophan abundance, resulting in the production of NAD^+ and a set of tryptophan catabolites similar to the host's own. Deletions in fungal *idoA, idoB,* or *idoC* not only resulted in a metabolic switch in the pathway of NAD^+ regeneration, but they also led to the production of a different tryptophan catabolites that increased fungal pathogenicity, promoted inflammation, and subverted local eubiosis in the host. Therefore, fungal and mammalian IDOs cooperate in shaping the type of interaction between host and microbes in local tissue microenvironments.

3.2 Introduction

Heme dioxygenase-encoding genes are widely distributed across species, from metazoans to bacteria to fungi(1, 2). During evolution, they have diverged through speciation and genetic duplication, with the emergence, in vertebrates, of paralogous genes. L-Tryptophan (Trp) degradation by indoleamine 2,3-dioxygenase (IDO) [1 and 2 in mammals and IdoA/B/C in fungi] generates a series of catabolites collectively known as kynurenines. The kynurenine pathway of Trp degradation contributes in mammals to immune tolerance(3-5) mediated by one of the first catabolites in the pathway, L-kynurenine, an amino acid itself. In fungi, the primary role of *IDO*-encoded dioxygenases (Idos) is thought to supply NAD^+ *via* the kynurenine pathway(6, 7). Since, both fungal Idos and mammalian IDO1 have high affinity for Trp and high catalytic efficiency, this suggests similar metabolic roles for these enzymes(8).

Different metabolic pathways in different eukaryotic clades lead to *de novo* biosynthesis of NAD^+. Tryptophan can be degraded to other parallel catabolite products to Kynurenines. One is via the Ehlrich pathway, which catabolizes Trp to Indole pyruvates, and involves the enzyme aromatic aminotransferase (AroH and AroI). These aromatic aminotransferases in *Saccharomyces cerevisiae* are also involved in the synthesis of the essential amino acid Phenylalanine (Phe) and Tyrosine (Tyr), as the deletion of Aro8 and Aro9 resulted in an auxotrophy for Phe and Tyr(9). Studies on the yeast pathogen *Candida glabrata* have shown that deletion of *ARO8* – encoding AroH/I – reduces fungal pigmentation and suggests a linkage to virulence with increased sensitivity to oxidative stress(10).

The opportunistic fungal pathogen *A. fumigatus* possesses three putative *IDO* genes (*idoA,B,C*) in its genome and two putative *ARO* genes (*aroH* and *aroI*) (6, 7). Enzymatic studies suggest that Idos of *A. oryzae*, participates in Trp degradation(11). Additionally, previous studies on

A.fumigatus grown on Trp showed upregulation of these *ido* genes(6), however, the relative contributions of individual Idos to *Aspergillus* metabolic pathways and adaptation to the host's environment have remained unclear.

In this study, we characterized the function of *A. fumigatus* Idos by generating *Aspergillus* mutants with single and triple deletions of Idos and analyzed them for growth and metabolism, along with pathogenicity under *in vitro* and *in vivo* conditions. Idos were responsible for L-kynurenine production and contributed to NAD^+ biosynthesis. Genetic deletion of the three paralogous genes activated the Ehrlich pathway, involving AroH and AroI. Such a metabolic switch compromised fungal fitness (i.e., growth ability) as well as fitness of the host, in which the release of other Trp metabolites, promoted inflammation and allergy, subverted disease-tolerance mechanisms and compromised microbial-community stability in the lungs of *A. fumigatus*-colonized mice.

3.3 Materials and Methods

3.3.1 Ethics statement

The animal studies described in this manuscript were performed according to the Italian Approved Animal Welfare Authorization 360/2015-PR and Legislative Decree #26/2014, which provided *ad hoc* clearance by the Italian Ministry of Health over a 5-yr period (2015–2020). Animals were assessed twice daily for physical conditions and behavior. Animals ranked as *moribund* were humanely euthanized by CO_2 asphyxiation.

3.3.2 Computational modeling.

The comparative model was built using Prime software (Schrödinger Release 2016-4), using the 2D0T crystal structure as a template, chain A(12), the best available structure on commencing this study. The overall goodness of the models was checked by Ramachandran plots, *via*

PROCHECK(13), whereby >97% of the IdoA and IdoB residues fitted in the allowed region of the plot)

3.3.3 Strains and medium.

Strains used or created in this study are listed in Table 1. The genetic background of the primary strain used in this study is *A. fumigatus* CEA17 (14). All strains were maintained as glycerol stocks at -80 °C and activated on solid glucose minimal media (GMM) at 37 °C (15). Growth media was supplemented with 1.26 g/L uridine and 0.56 g/L uracil for *pyrG* auxotrophs, 1 g/L L-arginine for *argB* auxotrophs, and 50uM Nicotinamide (NAM) in case of auxotrophy. Supplemental Trp (Sigma Aldrich) resulted in a final concentration of 60 μM.

3.3.4 Genetic manipulations for *A. fumigatus ido* and *aro* mutants.

Fungal DNA extraction, gel electrophoresis, restriction enzyme digestion, Southern blotting, hybridization and probe preparation were performed according to standard methods (16). For DNA isolation, *A. fumigatus* strains were grown for 24 h at 37 °C in static liquid GMM, supplemented as needed for auxotrophs. DNA isolation was performed as described by Sambrook and Russell (16). Gene deletion mutants in this study were constructed by targeted integration of the deletion cassette through transformation (17, 18). The deletion cassettes were constructed using a double-joint fusion PCR (DJ-PCR) approach (17, 18). *A. fumigatus* protoplast generation and transformation were carried out as previously described (17, 18). The primers used in this work are listed in Table S1 and the plasmids in Table S2. An *A. fumigatus idoB* (AFUB_034980) disruption consisted for the following: two 1 kb fragments flanking the ORF were amplified from CEA10 genomic DNA using the primer pair TC-1113/1114 and TC-1115/1116, respectively (Table S2). The selection marker, *A. parasiticus pyrG*, was PCR amplified from plasmid pJW24 (19) using the primer pair TC-4/TC-5 (Table S2). The deletion construct was transformed into

CEA17 (*pyrG1*) and TMN21 (*argB1, pyrG1*). Transformants were selected for pyrimidine prototrophy in media without any supplements and amended with 50uM NAM in case of auxotrophy. Transformants obtained were verified by PCR using primers pairs TC-1119/TC-1120, and Southern analysis using the flanking probes (Fig. S1). The obtained mutants were named TTC36.x (Δ*idoB, argB-*), and TTC37.x (Δ*idoB*) (Fig. S1). TTC36.15(Δ*idoB, argB-*) and TTC37.1 (Δ*idoB*) were chosen for further experiments.

The *A. fumigatus idoA* (AFUB_066940) disruption cassette was constructed similarly utilizing a 2.7 kb selectable auxotrophic marker, *A. fumigatus argB*, cloned from plasmid pJMP4 (20) with primers TC-20/TC-21 and the primer pairs TC-1131/1134 and TC-1132/1135 for flanking regions. A 3rd round PCR product was amplified with primer pairs TC-1133/1136. The deletion construct was transformed into TJG1.6 (*argB1*) and TTC36.15 (Δ*idoB, argB-)*. Transformants obtained were verified by PCR using primers pairs TC-1137/TC-1138, and Southern analysis using the flanking probes (Fig. S2). The obtained mutants were named TTC38.x (Δ*idoA*) (Fig. S2), and TTC39.x (ΔΔ*idoAidoB*) (Fig. S4). TTC38.13(Δ*idoA*) and TTC39.5 (ΔΔ*idoAidoB*) were chosen for further experiments.

The *A. fumigatus idoC* (AFUB_088580) disruption cassette was constructed with the self-excising selection marker, *six-B-rec-hygroR-six*, which was purified from plasmid pKS29 (21) (Table S2) by digestion with *Fsp* I. Two 1 kb fragments flanking the ORF were amplified using the primer pair XL-1/XL-2 and XL-3/XL-4, respectively (Table S2). The deletion construct was transformed into TMN2.1 (*argB-, pyrG-*) and TTC39.6 (ΔΔ*idoAidoB*). Transformants were selected for hygromycin resistance in media with hygromycin at 200 μg/ml and amended with Nicotinamide in case of auxotrophy. Transformants were further screened by PCR (primer pair XL-1/XL-5 for Δ*idoC* mutants,) and Southern analysis using probe of Flanking regions (Fig. S3). The obtained

mutants were named TXL2.x (Δ*idoC, hph*^{R}*, argB-, pyrG-*) and TTC41.x (ΔΔΔ*idoAidoBidoC, hph*^{R}). The self-excising selection marker was recycled by growing TXL2.2 and TTC41.1 on Xylose (2%) Minimal Media and transformants were further screened by PCR (primer pair XL-1/ XL-4) and Southern analysis using probe for Flanking regions (Fig. S3). A construct containing argB-pyrG was introduced into the Ku locus, yielding transformant TXL3.x (Δ*idoC, hph*^{S}) (Fig. S3 and TTC42.x (ΔΔΔ*idoAidoBidoC, hph*^{s}) (Fig. S5). TXL3.2 (Δ*idoC*) and TTC42.1 (ΔΔΔ*idoAidoBidoC*) were chosen for further experiments.

To construct the *A. fumigatus aroI* (AFUB_051500) disruption cassette, the 2.7 kb selectable auxotrophic marker, *A. fumigatus argB*, cloned from plasmid pJMP4 was fused with 1 kb DNA fragment upstream and downstream of the *aroH* ORF were amplified from CEA10 genomic DNA using the primer pairs DAFUB_051500F1/DAFUB_051500R1 and DAFUB_051500F2/DAFUB_051500R2. The deletion construct was transformed into TJG1.6 (*argB*-) and TMN2.1 (pyrG-*, argB-)*. Transformants obtained were verified by PCR using primers TC-1147 and TC-1148, and Southern analysis using the flanking probes (Fig. S6). The obtained mutants were named TTC20.x (Δ*aroI, pyrG*-), and TTC21.x (Δ*aroI*) (Fig. S6). TTC21.6 (Δ*aroI*) and TTC20.1 (Δ*aroI, pyrG*-) were chosen for further experiments.

An *A. fumigatus aroH* (AFUB_029280) disruption consisted for the following: *A. parasiticus pyrG* as a selection marker amplified from plasmid pJW24 (19) using the primer pair TC-4/TC-5 (Table S2), two 1 kb fragments flanking the ORF were amplified from CEA10 genomic DNA using the primer pairs TC-1104/TC-1105 and TC-1106/TC-1107, respectively (Table S2). The deletion construct was transformed into CEA17 (*pyrG*-) and TTC20.1 (Δ*aroI, pyrG*-). Transformants were further screened by PCR using primer paor TC-1110/TC-1111 and Southern analysis using probe for Flanking regions (Fig. S7). The obtained mutants were named TTC22.x (Δ*aroH*) and TTC23.x

(ΔΔ*aroHaroI*) (Fig. S7). TTC22.4 (Δ*aroH*) and TTC23.2 (ΔΔ*aroHaroI*) were chosen for further experiments.

3.3.5 Physiology experiments

Colony diameters of strains were measured after 3 days of growth at 37 °C on solidified GMM and GMM supplemented with NAM (50uM) respectively. Strains were point-inoculated onto the media at 10^4 conidia total (in 5 µL). Germination was assessed as described in Fischer et. al in static liquid GMM and GMM supplemented with NAM (50uM) respectively as well. Briefly 1×10^5 spores/mL in GMM and GMM supplement with 50uM NAM were inoculated into each well of a Costar® 24-well dish (Corning, Corning, NY, USA). Microscopic images were captured using a Nikon Eclipse T*i* inverted microscope equipped with an OKO-Lab microscopic enclosure to maintain the temperature at 37°C for *A. fumigatus* (OKO Lab, Burlingame, CA, USA). Germinated spores were observed using a Nikon Plan Fluor 20xPh1 DLL objective and phase-contrast images captured every 1–2 h using the Nikon NIS Elements AR software package (v. 4.13). A spore is noted to be germinating if an emerging germ tube was clearly present. One hundred spores were observed for each strain ($n = 3$) and growth condition. Values in figures represent the average percentage of spores germinated ± SEM. The Student *t*-test was carried out to determine statistical significance using the GraphPad Prism software (La Jolla, CA, USA). Growth on various media was also assessed to display the phenotype of mutants.

3.3.6 Primary metabolites extraction and analysis.

Primary metabolites were assessed with slight modification as previously described in Wang et al., (2017). Briefly, 10^4 *A. fumigatus* conidia from control and *ido* mutant strains were inoculated on solid GMM supplement with NAM and Trp and cultured at 37 °C for 84 h in triplicates. Fungal tissue was collected and immediately frozen in liquid nitrogen. The fungal tissue was homogenized

in 3 mL extraction solvent (2/2/1 (v/v/v) acetonitrile/methanol/water) cooled on dry ice. After centrifugation, 2 mL of supernatant was filtered using a 0.45 μm PTFE Mini-UniPrep filter vial (Agilent). The supernatant of these hyphal metabolites was used for metabolite analysis. For metabolite measurement, samples were dried under N_2 and resuspended to 20ug/ml in LC-MS grade water (Sigma-Aldrich). Samples were analyzed using a HPLC-MS system consisting of Thermo Scientific Vanquish UHPLC coupled by electrospray ionization (ESI; negative mode) to a hybrid quadrupole-high-resolution mass spectrometer (Q Exactive orbitrap, Thermo Scientific) operated in full scan mode. Liquid chromatography separation was achieved using an ACQUITY UPLC® BEH C18 (2.1 x 100 mm column, 1.7 μm particle size, Waters). Solvent A was 97:3 water: methanol with 10 mM tributylamine and 10 mM acetic acid, pH 8.2; solvent B was methanol. The gradient was: 0 min, 5% B; 1.5 min, 5% B, 11.5 min, 95% B; 12.5 min, 95% B; 13 min, 5% B; 14.5 min, 5% B. Autosampler and column temperatures were 4 °C and 25 °C, respectively. Metabolite peaks were identified by their exact mass and matching retention time to those of pure standards (Fig. S7) (Sigma-Aldrich).

3.3.7 RNA extraction and Semiquantitative RT-PCR analysis.

Total RNA was extracted with Trizol reagent (Invitrogen) according to manufacturer's protocol. Semiquantitative RT-PCR analysis was performed using 10 μg RNA, which was digested with DNase I (NEB catalog no. M0303L) to remove any contaminating genomic DNA. cDNA synthesis reactions were performed using the Bio-Rad iScript cDNA synthesis kit (catalog no. 170-8891) according to the manufacturer's protocols. Fifty nanograms of cDNA was used per reaction to amplify specific fragments using gene-specific primers. The primers used are listed in Table S2 where Actin cDNA served as a loading control. Control and mutant strains were grown on solid

inoculated on solid GMM supplement with NAM and GMM supplemented with NAM and Trp and cultured at 37 °C for 84 h in triplicates.

3.3.8 RT-PCR.

Total fungal RNA was extracted with mortar and pestle in the presence of liquid nitrogen. The resulting powder was suspended in TRIzol (Invitrogen) and transferred to a 1.5 ml tube, and gently vortexed and inverted two or three times to homogenize the sample. RNA samples were reverse transcribed with the High capacity cDNA Reverse Transcription Kit (Applied Biosystems) according to the manufacturer's protocol. Real-time RT-PCR was performed using the 7500 Fast Real-Time PCR System (ThermoFisher) and FAST SYBR Green Master Mix (Applied Biosystems) following the manufacturer's directions. Real-time PCR reactions for single genes were performed using 100ng of reverse transcribed RNA, FAST SYBR Green Master Mix and gene-specific primers (sequence reported in Table S3). Total murine RNA was extracted from purified cells or different organs by the TRIzol method (Invitrogen) according to the manufacturer's protocol. All reactions were repeated at least three times independently and normalized with *18S* and *β-actin* gene expression for fungi and mouse studies respectively.

3.3.9 Invitro Killing and Phagocytosis Assay

Thioglycolate-induced peritoneal polymorphonuclear (PMN) cells were obtained from naïve C57BL/6 mice. PMN were plated at final concentration of 1×10^6 cells/well in 96-well plates, and fungicidal assays were performed incubating cultures at 37°C for 2h at 1:1 *A. fumigatus*:PMN ratio. The wells were washed with PBS-diluted TRITON X-100 (Sigma Aldrich) to lyse PMNs. Lysate suspensions were diluted and grown in Sabouraud agar overnight at 37 °C in individual plates. The percentage of CFU inhibition (mean ± SE) was determined as: percentage of colony

formation inhibition = 100 − (CFU experimental group/CFU control cultures) × 100. All assays were done with five wells per condition in more than three independent experiments.

Thioglycolate-induced peritoneal PMN cells were challenged with two conidia and were subsequently incubated at 4°C for 2 h. After culture, cells were put under centrifugation (7 min, 700 rpm), and cytospins were stained with May-Grünwald-Giemsa (Bio Optica). At least 200 PMNs per sample were counted under oil immersion microscopy (100×). All images were visualized using a BX51 Olympus equipped with a high-resolution DP71 camera (Olympus). One hundred randomly chosen cells were examined microscopically to calculate the number of PMNs with at least one associated conidium. Results are expressed as phagocytic index, where the average number of conidia phagocytized per 100 neutrophils, or as percentage of phagocytosis, the percentage of neutrophils containing at least 1 conidium. The experiments were repeated twice for each fungal species with two different primary cultures.

3.3.10 Infections

Female C57BL/6 8-10-week-old mice were purchased from Charles River. Homozygous *Ido1*$^{-/-}$ mice on a C57BL/6 background were bred under specific pathogen-free conditions at the Animal Facility of Perugia University. Mice (n=18) were anesthetized before instillation (for three consecutive days) of a suspension of 2×10^7 resting conidia per 20 µl of saline intranasally of the *Aspergillus* CEA17 *akuB*^{KU80} wild-type or the different Δ*ido* mutant strains. Mice were monitored for fungal growth and lung inflammation and histology. The extent of infection was measured by euthanizing mice at 7 or 14 days post infection, removing the lungs and culturing serial dilutions of the homogenized tissue on Sabouraud agar plates, in triplicate, to allow calculation of the mean number of colony-forming units per organ (c.f.u. per organ; mean ± s.d.).

3.3.11 Histology

For histology, lungs were removed and immediately fixed in 10% neutral buffered formalin (Bio-optica) for 24 h. Lungs were then dehydrated, embedded in paraffin, sectioned into 3–4 μm slices and stained with periodic acid-Schiff reagent (PAS), Alcian blue reagent or Masson reagent (Bio-optica). All images were visualized using a BX51 Olympus equipped with a high-resolution DP71 camera (Olympus) with a ×4, ×20 and ×40 objective with the analySIS image processing software (Olympus) or EVOS® FL Color Imaging System with a ×40 objective.

3.3.12 Cytokine detection

ELISAs were performed on lung homogenates or lung supernatants to measure cytokine production. IL-33, IL-17A, IL-4, IFN-γ and IL-10 were assayed using commercially available antibody pairs and standards from Biolegend and eBiosciences according to the manufacturer's protocol.

3.4 Results

3.4.1 Structure, function and regulation of *A. fumigatus* Ids

BLAST analysis showed that *A. fumigatus* has three *IDO*-related genes, namely, *idoA* (Afu3g14250), *idoB* (Afu4g09830), and *idoC* (Afu7g02010) (Fig. 1a). Phylogenetic analysis revealed that IdoA and IdoB were more closely related to each other than to IdoC (Fig. 1a), indicating that they might represent paralogues evolved from a common ancestral gene, a previously suggested for *A. oryzae*(7). IdoA and IdoB were the most similar to human IDO1 and IDO2, both of which showed considerable identity to IdoA (49–49.5%) and IdoB (49–49.9%) (Fig. 1b). IdoC had the lowest homology with the other two proteins (37–38%) as well as with human IDO1 and IDO2 (38.1%) (Fig. 1b).

To functionally analyze the specific roles of the different *A. fumigatus* Idos, we deleted their respective *IDO* gene (Fig. S1) and assessed single, double as well as triple mutants for biological activity. All three *ido* mRNAs were upregulated in minimal medium (MM) enriched in Trp (MM + Trp) (Fig. 1c). Genetic ablation of *idoA* and *B* contributed to kynurenine production (Fig. 2a-c and Fig. S1) and *de novo* NAD^+ biosynthesis (Fig. 2c), and fungal growth (Fig. 2a).

Since deletion of both IdoA and IdoB contributed to the *de novo* NAD^+ biosynthesis, we supplemented nicotinamide (NAM) to the growth medium to rescue this lethality via the activation of the NAD+ salvage pathway. We assessed fungal physiology on GMM+NAM media for germination difference (Fig. S3a) and observed no significant difference in these two media for wild type strain. Furthermore, no significant difference in germination was observed between wild-type and *ido* mutant strains (Fig. S3b). Interestingly, with the deletion of *idoA* gene, we observed an NAD auxotrophy, that could be slightly rescued with the addition of Trp. Since, *A. fumigatus ido* genes are highly induced on tryptophan supplemented media (Fig. 1c), the auxotrophy of *idoA* mutant was slightly rescued with some poor growth of *idoA* mutant on Trp supplementation (Fig. 2a). When both *idoA* and *idoB* were deleted, we were not able to rescue the NAD auxotrophy with Trp supplementation (Fig. 2a). Metabolic profiling of the wild type (*akuB* KU80) and the double and triple *ido* mutants show that kynurenine, a precursor in the *de novo* NAD+ pathway is not produced in the two mutants (Fig. 2b-c).

3.4.2 Ido deficiency increases *A. fumigatus* pathogenicity *in vivo*

To assess the impact of the metabolic adaptation on fungal pathogenicity *in vivo*, we infected C57BL/6 mice intranasally with the WT and fungal *ido* mutants; we then evaluated parameters of infection, inflammation, and immune responses. We found that all three fungal Idos transcriptionally expressed in infection (Fig. 3a). The *ΔidoA/B/C* mutant was more virulent, as

shown by decreased survival of mice (Fig. 3b), increased fungal burden (Fig. 3c), inflammatory cell recruitment on Broncho alveolar lavages (BAL) (Fig. 3d) and pathology (Fig. 3e) in the lungs, as well as by an altered inflammatory/anti-inflammatory cytokine balance (Fig. 3f).

Because susceptibility to phagocytosis and killing by effector phagocytes was not different between the *ΔidoA/B/C* mutant and the wild-type strain (Fig. S4a-b), these findings indicated that Ido deficiency contributes to inflammatory pathology *in vivo*. In particular, mice infected with each individual mutant survived infection and cleared the fungus in a manner similar to counterparts infected with wild-type *Aspergillus* (Fig. S5a-d), a finding only apparently arguing for a degree of redundancy among the three Idos. In fact, the double *ΔidoA/B* mutant showed more PMN recruitment (Fig. S5d). In highly susceptible mice to invasive aspergillosis, we also observed the highest virulence for the *ΔidoA/B/C* mutant compared to *A. fumigatus* control strain (Fig. 3b-f).

Trp metabolites along the kynurenine pathway pivotally contribute to the host's mucosal immune homeostasis as related to luminal microbiota(22). L-kynurenine, in particular, is known to contribute to immune tolerance at the host/fungal interface(23). To assess whether the observed failure to produce kynurenine *in vitro* could impact fungal pathogenesis *in vivo*, mice not competent for L-kynurenine production – namely, *Ido1*$^{-/-}$ mice – were infected with the wild-type or the Δ*idoA/B/C* mutant strain (Fig.3g-j). On comparing, indeed, the response of *Ido1*$^{-/-}$ mice challenged with either wild-type *A. fumigatus* or the triple *ido* mutant, we found that all 3 *A. fumigatus ido* genes were expressed in *Ido1*$^{-/-}$ mice infected with WT *A. fumigatus* (Fig. 3g) We also observed inflammatory pathology (Fig.3h) increased in the *Ido1*$^{-/-}$ mice harboring *A. fumigatus ido* mutant. Fungal burden increased in those mice as well (Fig. 3i). These data suggest that the *A. fumigatus* will produce an immunologically active L-kynurenine during infection that

contributes to the host response in the absence of a functional kynurenine pathway in the latter. However, besides lack of L-kynurenine production, other factors might reasonably contribute to the increased pathogenicity of the triple *Aspergillus* mutant in *Ido1*-deficient hosts.

3.4.3 Ido deficiency enhances *A. fumigatus* Indole pyruvate production in vitro and *aroH* expression *in vivo.*

The increased pathogenicity of the *A. fumigatus* ΔIdoA/B/C mutants led us to hypothesize that the production of other Tryptophan catabolites such as indole pyruvate could contribute to the increased pathogenicity of the ΔIdoA/B/C mutant. Tryptophan can also be metabolized via the indole pyruvate pathway, initiated through the transamination of Trp by aromatic aminotransferases (termed Aro8 and Aro9 in *S. cerevisiae*).(2) These aromatic aminotransferases are also involved in the synthesis of Phe and Tyr in *S. cerevisiae*, and their orthologs are present in *A. fumigatus* (AroH/AroI)(2). In *Candida* spp., where filamentation and pigment production play a role in virulence, the products of these enzymes have been described to influence both phenotypes(24). The deletion of *aro*8 in *C. glabrata* results in a reduced pigment production and leads to an increased sensitivity to hydrogen peroxide(24).

Indole-derivatives such as indole pyruvate and indole acetate production downstream of Trp breakdown occurs *via* the aromatic aminotransferases such as AroH and AroI in *A. fumigatus(2)* (Fig. 4a). Since this pathway is parallel to the Ido pathway, we assessed *aroH* and *aroI* expression in response to the addition of Trp in the WT control and in the *A. fumigatus ido* mutants (Fig. 4b). We observed higher *aroH* expression in the presence of Trp, and in the *idoA*, *idoA/B*, and *idoA/B/C* mutants even in the absence of Trp. The expression of *aroI* was transient, however, increased in the *idoA/B/C* mutant (Fig. 4b). The expression patterns of the *aroH* and *aroI* complements indole

pyruvate and indole acetate metabolite production (Fig. 4c). This suggested that the AroH/AroI pathway was activated also in the absence of Trp where Idos were inactive.

We then measured *aroH* expression in mice after infection with the Δ*idoA/B/C* mutant. Although undetectable in uninfected mice, *aroH* mRNA expression did increase in infection (Fig. 5a). This supported the notion that alternative tryptophan-derived metabolic products may enhance fungal pathogenesis *in vivo*, likely accounting for the higher pathogenicity of to the triple mutant as compared to single or double mutants over that of *ΔidoA/B* (Supplementary Fig. 5).

3.4.4 Deletion of *A. fumigatus aro* genes reduces fungal pathogenicity.

Little is known of any possible role of indolepyruvate or indole acetate, as downstream products of Aro activity, in lung inflammatory pathology. Therefore, we deleted *A. fumigatus aroH* and *aroI* (Supplementary Fig. 2) genes and infected mice with wild-type *A. fumigatus* and Δ*aroI*, Δ*aroH* and *ΔaroH/I*. The Δ*aroH*, Δ*aroI* and Δ*aroH/I* mutants did not display any growth differences in comparison to WT *A. fumigatus*. Mice infected with Δ*aroH*, Δ*aroI* and Δ*aroH/I* mutant strains showed minor inflammatory pathology occurring in the lungs (Fig. 5b-c), together with a reduced production of inflammatory cytokine, in particular IL-33, which represents a sign of epithelial damage given by the infection pathology in the lung (Fig. 5d).

3.5 Discussion

Originally identified in mammals, IDO-related proteins have been subsequently found in lower vertebrates, several invertebrates, fungi, and a number of bacterial species(8). While the affinity and catalytic efficiency for Trp catabolism of IDOs varies greatly among vertebrates and invertebrates(8), the high affinity and catalytic efficiency for Trp catabolism of fungal and mammalian IDOs suggest similar biological roles for those enzymes(8). The results of the present study demonstrate that, similar to mammalian IDO1 – and besides fulfilling the need for NAD^+

supply – fungal Idos have a significant impact on the host-fungal interaction. All 3 of the fungal Idos were inducted by Trp. The data in our current study suggests a complementary role for the the fungal kynurenine supply in maintaining lung immune homeostasis provided by the enhance inflammation observed upon the infection of fungal strains lacking Idos. The data also suggest a degree of mutualistic/symbiotic relationship between the fungus and its mammalian host in the lung. Whether the differences observed in protein structure between fungal and human IDOs may predict alternative pathways of activation remains to be defined.

Our results also show how the flux of Tryptophan pathways is altered upon the deletion of Idos, as the Ehrlich pathway of Trp degradation involving Aros is increased. These aromatic amino transferases are key enzyme in the transamination of Trp, and involved in generating among other metabolites, indolepyruvate(6). Therefore, opposing activation of fungal Aros via the loss of fungal Idos may further contribute to the host/fungi interplay in the lung (Fig. 5e).

All together, these results point to a previously undescribed mechanism of fungal adaptation, involving Trp catabolism *via* Ido and Aro. IdoA and IdoB contributed to L-kynurenine/NAD^+ production and the loss of IdoA and B drives tryptophan catabolism toward Indole pyruvates via Aros. Moreover, the assessment of metabolic molecules on fungal supernatants suggest that *Aspergillus* metabolites may impact host immune system during infection.

3.6 Acknowledgements

The Italian Grant “Programma per Giovani Ricercatori - Rita Levi Montalcini 2013”, the Specific Targeted Research Project FunMeta (ERC-2011-AdG-293714), the Italian Cystic Fibrosis Research Foundation (Research Project number FFC #22/2014), AIRC Investigator Grant #16851 and Telethon Research Grant GGP14042 supported this study. We would like to thank support from Dalai Lama Trust MSN178745 awarded to TC. We thank Dr. Cristina Massi-Benedetti for

digital art and editorial assistance. We thank Nir Osherov (Sackler School of Medicine, Tel Aviv University, Tel Aviv, Israel) for the hypoxic *Aspergillus* strains.

3.8 Figures

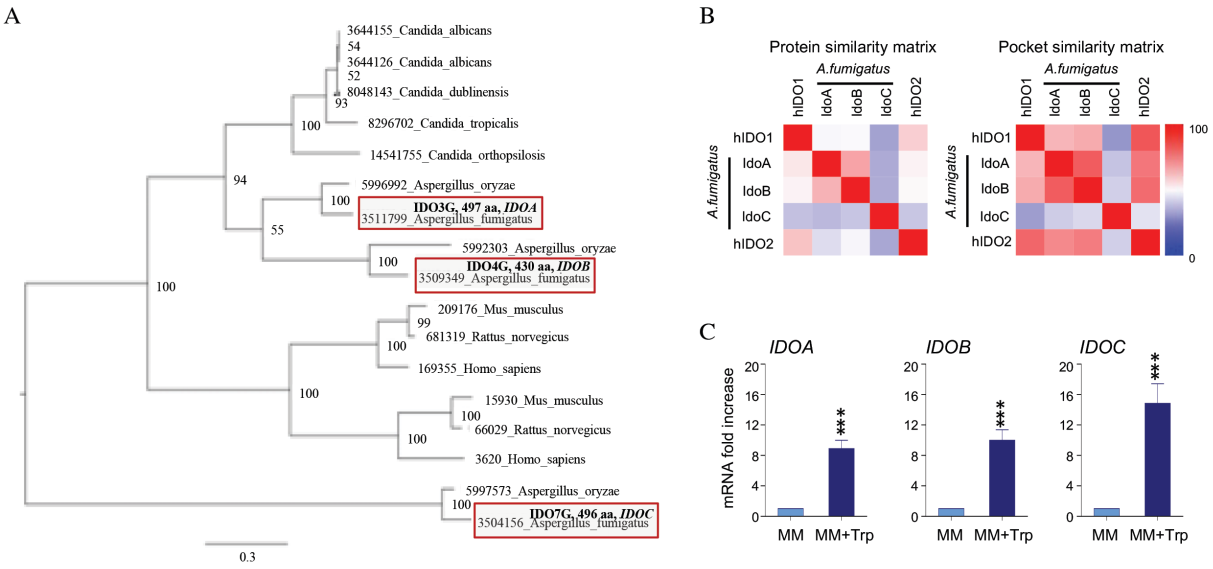

Figure 1. *Aspergillus fumigatus* Ids are expressed highly in the presence of L-Trp.

A. Maximum likelihood phylogenetic analysis of Ido proteins. **B.** Protein similarity and pocket matrix of human and *A. fumigatus* Ids. **C.** mRNA fold increase of *A. fumigatus idoA, idoB* and *idoC* in MM and MM+ Trp at 24h of culture. Data are represented as Mean±S.D of triplicate measurements. Statistical significance for C. (***P<0.0001) was determined comparing against MM.

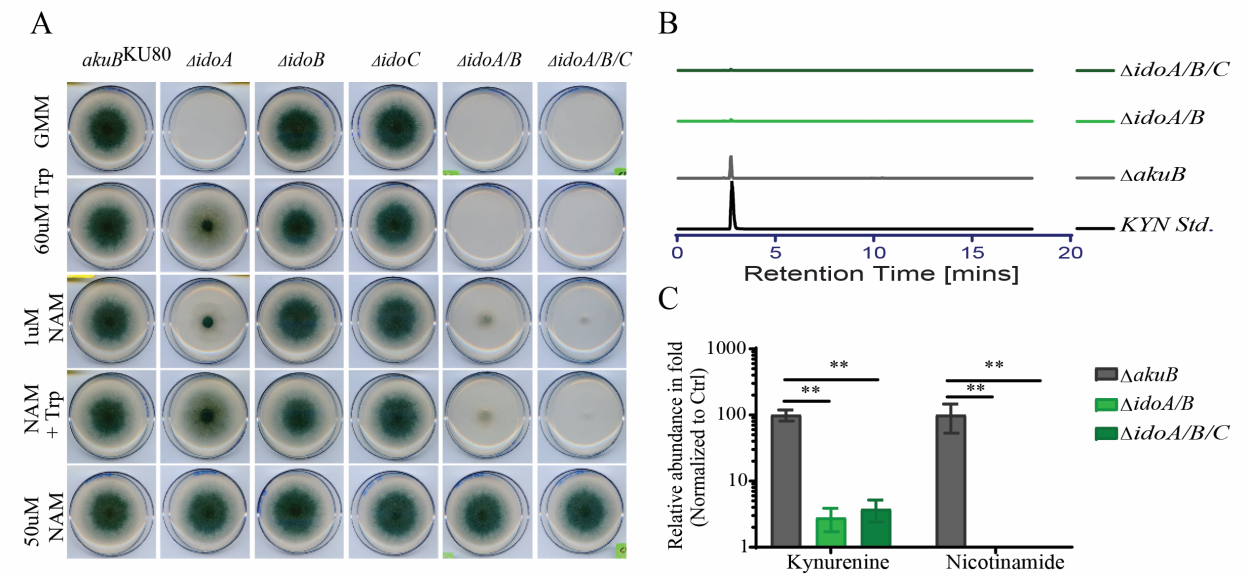

Figure 2. *Aspergillus fumigatus* Idos catabolize tryptophan for de novo NAD+ biosynthesis.

A. Colony morphologies of parental akuBKU80 (WT) and indicated mutant strains in MM, MM+ Trp, and MM+Nam. **B.** Peak levels of L-Kynurenine in *idoA/B* and *idoA/B/C* mutants in comparison to parental akuBKU80. **C.** Quantification of the loss of Kyn and Nicotinamide in *idoA/B* and *idoA/B/C* mutants in comparison to parental akuBKU80. Abbreviations: MM-Minimal Media; Trp-Tryptophan; NAM: Nicotinamide. Data are represented as Mean±SEM of triplicate measurements. Statistical significance for **C** (**P<0.001) was determined comparing against WT *akuB*^{KU80}.

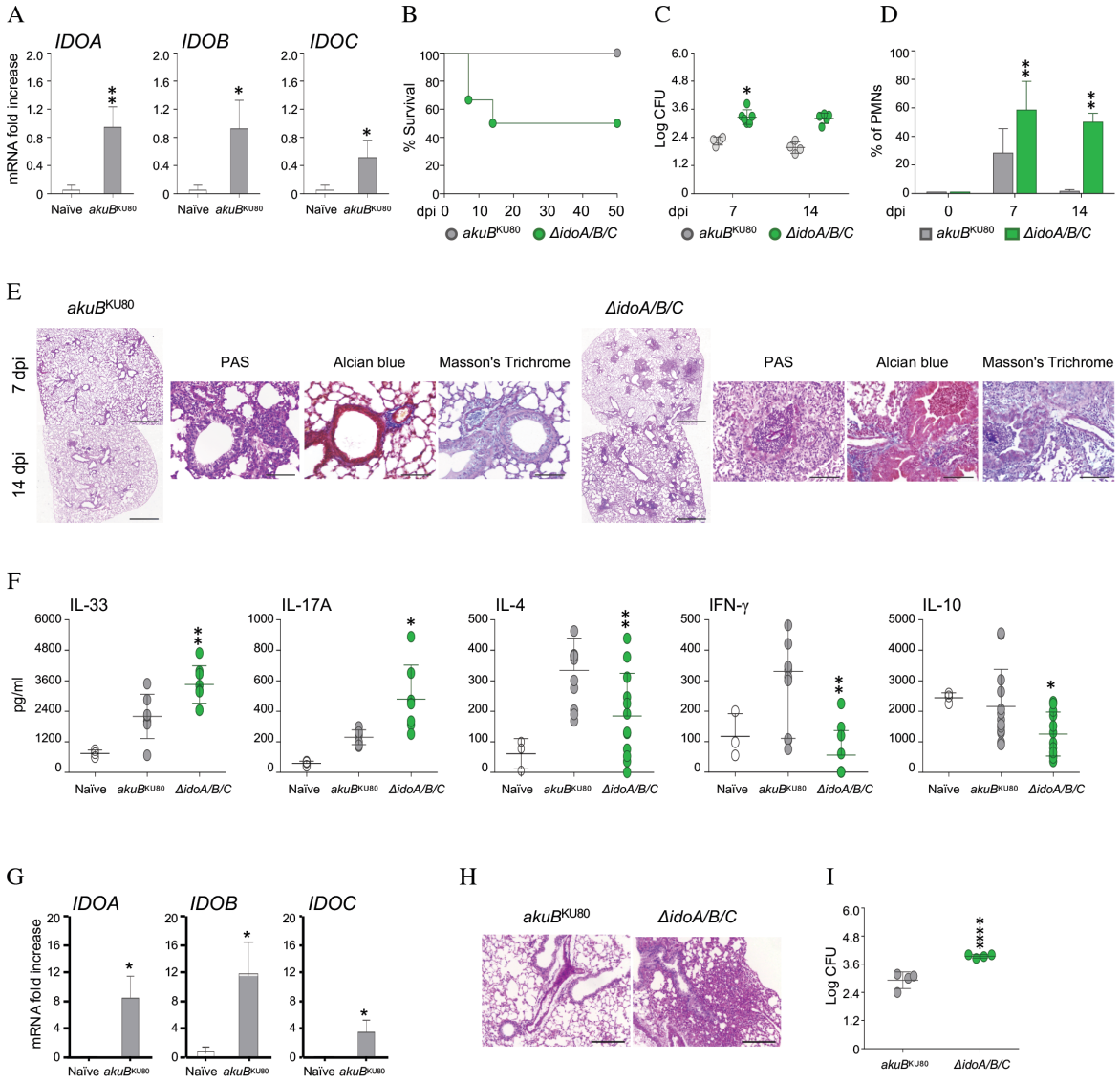

Figure 3. Loss of *Aspergillus fumigatus* Idos impacts on lung pathogenic inflammation in an invasive aspergillosis murine model.

A. mRNA fold change of IdoA, IdoB and IdoC at 7 days post fungal infection in the lung of wild type (C57/BL6) mice. **B.** Survival rates of C57/BL6 intranasally infected mice with the indicated strains. **C.** *A. fumigatus* cfu isolated from lungs of mice sacrificed at the indicated time points post-infection. **D.** Analysis of lung cells showing the percentage of pulmonary PMNs ($CD11b^+$ (FITC) and $GR1^+$ cells) at indicated days post infection. **E.** Histopathological analyses on lung tissue isolated from mice at 7 and 14 days post infection with PAS staining to visualize lung infiltrate, scale bar represents 20 µm (insets). Alcian blue for lung mucins and Masson's Trichrome for collagen deposition, scale bar represents 100µm. **F.** ELISA of indicated cytokines in total lung homogenate supernatant at 7 days post infection. **G.** *A. fumigatus idoA*, *idoB* and *idoC* mRNA expression during fungal infection in the lung of C57/BL6 and $Ido^{-/-}$ mice at 7 days post infection. **H.** Representative PAS stain histopathological analyses of lung infiltrate of $Ido^{-/-}$ mice infected with WT and IdoABC *A. fumigatus* mutants at 7 days post infection, scale bar represents 100µm. **I.** *A. fumigatus* cfu isolated from lungs of $Ido^{-/-}$ mice infected with WT and IdoABC *A. fumigatus* mutants at sacrificed at 7 days post infection. Data are represented as Mean±S.D of triplicate measurements. Statistical significance for **A, G,** and **I** (**P<0.001), (*P<0.01) was determined compared against naïve uninfected murine lung sample. Statistical significance for **C, D, and F** (***P<0.0001), (**P<0.001), (*P<0.01) was determined compared against mice infected with $akuB^{KU80}$.

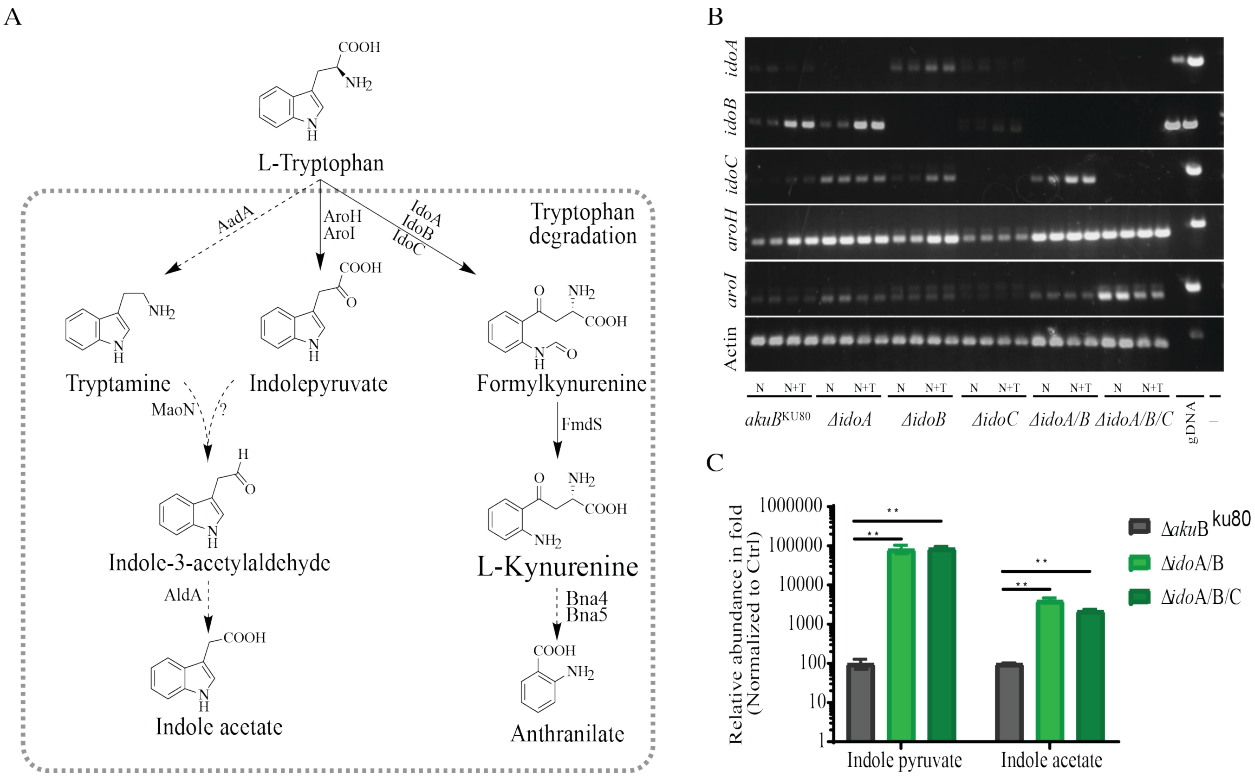

Figure 4. Aro as a backup pathway for loss of Ido in *A. fumigatus*.

A. Pathway depiction of Trp catabolism in *A. fumigatus* (modified from Choera et al. 2017 (2)). **B.** Semi qPCR gene expression of WT and *ido A. fumigatus* mutants. **C.** Quantification of the enhanced of Indole pyruvate and indole acetate metabolites in *idoA/B* and *idoA/B/C* mutants in

comparison to parental akuBKU80. Abbreviations: N: Nicotinamide; T: Tryptophan. Data are represented as Mean±SEM of triplicate measurements. Statistical significance for **C** (**P<0.001) was determined comparing against WT *akuB*^{KU80}.

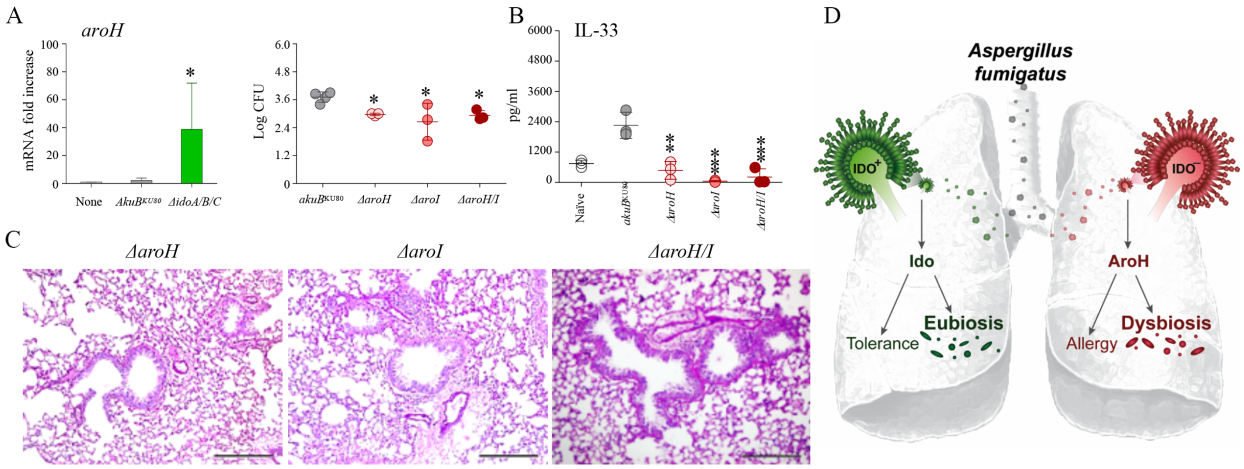

Figure 5. *A. fumigatus* Aro pathways impact on infection.

A. mRNA fold increase of *aroH* in indicated *A. fumigatus* strains at 7 days post infections. **B.** *A. fumigtus* cfu isolated from mice infected with WT and Aro *A. fumigatus* mutants sacrificed at 7 days post infection. **C.** Representative PAS staining of mice infected with indicated *A. fumigatus aro* mutants, scale bar represents 100µm. **D.** ELISA of IL-33 in total lung homogenate supernatant at 7 days post infection. **E.** Model of the role of *A. fumigatus* Ido in infection and inflammation. Data are represented as Mean±S.D of triplicate measurements. Statistical significance (***P<0.0001), (**P<0.001), (*P<0.01) was determined against mice infected with *akuB*^{KU80} (Two tailed Student's t Test unpaired parametric).

3.9 Supplemental Figures and Tables

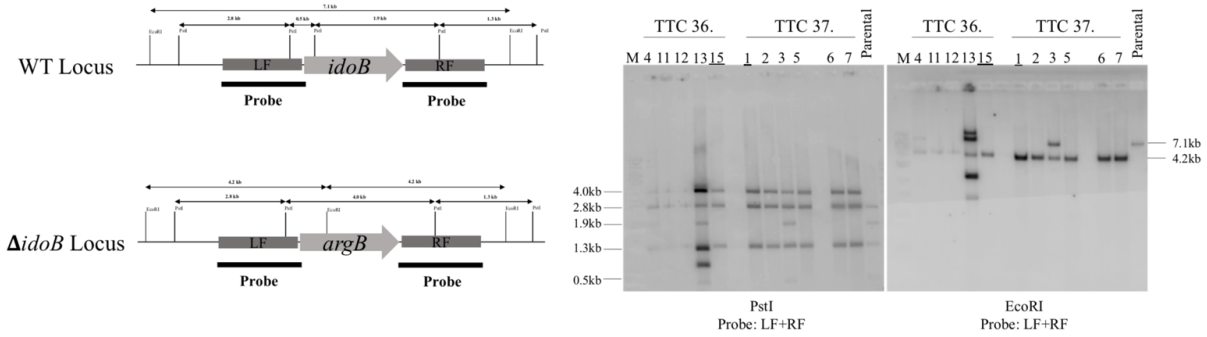

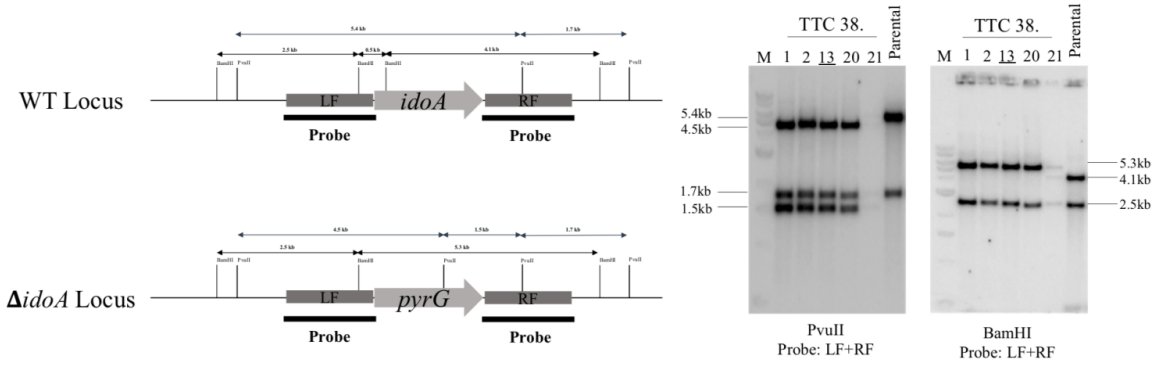

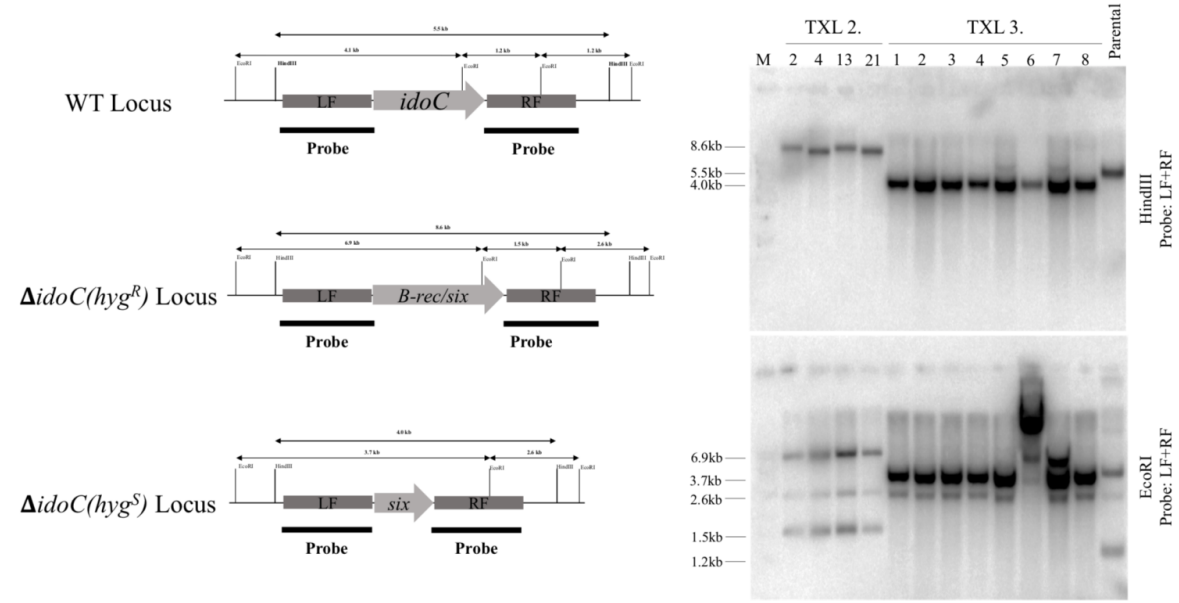

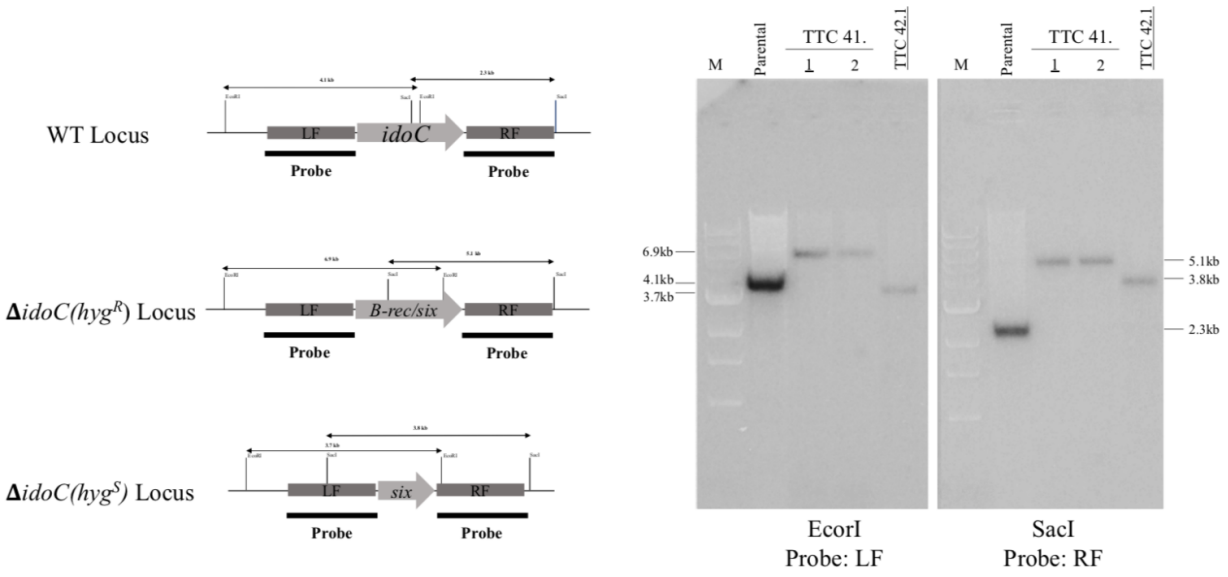

Figure S1. Southern confirmation of deletion of *A. fumigatus ido* mutants.

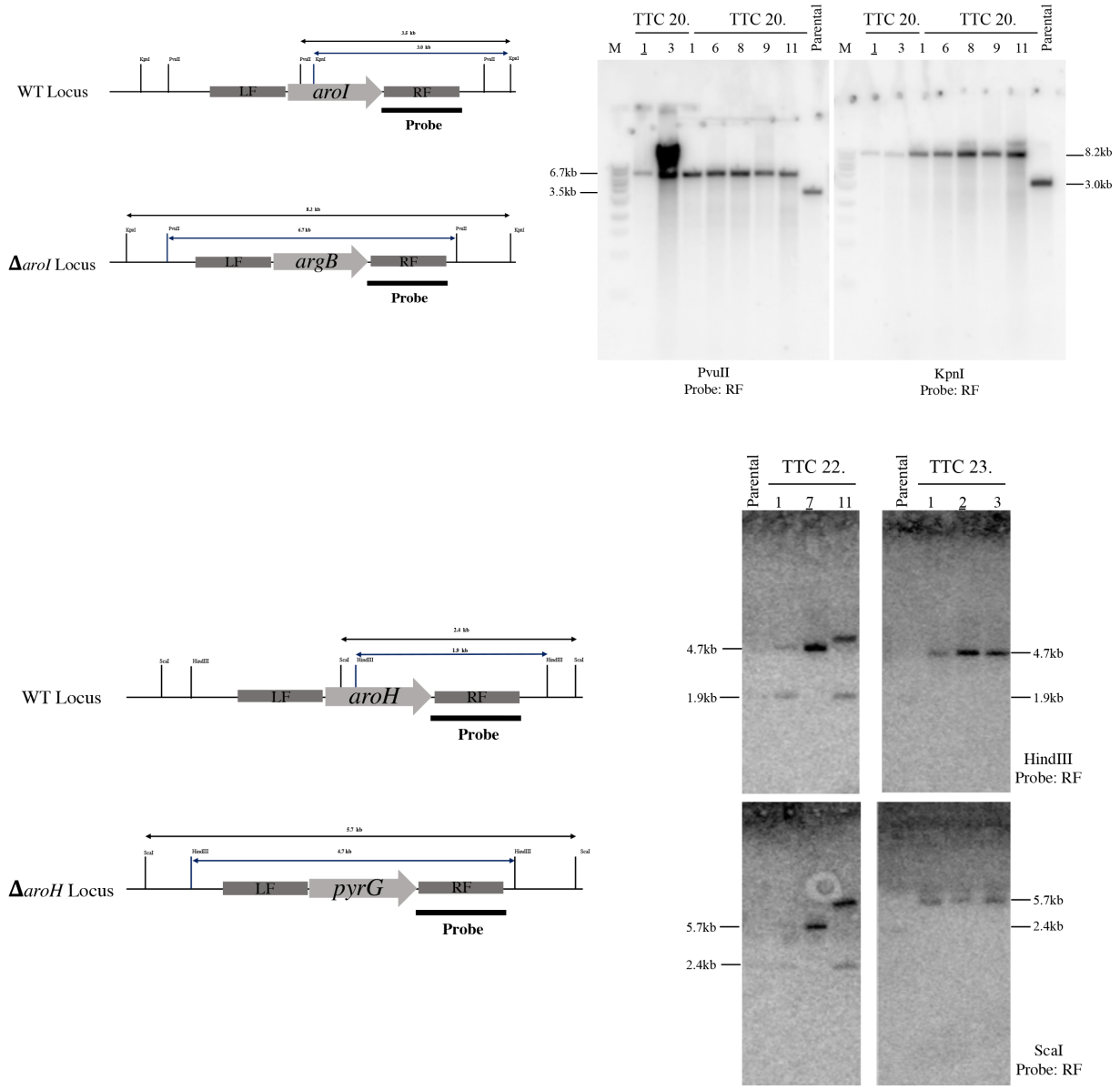

Figure S2. Southern confirmation of deletion of *A. fumigatus aro* mutants.

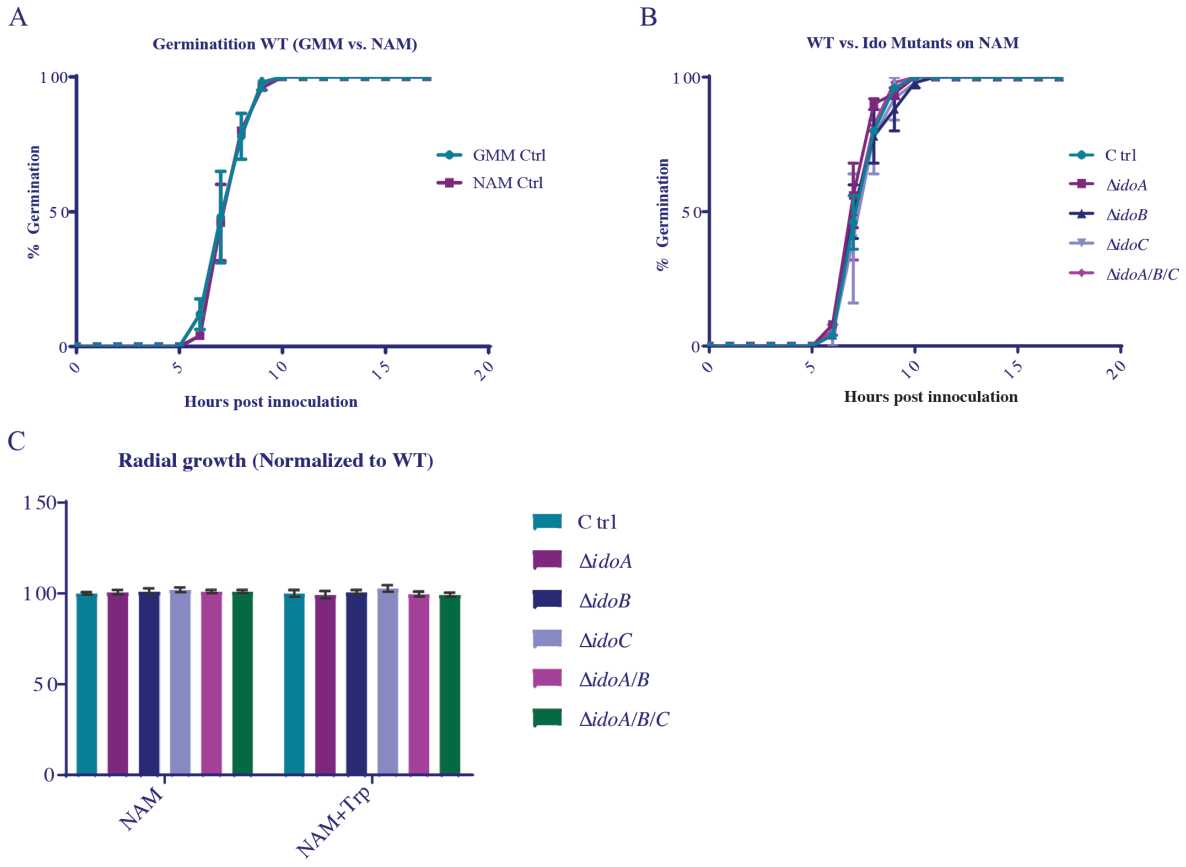

Figure S3. Germination assessment of *A. fumigatus ido* mutants.

A. fumigatus WT control on MM vs. MM+NAM (A); and *A. fumigatus ido* mutants vs. WT on MM+NAM. Radial growth (C) was also measured for *ido* mutants vs. WT on MM+NAM. Abbreviation: MM: Minimal media; NAM: Nicotinamide

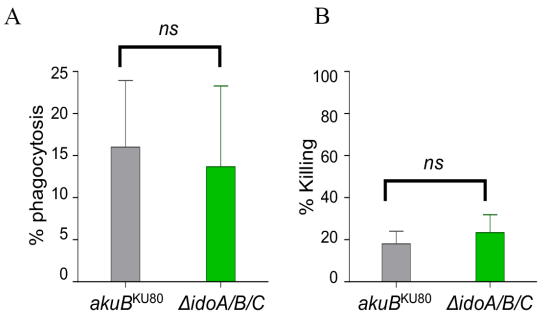

Figure S4. Macrophage interactions with *idoABC* mutants.

Macrophage phagocytosis (A) and Killing (B) of *A. fumigatus ido* mutants and WT control

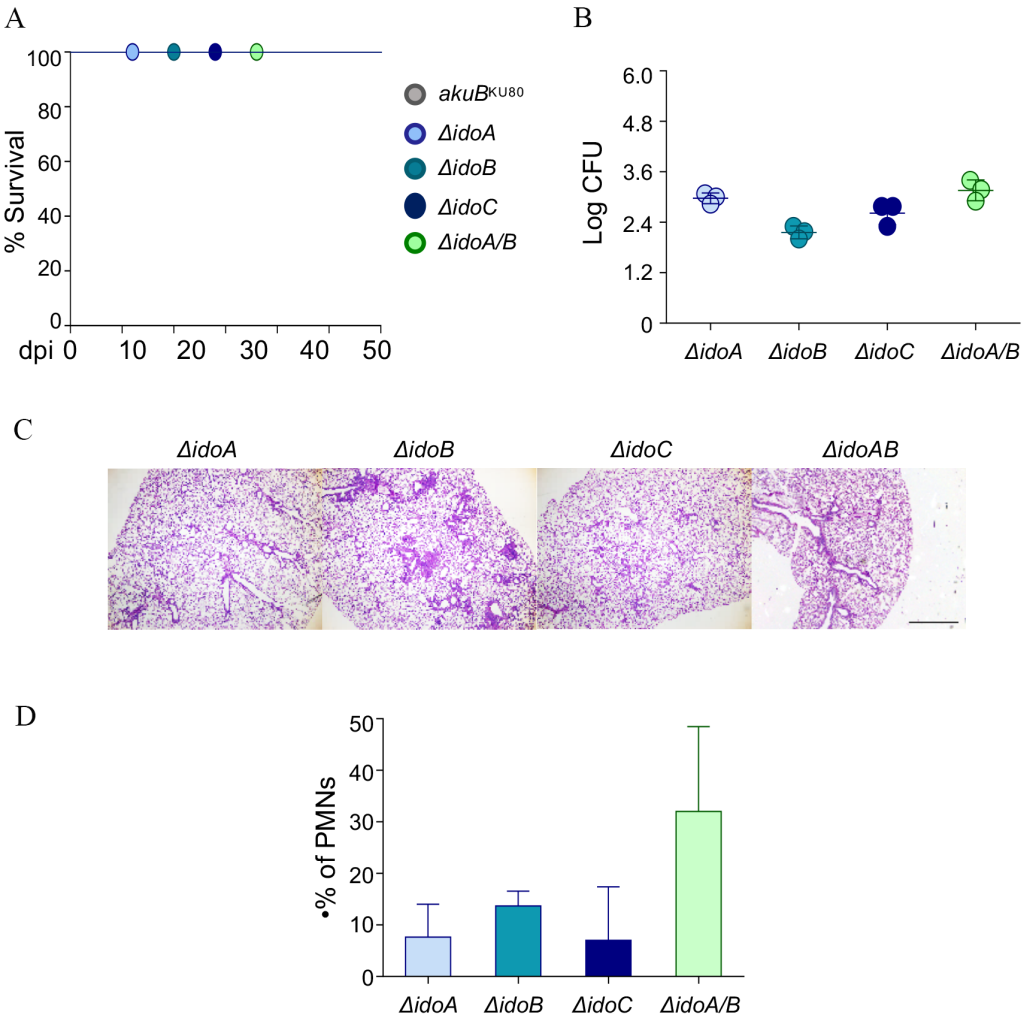

Figure S5. Virulence of *ido* mutants

Survival (A) of mice infected with *ido* mutants vs. WT. Fungal burden(B) in lungs of mice infected with with *ido* mutants vs. WT. Histopathology (C) of mice infected with with *ido* mutants vs. WT. PMN recruitment (D) of mice infected with *ido* mutants vs. WT.

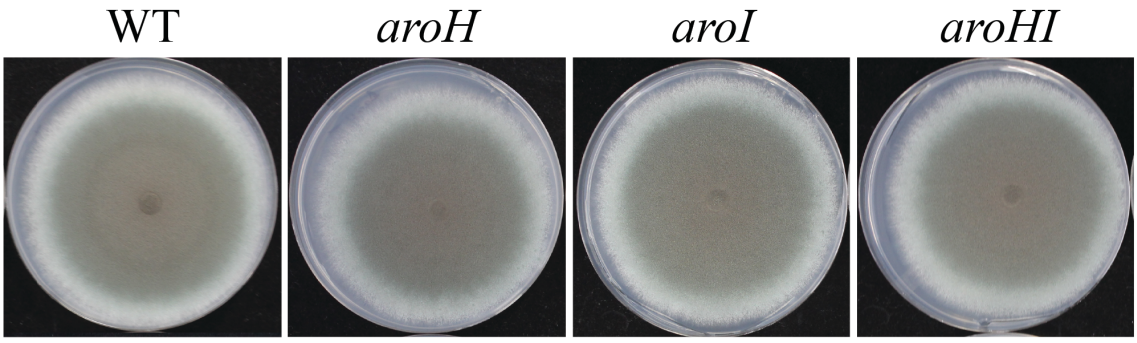

Figure S6. Radial growth of *A. fumigatus aro* mutant

Compared to WT grown on GMM for 5days at 37C.

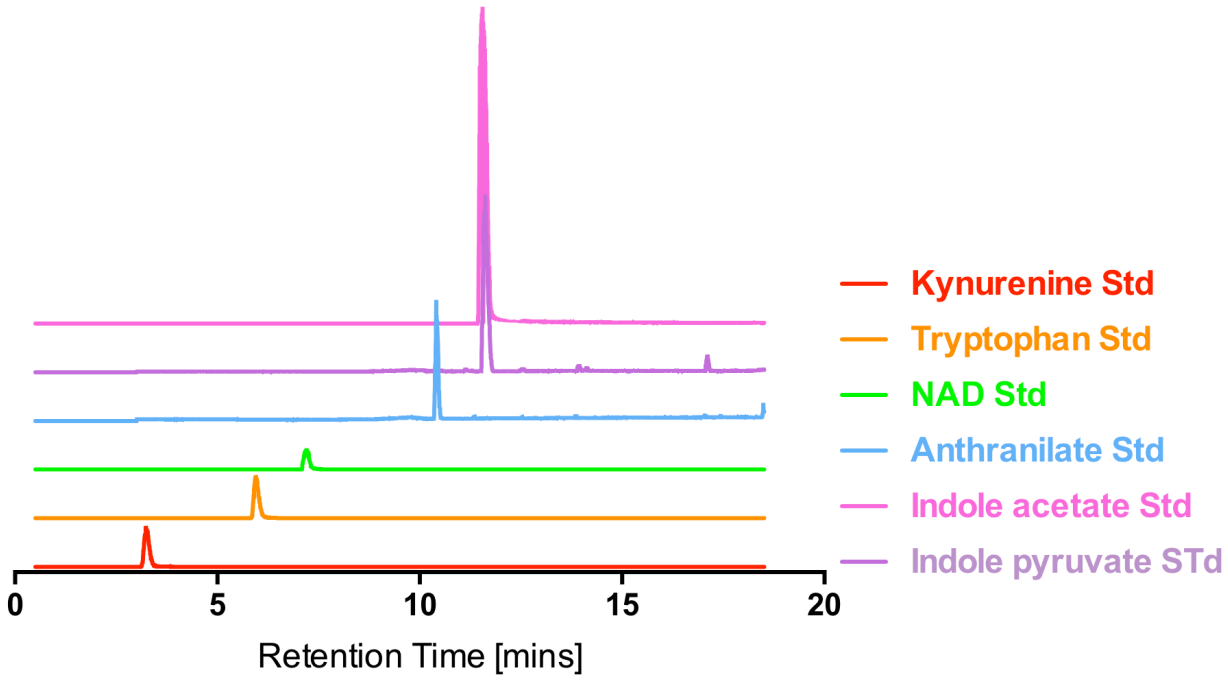

Figure S7. Traces of standards measured on LCMS.

Table S1. Fungal Strains used in this study

ID	Strain	Genotype	Reference
Control	CEA17 *pyrG*+ KU80	*pyrG1*, Δ*akuB*::*pyrG*	da Silva Ferreira et al., 2006
CEA17	CEA17 *pyrG*- KU80	*pyrG1,* Δ*akuB*::*pyrG, pyrG1*	da Silva Ferreira et al., 2006 (25)
TJG1.6	Δ*argB*	*pyrG1*, Δ*akuB*::*pyrG*, *pyrG1*, Δ*argB*::*pyrG*	Wiemann et al., 2017 (26)
TMN2.1	ΔΔ*argB/pyrG*	*pyrG1,* Δ*akuB*::*pyrG, pyrG1,* Δ*argB*::*pyrG*, Δ*pyrG*	Wiemann et al., 2017 (26)
TTC38.13	Δ*idoA*	*pyrG1,* Δ*akuB::pyrG, pyrG1, argB::pyrG,* Δ*AFUB_066940::argB*	This study
TTC37.1	Δ*idoB*	*pyrG1,* Δ*akuB::pyrG, pyrG1,* Δ*AFUB_034980::pyrG*	This study
TXL3.2	Δ*idoC*	*pyrG1,* Δ*akuB::pyrG, pyrG1,* Δ*argB::pyrG,* Δ*pyrG,* Δ*AFUB_088580::six, pyrG, argB*	This study
TTC39.5	ΔΔ*idoA/B*	*pyrG1,* Δ*akuB::pyrG, pyrG1,* Δ*argB::pyrG,* Δ*pyrG,* Δ*AFUB_034980::pyrG,* Δ*AFUB_066940::argB*	This study
TTC42.1	ΔΔΔ*idoA/B/C*	*pyrG1,* Δ*akuB::pyrG, pyrG1,* Δ*argB::pyrG,* Δ*pyrG,* Δ*AFUB_034980::pyrG,* Δ*AFUB_066940::argB,* Δ*AFUB_088580::six*	This study
TTC 21.6	Δ*aroI*	*pyrG1,* Δ*akuB::pyrG, pyrG1,* Δ*argB::pyrG,* Δ*akuB*::*pyrG,* Δ*AFUB_051500*::*argB*	This study
TTC 22.7	Δ*aroH*	*pyrG1,* Δ*akuB::pyrG, pyrG1,* Δ*AFUB_029280*::*pyrG*	This study
TTC 23.1	ΔΔ*aroH/I*	*pyrG1,* Δ*akuB::pyrG, pyrG1,* Δ*argB::pyrG,* Δ*pyrG,* Δ*AFUB_051500::argB,* Δ*AFUB_029280::pyrG*	This study
	*Δ*srbA*	*Afu2g01260::hph*	Vaknin Y. *et al.*, 2016 (27)
	*Δ*dscE*	*Afu1g14320::hph*	Vaknin Y. *et al.*, 2016 (27)
	*Δ*rbdA*	*Afu6g12750::hph*	Vaknin Y. *et al.*, 2016 (27)

Table S2. Primers used in this study

Number	Name	Sequence 5'- 3'	Associated Gene
TC-1131	TC-DAfu3g14250 F1	ATTACCCTGGATGCGTCAACG	*idoA*

TC-1134	TC-DAfu3g14250 R1	TTCGATATCAAGCTATCGATACCTCGACTC TGTAGGCAGGATTCAATGCAC	*idoA*
TC-1132	TC-DAfu3g14250 F2	CTGTCGCTGCAGCCTCTCCGATTGTCGAAT CCCGATCAGGGTATTGAGAGT	*idoA*
TC-1135	TC-DAfu3g14250 R2	TCGTGAAGAAGACTTCGGAGC	*idoA*
TC-1133	TC-DAfu3g14250 F3	ATTGACTACGTCCTCAAGGCTG	*idoA*
TC-1136	TC-DAfu3g14250 R3	TGTTTGAGATGCAGGACTGC	*idoA*
TC-1137	TC-diAfu3g14250 F	ATTGGCCAGGATATATTGTCTCC	*idoA*
TC-1138	TC-diAfu3g14250 R	GATCCGAGAGCCCCCTTAG	*idoA*
TC-20	Arg F	GAACGCGGTCTGCATCCAAG	*argB*
TC-21	ArgR	GAAGGAGAGACCCATACATCC	*argB*
TC-1113	TC-DAfu4g09830 F1	ACCAAGCTGCAAAATCGACG	*idoB*
TC-1114	TC-DAfu4g09830 R1	TGTCTTGGATGCAGACCGCGTTCTGTCGAA GCCAGAATATAAGGGGACG	*idoB*
TC-1115	TC-DAfu4g09830 F2	ATCAAATGGATGTATGGGTCTCTCCTTCAC TCATTTGAGTGGAAACTCAGC	*idoB*
TC-1116	TC-DAfu4g09830 R2	TTCGAAATCCAAATCAAGC	*idoB*
TC-1117	TC-DAfu4g09830 F3	ACTGGATTCCCGGAAGCAGG	*idoB*
TC-1118	TC-DAfu4g09830 R3	AGCCCATGGAACCGTTCTACG	*idoB*
TC-1119	TC-diAfu4g09830 F1	TCGCTGATTTACCAGCTCTGC	*idoB*
TC-1120	TC-diAfu4g09830 R1	TGCTGGAGTGTCCTTCGAACG	*idoB*
TC-4	pyrG_prom_F	CGTAATACGACTCACTATAGGG	*pyrG*
TC-5	pyrG_term_R	ATTCGACAATCGGAGAGGCTGC	*pyrG*
XL-1	DAfu7g02010 F1	TCGAGTTCGTTGCTTGGATGC	*idoC*
XL-2	DAfu7g02010 R1	CTATTGACCTATAGGACCTGAGTGATGCGG TAGAAGTTGACAAGAAGAGAG	*idoC*
XL-3	DAfu7g02010 F2	TAAGTTGAGCATAATATGGTCCATCTAGTG CTTGTCCGTAGATTGTGTAGGTAG	*idoC*
XL-4	DAfu7g02010 R2	GCAGGCTCCTGCTCTTCATCTT	*idoC*
XL-5	diAfu7g02010R	TGGTGTCACCATCAAGACCCA	*idoC*
XL-6	DAfu7g02010F3	TAGTTGGTGAGCTGTACGGTG	*idoC*
XL-7	DAfu7g02010R3	GCGTCTTTCGACATGTCTTCC	*idoC*
TC-1104	TC- DAfu2g13630F1	CGATTGTGCTAAACAACAGGGGC	*aroH*
TC-1105	TC- DAfu2g13630R1	GTCGCTGCAGCCTCTCCGATTGTCGAATTC AGAATACGATGCTCTCAAGTTCAGCCGG	*aroH*
TC-1106	TC-DAfu2g13630 F2	CGATATCAAGCTATCGATACCTCGACTCAC AATACCAACGCCATTTTTGTCTCCGCCG	*aroH*
TC-1107	TC-DAfu2g13630 R2	ATTGGCTATGGATCGAGATGGCC	*aroH*
TC-1108	TC-diAfu2g13630 F1	ACGGCATTCAAGCAGATCAACG	*aroH*
TC-1109	TC-diAfu2g13630 R1	AGTCATGCACTAGCCACACG	*aroH*

TC-1110	TC-diAfu2g13630F1	GCAGTGATATGTTCAAGAGCCC	*aroH*
TC-1111	TC-diAfu2g13630R1	CACGCTAATCTCTTCGAAAGGG	*aroH*
TC-1141	TC-DAfu5g02990 F1	TGAGGATGCAGGTTTACTGACAC	*aroI*
TC-1142	TC-DAfu5g02990 R1	GAAAATTTGTCTTGGATGCAGACCGCGTTC CTTGAGCAATCAAGTCCTTTACAGC	*aroI*
TC-1143	TC-DAfu5g02990 R3	TACTGATTTGGCTGGCAAGG	*aroI*
TC-1144	TC-DAfu5g02990F2	ATCAAATGGATGTATGGGTCTCTCCTTCTT GTTTATAATAGCATCGAGACG	*aroI*
TC-1145	TC-DAfu5g02990F3	AGGTTCAAAAGTGCCTGATCTTG	*aroI*
TC-1146	TC-DAfu5g02990R2	AGGTGGTCCCATAATCAAACG	*aroI*
TC-1147	TC-diAfu5g02990F	TGATTTCTATCGAAAAATGGTGG	*aroI*
TC-112	TC-Act 1 F2	CTTCCAGCCTAGCGTTCTG	*actA*
TC-113	TC-Act 1 R2	ATCCACATCTGCTGGAAGG	*actA*
TC-1206	IdoA qPCR F	ATGCTTCCTCCTATCCCCGCTC	*idoA*
TC-1207	IdoA qPCR R	GAGGGAGCTCTAGATGGTCGC	*idoA*
TC-1119	IdoB qPCR F	TCGCTGATTTACCAGCTCTGC	*idoB*
TC-1208	IdoB qPCR R	TGAAGAACCATTCTTCGTCCTTGG	*idoB*
TC-1210	IdoC qPCR F	AAAGTGGTCGATACCCTTGAGC	*idoC*
TC-1211	IdoC qPCR R	AACTCGTGTAGGATCTTGGTGAG	*idoC*
TC-1139	AroH qPCR F	TTCGTACCTGAGCCTAGATGTCG	*aroH*
TC-1140	AroH qPCR R	GATGCTTCTGCCAATCGATCTC	*aroH*
TC-1234	AroI qPCR F1	AACTGGGATTGCACCAAAGGACG	*aroI*
TC-1235	AroI qPCR R1	AGTCTCAGTAAGGCGGGTGATCC	*aroI*

Table S3. RT-PCR primers used in this study

GENE	**PRIMERS SEQUENCE (5'-3')**	**ANNEALING TEMPERATURE (°C)**
18S	Sense ➲ GAGCCGATAGTCCCCCTAAG αSense ➲ATGGCCGTTCTTAGTTGGTG	58
AroH	Sense➲AAAGTCCCGACAGCAATCTACA αSense➲TGGGACTTTCACGCTAATCTCT	60
IdoA	Sense ➲ ATGCCTGTCTCGCTATGC αSense ➲ CTCGGGTGTACGGTTTCG	55
IdoB	Sense➲ AGGAAGTTGTCGCTGATTTACC αSense ➲ ATGCTCGCCGCCATTCTG	54
IdoC	Sense ➲ TCAGCCAGGATGGCAGTC αSense ➲ TCGTCAGTCAGGTCAGGAAG	55
β-actin	Sense ➲ AGCCATGTACGTAGCCATCC αSense ➲ CTCTCAGCTGTGGTGGTGAA	59

Il33	Sense ➲ TCCTGCCTCCCTGAGTACAT	58
	αSense ➲ CACCTGGTCTTGCTCTTGGT	
Il4	Sense➲CGGCATTTTGAACGAGGTCACAGG	56
	αSense➲AGCACCTTGGAAGCCCTACAGACG	
Il17a	Sense ➲ GACTACCTCAACCGTTCCAC	56
	αSense ➲ CCTCCGCATTGACACAGC	
Cyp1a1	Sense ➲ ACAGTGATTGGCAGAGATCG	60
	αSense ➲ GAAGGGGACGAAGGATGAAT	
Il10	Sense ➲ CCCTTTGCTATGGTGTCCTT	56
	αSense ➲ TGGTTTCTCTTCCCAAGACC	
Foxp3	Sense ➲ CCCAGGAAAGACAGCAACCTTTT	59
	αSense ➲ TTCTCACAACCAGGCCACTTG	
pqsH	Sense ➲ TGATGTCGATGCCTTCCAGT	55
	αSense ➲CTCATCCAGCCCCTCCAGTA	

3.10 References

1. Yuasa HJ, Ushigoe A, Ball HJ. Molecular evolution of bacterial indoleamine 2,3-dioxygenase. Gene. 2011;485(1):22-31.
2. Choera T, Zelante T, Romani L, Keller NP. A Multifaceted Role of Tryptophan Metabolism and Indoleamine 2,3-Dioxygenase Activity in *Aspergillus fumigatus*-Host Interactions. Front Immunol. 2017;8:1996.
3. Grohmann U, Fallarino F, Puccetti P. Tolerance, DCs and tryptophan: much ado about IDO. Trends Immunol. 2003;24(5):242-8.
4. Metz R, Smith C, DuHadaway JB, Chandler P, Baban B, Merlo LM, et al. IDO2 is critical for IDO1-mediated T-cell regulation and exerts a non-redundant function in inflammation. International immunology. 2014;26(7):357-67.
5. Munn DH, Mellor AL. Indoleamine 2,3 dioxygenase and metabolic control of immune responses. Trends Immunol. 2013;34(3):137-43.
6. Wang PM, Choera T, Wiemann P, Pisithkul T, Amador-Noguez D, Keller NP. TrpE feedback mutants reveal roadblocks and conduits toward increasing secondary metabolism in *Aspergillus fumigatus*. Fungal genetics and biology : FG & B. 2016;89:102-13.
7. Yuasa HJ, Ball HJ. Indoleamine 2,3-dioxygenases with very low catalytic activity are well conserved across kingdoms: IDOs of Basidiomycota. Fungal Genet Biol. 2013;56:98-106.
8. Yuasa HJ, Ball HJ. Efficient tryptophan-catabolizing activity is consistently conserved through evolution of TDO enzymes, but not IDO enzymes. Journal of experimental zoology Part B, Molecular and developmental evolution. 2015;324(2):128-40.
9. Iraqui I, Vissers S, Cartiaux M, Urrestarazu A. Characterisation of *Saccharomyces cerevisiae* ARO8 and ARO9 genes encoding aromatic aminotransferases I and II reveals a new aminotransferase subfamily. Mol Gen Genet. 1998;257(2):238-48.
10. Brunke S, Seider K, Richter ME, Bremer-Streck S, Ramachandra S, Kiehntopf M, et al. Histidine degradation via an aminotransferase increases the nutritional flexibility of Candida glabrata. Eukaryot Cell. 2014;13(6):758-65.
11. Yuasa HJ, Ball HJ. Molecular evolution and characterization of fungal indoleamine 2,3-dioxygenases. Journal of molecular evolution. 2011;72(2):160-8.
12. Sugimoto H, Oda S, Otsuki T, Hino T, Yoshida T, Shiro Y. Crystal structure of human indoleamine 2,3-dioxygenase: catalytic mechanism of O2 incorporation by a heme-containing dioxygenase. Proceedings of the National Academy of Sciences of the United States of America. 2006;103(8):2611-6.
13. Laskowski RA, Rullmannn JA, MacArthur MW, Kaptein R, Thornton JM. AQUA and PROCHECK-NMR: programs for checking the quality of protein structures solved by NMR. Journal of biomolecular NMR. 1996;8(4):477-86.
14. Osherov N, Kontoyiannis DP, Romans A, May GS. Resistance to itraconazole in *Aspergillus nidulans* and *Aspergillus fumigatus* is conferred by extra copies of the *A. nidulans* P-450 14α-demethylase gene, *pdmA*. Journal of Antimicrobial Chemotherapy. 2001;48(1):75-81.

15. Shimizu K, Keller NP. Genetic involvement of a cAMP-dependent protein kinase in a G protein signaling pathway regulating morphological and chemical transitions in *Aspergillus nidulans*. Genetics. 2001;157(2):591-600.
16. Sambrook J, Russell D. Molecular cloning: a laboratory manual. Cold Spring Harbor, New York: Cold Spring Harbor Laboratory Press; 2001.
17. Szewczyk E, Nayak T, Oakley CE, Edgerton H, Xiong Y, Taheri-Talesh N, et al. Fusion PCR and gene targeting in *Aspergillus nidulans*. Nature protocols. 2006;1(6):3111-20.
18. Lim FY, Sanchez JF, Wang CC, Keller NP. Toward awakening cryptic secondary metabolite gene clusters in filamentous fungi. Methods in enzymology. 2012;517:303-24.
19. Calvo AM, Bok J, Brooks W, Keller NP. veA is required for toxin and sclerotial production in *Aspergillus parasiticus*. Applied and Environmental Microbiology. 2004;70(8):4733-9.
20. Palmer JM, Bok JW, Lee S, Dagenais TR, Andes DR, Kontoyiannis DP, et al. Loss of CclA, required for histone 3 lysine 4 methylation, decreases growth but increases secondary metabolite production in *Aspergillus fumigatus*. PeerJ [Internet]. 2013; 1:[e4 p.].
21. Muszkieta L, Aimanianda V, Mellado E, Gribaldo S, Alcazar-Fuoli L, Szewczyk E, et al. Deciphering the role of the chitin synthase families 1 and 2 in the in vivo and in vitro growth of *Aspergillus fumigatus* by multiple gene targeting deletion. Cell Microbiol. 2014;16(12):1784-805.
22. Santhanam S, Alvarado DM, Ciorba MA. Therapeutic targeting of inflammation and tryptophan metabolism in colon and gastrointestinal cancer. Translational research : the journal of laboratory and clinical medicine. 2016;167(1):67-79.
23. Romani L, Fallarino F, De Luca A, Montagnoli C, D'Angelo C, Zelante T, et al. Defective tryptophan catabolism underlies inflammation in mouse chronic granulomatous disease. Nature. 2008;451(7175):211-5.
24. Rao RP, Hunter A, Kashpur O, Normanly J. Aberrant synthesis of indole-3-acetic acid in *Saccharomyces cerevisiae* triggers morphogenic transition, a virulence trait of pathogenic fungi. Genetics. 2010;185(1):211-20.
25. da Silva Ferreira ME, Kress MR, Savoldi M, Goldman MH, Hartl A, Heinekamp T, et al. The akuB(KU80) mutant deficient for nonhomologous end joining is a powerful tool for analyzing pathogenicity in *Aspergillus fumigatus*. Eukaryot Cell. 2006;5(1):207-11.
26. Wiemann P, Perevitsky A, Lim FY, Shadkchan Y, Knox BP, Landero Figueora JA, et al. *Aspergillus fumigatus* Copper Export Machinery and Reactive Oxygen Intermediate Defense Counter Host Copper-Mediated Oxidative Antimicrobial Offense. Cell Rep. 2017;19(10):2174-6.
27. Vaknin Y, Hillmann F, Iannitti R, Ben Baruch N, Sandovsky-Losica H, Shadkchan Y, et al. Identification and Characterization of a Novel *Aspergillus fumigatus* Rhomboid Family Putative Protease, RbdA, Involved in Hypoxia Sensing and Virulence. Infect Immun. 2016;84(6):1866-78.

CHAPTER 4

Environmental origins of *Aspergillus fumigatus* alter the preloaded metabolic state of the spore and long lasting, subsequent virulence.

Tsokyi Choera, Alysia Vang, Nancy P. Keller. [In Prep]

I designed and conducted all the experiments in this chapter with assistance from my undergraduate Alysia Vang. The RNA Sequencing was conducted through Protein CT- a paid service

4.1 Abstract

Aspergillus fumigatus disease is primarily initiated upon the inhalation of the ubiquitous airborne conidia – the initial inoculum – produced by *A. fumigatus.* This opportunistic pathogen is able to thrive and grown on diverse substrates ranging from soils, decaying animal/vegetative matter to building materials. Subsequently the conidia derived from these various environmental milieus are prepacked with metabolic pools reflective of their substrate. We found ranges in the metabolic profiles of a single isolate of *A. fumigatus* grown on different substrates. Using a triamcinolone murine model of invasive aspergillosis, we investigated one of the substrates in detail (minimal medium grown spores versus spores harvested from $_{L}$-Trp+ amended medium). Infection with $_{L}$-Trp+ spores resulted in significantly higher virulence compared to wild type spores. To gain an understanding of the metabolic processes leading to long lasting and increased virulence of $_{L}$-Trp+ spores, RNA-Seq profiles were analyzed between $_{L}$-Trp+ and wild type spores. Strikingly, there was an ~ 5-fold upregulation of all 14 of the core mitochondrial genes encoding members of the respiration oxidative phosphorylation complex. Nuclear upregulated genes included two prominent tryptophan catabolic pathways: the fumigaclavine biosynthetic cluster genes and a critical member of the NAD *de novo* pathway. Gene expression correlated with increases in fumigaclavine (~ 7-fold) production and the *de novo* pathway metabolites kynurenine (~ 60-fold) and NAD+ (~ 2-fold). Increased virulence was not associated with fumigaclavine production however, as $_{L}$-Trp+ grown fumigaclavine-null strains were still more virulent than wild type. instead, we found that enhanced mitochondrial respiration is a likely contributor to the virulence attributes of $_{L}$-Trp+ spores, as indicated by the increased tolerance of $_{L}$-Trp+ spores to the cytochrome C oxidase inhibitor KCN. Considered all together, this work strongly supports a view

that *A. fumigatus* virulence is a function of the preloaded metabolic state of the spore and hence a consequence of the environmental origin of inocula.

4.2 Introduction

Over the past decades, there has been a marked increase in the incidence of fungal infections (1, 2). Invasive fungal infection caused by the ubiquitous mold *Aspergillus fumigatus* is the most common filamentous fungal infection in susceptible patient populations (3, 4). Invasive aspergillosis can develop in immunocompromised patients including those undergoing steroid or chemotherapy treatments, bone marrow or solid-organ transplantations, or those with hematologic malignancies. Poor prognosis and limited treatment options lead to very high mortality rates (5). While it is known that the status of the host immune system (i.e. host heterogeneity) can influence disease outcomes, recent studies have highlighted how intraspecies heterogeneity (i.e strain heterogeneity) influence fungal pathogenesis (6-9). This notion of strain heterogeneity has been observed not only in *A. fumigatus* strains, but also in other medically important fungal pathogens with intra-species genetic and phenotypic differences in *Candida albicans and in Cryptococcus neoformans strains (6, 10). In C. albicans, an evaluation of 21 different strains revealed* marked differences in virulence, growth rates, filamentation, biofilm formation, stress resistance, and resistance to antifungal drugs *(10)*. In *C. neoformans* studies revealed 54 clinical isolates exhibited difference in capsule size, growth rate, and resulted in variable virulence in mice (6). Similarly in a comparative study of *A. fumigatus* strains isolated from the international space station revealed normal *in vitro* growth and chemical stress tolerance yet caused higher lethality in a zebrafish model of invasive disease, when compared against two commonly utilized patient derived strains, Af293 and CEA10 (9). Furthermore, differences in virulence between Af293 and CEA10 have been observed in triamcinolone-immunosuppressed mouse model, where CEA10 is more virulent(8, 9). The investigations of strain heterogeneity of *A. fumigatus* has led to several factors including germination differences (11), altered activation of the host immune response (11, 12),

secondary metabolism (13, 14), and response to light (15). A recent study also highlighted the increased fitness in hypoxia of the CEA10 strain *in vitro* led to a better fungal infection *in vivo* as hypoxia is a hallmark of the microenvironment in a triamcinolone immunosuppressed murine model (8).

While these previous studies have established that host susceptibility along with strain heterogeneity is crucial for establishing an infection, the function of environmental conditions (specifically growth substrates) remains to be explored further. *Aspergillus fumigatus* produces abundant airborne spores that have a worldwide distribution and can therefore survive in a very diverse range of environment exposed to continuous stressors, both in the environment and in the host (7, 13). While growing in compost, *A. fumigatus* is commonly found at temperatures exceeding 50C, whereas in the host, the fungus is subjected to nutrient deprivation, hypoxia, and oxidative stresses (16-19) . There is growing body of evidence that different environment such as temperature and light can influence disease outcomes (13, 15). Additionally, in several insect pathogens, growth substrates yielded differentially virulent conidia (20). These studies present a plausible impact of the growth substrate in priming *A. fumigatus* spores fitness to enhance survival and thrive within the harsh host's microenvironment.

In our study, we hypothesized that the heterogeneity of the *A. fumigatus* growth substrate contributes to a preloaded, more metabolically primed spore leading to a more aggressive infection. We show that WT (Af293) spores grown on varied substrates yield a different metabolite profile and expand on one of them, a defined minimal media supplemented with the essential amino acid, Tryptophan ($_{L}$-Trp). The conidia derived from $_{L}$-Trp led to higher virulence in triamcinolone immunosuppressed murine model. The metabolite profile of the supplementation of $_{L}$-Trp resulted in a higher fumigaclavine synthesis but doesn't account for the virulence

phenotype observed with the L-Trp supplementation. With transcriptional profiling of the spores grown on the minimal media with or without L-Trp, we show a strong correlation between the mitochondrial activity and virulence.

4.3 Materials and Methods

4.3.1 Ethics Statement

We carried out our animal studies in strict accordance with the recommendations in the *Guide for the Care and Use of Laboratory Animals* (21). The animal experimental protocol was approved by the Institutional Animal Care and Use Committee (IACUC) at University of Wisconsin-Madison (Protocol # M005786-A02).

4.3.2 Strains and medium.

The genetic background of the primary strain used in this study is *A. fumigatus* Af293 (22). All strains were maintained as glycerol stocks at -80 °C and activated on solid glucose minimal media (GMM) at 37 °C (23). Growth media was supplemented with 1.26 g/L uridine and 0.56 g/L uracil for *pyrG* auxotrophs. All media supplemented with tryptophan, tyrosine, or phenylalanine utilized a concentration of 5mM. Blood media is blood agar plates obtained from Thermo Fischer. Grass media was made utilizing fresh grass cutting and adding agar (16g/L); this media was autoclaved for one hour prior to plating.

4.3.3 Genetic manipulations for *A. fumigatus dmaW* mutant

Fungal DNA extraction, gel electrophoresis, restriction enzyme digestion, Southern blotting, hybridization and probe preparation were performed according to standard methods (24). For DNA isolation, *A. fumigatus* strains were grown for 24 h at 37 °C in static liquid GMM, supplemented as needed for auxotrophs. DNA isolation was performed as described by Sambrook and Russell (24). Gene deletion mutants in this study were constructed by targeted integration of the deletion

cassette through transformation (25, 26). The deletion cassettes were constructed using a double-joint fusion PCR (DJ-PCR) approach (25, 26). *A. fumigatus* protoplast generation and transformation were carried out as previously described (25, 26). The primers used in this work are listed in Table S1. An *A. fumigatus dmaW* (Afu2g18040) disruption consisted for the following: two 1 kb fragments flanking the ORF were amplified from Af293 genomic DNA using the primer pair TC-1149/ TC-1151/1152, respectively (Table S2). The selection marker, *A. parasiticus pyrG*, was PCR amplified from plasmid pJW24 (27) using the primer pair TC-4/TC-5 (Table S2). A nested primer sets TC1153/1154 were used to during the 3rd round of PCR. The deletion construct was transformed into Af293.1 (*pyrG1*). Transformants were selected for pyrimidine prototrophy in media without any supplements. Transformants obtained were verified by PCR using primers pairs TC-1155/1156, and Southern analysis using the flanking probes (Fig. S1). The obtained mutants were named TTC31.x (Δ*dmaW*), and TTC31.15 was chosen for further experiments.

4.3.4 Physiology experiments

Colony diameters of strains were measured after 3, 5, and 7 days of growth at 37 °C on solidified GMM, GMM supplemented with indicated aromatic amino acids, blood, and grass media. Strains were point-inoculated onto the media at 10^4 conidia total (in 5 μL). For germination, spores were collected from GMM with and without Trp grown at 37C for 5 days. Spore were washed twice prior to the germination assay. Germination was assessed as described in Fischer et. al in static liquid GMM (28). When KCN was added, it was added at a final concentration of 1mM (16). Briefly 1×10^5 spores/mL in GMM and GMM (or with KCN) were inoculated into each well of a Costar® 24-well dish (Corning, Corning, NY, USA). Microscopic images were captured using a Nikon Eclipse T*i* inverted microscope equipped with an OKO-Lab microscopic enclosure to

maintain the temperature at 37°C for *A. fumigatus* (OKO Lab, Burlingame, CA, USA). Germinated spores were observed using a Nikon Plan Fluor 20xPh1 DLL objective and phase-contrast images captured every 1–2 h using the Nikon NIS Elements AR software package (v. 4.13). A spore is noted to be germinating if an emerging germ tube was clearly present. One hundred spores were observed for each strain ($n = 3$) and growth condition. Values in figures represent the average percentage of spores germinated ± SEM. The Student *t*-test was carried out to determine statistical significance using the GraphPad Prism software (La Jolla, CA, USA).

4.3.5 Secondary metabolites extraction and analysis

Secondary metabolites of strains were extracted after 7 days of growth at 37 °C on solidified GMM, GMM supplemented with indicated aromatic amino acids, blood, and grass media. Strains were point-inoculated onto the media at 10^4 conidia total. Agar cores (1.5 cm in diameter) were prepared in triplicate for each strain cultured. Three cores from each plate were extracted with 2.5 mL of ethyl acetate. The solvent was evaporated and suspended in 500 µL 19.5/79.5/1 (v/v/v) acetonitrile/water/formic acid. Subsequently, the samples were filtered using a 0.45 µm PTFE Mini-UniPrep filter vial (Agilent) and 50 µL of the filtrate analyzed by high-performance liquid chromatography (HPLC) (Perkin Elmer) coupled to a photo diode array (PDA) as described by Wiemann et al. (29). For secondary metabolites extracted from spores only, conidial fraction was harvested following the protocol in Lim *et al*., (30).

4.3.6 RNA isolation and RNA Sequencing

Total RNA was extracted with QIAzol reagent (Qiagen) from spores grown on MM (with or without Trp) following the manufacturer's protocol and further purified using silica membrane spin columns from the RNeasy Plant minikit (Qiagen). Total RNA was subjected to DNase I digestion to further remove genomic DNA contamination. RNA was sent out to be sequenced and

analyzed by Protein CT (http://www.proteinct.com/). Libraries were prepared using the Illumina TruSeq strand specific mRNA sample preparation system (Illumina). Briefly, mRNA was extracted from total RNA using polyA selection, followed by RNA fragmentation. Strand specific library was constructed by first-strand cDNA synthesis using random primers, sample cleanup and second-strand synthesis using DNA Polymerase I and RNase H. A single 'A' base was added to the cDNA fragments followed by ligation of the adapters. Final cDNA library was achieved by further purification and enrichment with PCR, quality checked using Bioanalyzer 2100. The libraries were sequenced (Single end 100bp reads) using the Illumina HiSeq4000, final of around 30-60 million reads per sample.

4.3.7 RNA Sequencing Data QC and analysis

The fastQC program was used to verify raw data quality of the Illumina reads. The latest A_fumigatus_Af293 genome and gene annotations (version s03_m05_r08) were downloaded from AspGD and used for mapping. The raw sequence reads were mapped to the genome using Subjunc aligner from Subread (31), with majority of the reads (over 96% for all samples) aligned to the genome. The alignment bam files were compared against the gene annotation GFF file, and raw counts for each gene were generated using the featureCounts tool from Subread, with 85-89% of reads overall assigned to genes. The raw counts data were normalized using voom method from the R Limma package (32), then used for differential expression analysis.

4.3.8 Infections

Female and Male (50:50 ratio) C57BL/6 8-10-week-old mice were utilized for infections. Mice (n=10) were immunosuppressed as previously described with Kenalog (40mg/kg delivered sub cutaneously) 1 day prior to infection. Mice (n=18) were anesthetized before instillation of a suspension of 2×10^6 conidia per 50 µl of saline intranasally of the *A. fumigatus* Af293 wild-type

or *dmaW* mutants derived from the different growth substrates. Mice were monitored every 12 hours post infection for 14 days. For fungal burden, mice (n=5) were euthanized and fungal burden was assessed by amplification of fungal 18s rDNA as previously described (8).

4.4 Results

4.4.1 Growth of spores on $_{L}$-Trp results in different metabolic profile and increased virulence in an invasive aspergillosis mouse model.

To explore how growth substrates, influence the outcome of the spore, we grew WT Af293 conidia on defined and complex substrate sources utilizing glucose minimal media (GMM) as the control growth substrate (Fig. 1 A-C). Differences were noted in radial growth on the various media (Fig. 1A, C). Some of the defined growth media included supplementation of the aromatic amino acids, tryptophan, phenylalanine, and tyrosine. These amino acids often feed into synthesis of toxins such as the virulent toxin, gliotoxin-incorporating a phenylalanine and serine into its biosynthesis (33-35). Tryptophan is also incorporated in toxins such as fumigaclavine and fumitremorgins; of which the former is a virulence factor in the insect model of aspergillosis (36). Tyrosine is incorporated in imizoquins which has been linked to influencing germination, a major factor for fungal pathogenesis (37). Since *Aspergillus fumigatus* is a prominent producer of a variety of biologically active natural products, we measured the secondary metabolite profile of the fungus derived from the complex and defined media (Fig. 1B). The metabolite profile of *A. fumigatus* derived from the various substrates was altered. We noted a significant increase in fumigaclavine synthesis when *A. fumigatus* was grown on tryptophan and tested whether this increase in fumigaclavine would impact virulence (Fig. 1B). We also measured the metabolites from the spore alone and observed a high increase in fumigaclavine production (Fig. 2A).

We tested the virulence of WT spores derived from these MM with and without L-Trp and saw a significant reduction in mice survival when the WT spores were derived from MM with L-Trp (Fig. 2B). We also measured higher fungal burden in the lungs of the mice infected with spores derived from L-Trp. (Fig. 2C).

4.4.2 Deletion of fumigaclavine biosynthesis does not account for increased virulence.

To test if the increased fumigaclavine was responsible for the increased virulence of spores grown on L-Trp, we deleted *dmaW*, the gene catalyzing the first step of fumigaclavine biosynthesis, the dimethylallyl tryptophan synthase (DMAT) (36, 38). We measured fumigaclavine in this mutant and show a significant reduction in this mutant. However, the *dmaW* mutant derived on L-Trp did not reduce virulence in comparison to WT spores derived on L-Trp (Fig. 2D). Upon further metabolite profiling of the *dmaW* mutants, we observed that growth of *dmaW* mutants grown on L-Trp alters other DMAT derived metabolites such as fumitremorgins indicating an interesting dynamic among these DMAT derived metabolites (data not shown).

4.4.3 Transcriptional profiling of spores derived from media with and without L-Trp.

To further explore why conidia derived on L-Trp was increasing virulence, we hypothesized that in fact the catabolites product of tryptophan could be impacting virulence. As previously shown by Wang et al., (39), *A. fumigatus* grown on excess L-Trp can be driven to enhance both secondary metabolism as well as kynurenine production; the latter of which could subsequently be responsible for the de novo synthesis of NAD (+). Following this previous observation of the increase in the Trp catabolite and fumigaclavine not accounting for the enhanced virulence, we took a transcriptomic approach by conducting an RNA Sequencing experiment of the spores derived in MM with or without L-Trp. The RNA Seq experiment revealed 422 significantly differentially expressed gene in the spores derived from the two substrates (Fig. 3A). Of these,

233 genes were upregulated, and 189 genes were downregulated in the L-Trp derived spores (Fig. 3A). Confirming the toxin production, members of the fumigaclavine gene cluster were significantly upregulated in the spores derived on L-Trp (Table S4). Among the highly upregulated genes were the mitochondrially encoded genes of the electron transport chain complexes (ETC) (Fig. 4A, Table S5). Among the nuclear encoded genes were the *ido* genes (*idoB* and *idoC*) and the transcription factors governing fatty acid β-oxidation (*farB1* and *farB2*) (Table S3).

4.4.4 Mitochondrial activity is enhanced in spores derived from L-Trp.

We show that the substrate source (in this case growth L-Trp) of *A. fumigatus* spores greatly enhanced the virulence of the fungus (Fig. 2B-D) and our RNA Seq results reveals that mitochondrial genes encoding the complexes (Complex I, II, and IV) involved in respiration are highly upregulated (Fig. 4A). Therefore, we hypothesized that growth on the L-Trp enhances mitochondrial activity making it more fit in the hypoxic lung micro-environment. Complex IV, a cytochrome c oxidase is the terminal oxidase of the core respiratory chain; the activity of which is inhibited by both Potassium cyanide (KCN) and hypoxia (16). Considering the hypoxic nature of the infected lung, we tested germination of spores derived from MM with and without L-Trp in the presence and absence of the complex IV inhibitor, KCN. Spores derived from L-Trp with or without KCN germinated at a slower rate than the spores derived from MM without L-Trp (Fig. 4B-D). However, the number of spores germinated between MM with and without L-Trp did not differ (Fig. 4B, D). Interestingly, we did not observe an increase in ATP production in WT spores grown on MM with L-Trp (Fig. S3). Complementing the RNA Seq results of the upregulation of Complex IV genes, the spores derived from L-Trp were more tolerant of the KCN stressor as germination rates were higher in the spores derived from MM with L-Trp than those derived from MM without L-Trp (Fig. 4C-D). Additionally, the spores derived from MM without L-Trp began

sporulating in the presence of KCN, whereas the spores derived from MM with L-Trp did not (Fig. 4C-D).

4.5 Discussion

The conidia of *A. fumigatus*, are ubiquitous, yet resilient. While normally existing as a saprobe in soil and on decaying organic matter such as compost piles and animal remains, *A. fumigatus* spores are able to successfully colonize a human lung (4). During infection, the conidia needs to quickly adapt to the lung environment; not only has to evade the attacks of immune cells and upregulate an effective nutrient uptake system, but also has to adjust to low oxygen levels in the host (18). In this study, we demonstrate that adaptation can be a primed trait based on the growth substrate the conidia are derived from. As shown by previous studies, oxidative phosphorylation processes of *A. fumigatus* are enhanced under hypoxic conditions and the ability of some strains to grow under hypoxia is a fitness trait that allows *A. fumigatus* to be more virulent (8, 17, 18). Complementing this virulent trait, we report that growing *A. fumigatus* conidia derived on L-Trp enhances mitochondrial functions, a trait favored under hypoxia.

We demonstrate that not only are the mitochondrial genes upregulated, but the functions of ETC, specifically Complex IV are more active. The inhibitor of Complex IV, KCN has been shown to induces a decrease in the oxygen consumption (18). While our germination of spore derived from media with L-Trp displayed a delayed germination, more of these spores germinated in the presence of CIV inhibitor KCN in comparison to the spores derived from media without L-Trp. We hypothesize that this delayed germination could be due to the upregulation of genes involved in trehalose biosynthesis as observed in the RNA Seq results. The mitochondrial ETC process is deeply involved in the production of reactive oxygen species, therefore *A. fumigatus* must find mechanism to protect against this self-oxidative stressor (16, 40, 41) . Overproduction of trehalose

has not only been implicated in protecting the fungus against oxidative stress, but also in germination. Increased trehalose content in *C. albicans* demonstrated a reduction of elongated cell phenotypes observed at 37 °C (42).

Our RNA Seq experiments revealed upregulation of genes not only in the mitochondrial ETC, but also displayed upregulation of genes in fatty acid b-oxidation. The fatty acid beta oxidation process breaks down the acyl-CoA to acetyl-CoA generating NADH and FADH2, the two molecules that initiate and drive the mitochondrial ETC (43). The process of ETC generates a proton gradient over the inner mitochondrial membrane, which is then used for ATP synthesis as the mitochondria is responsible for about 95 % of the ATP synthesis (16).

The respiration process in also implicated in other fungal pathogenesis, since petit mutants of *Candida glabrata* that fully lack mitochondrial function are severely attenuated in virulence (Brun *et al*., 2005) and the hypervirulent *Cryptococous* strains has been associated with increased mitochondrial activity. Here, we display that growth substrate ($_{L}$-Trp) can enhance mitochondrial respiration and conidia derived from $_{L}$-Trp causes more virulence in a triamcinolone murine model of invasive aspergillosis. Future investigation of the mechanisms behind the fungal mitochondrial functions can potentially lead to new therapeutic for invasive fungal infections.

4.6 Acknowledgements

We would like to thank support from Dalai Lama Trust MSN178745 awarded to TC.

4.7 Figures

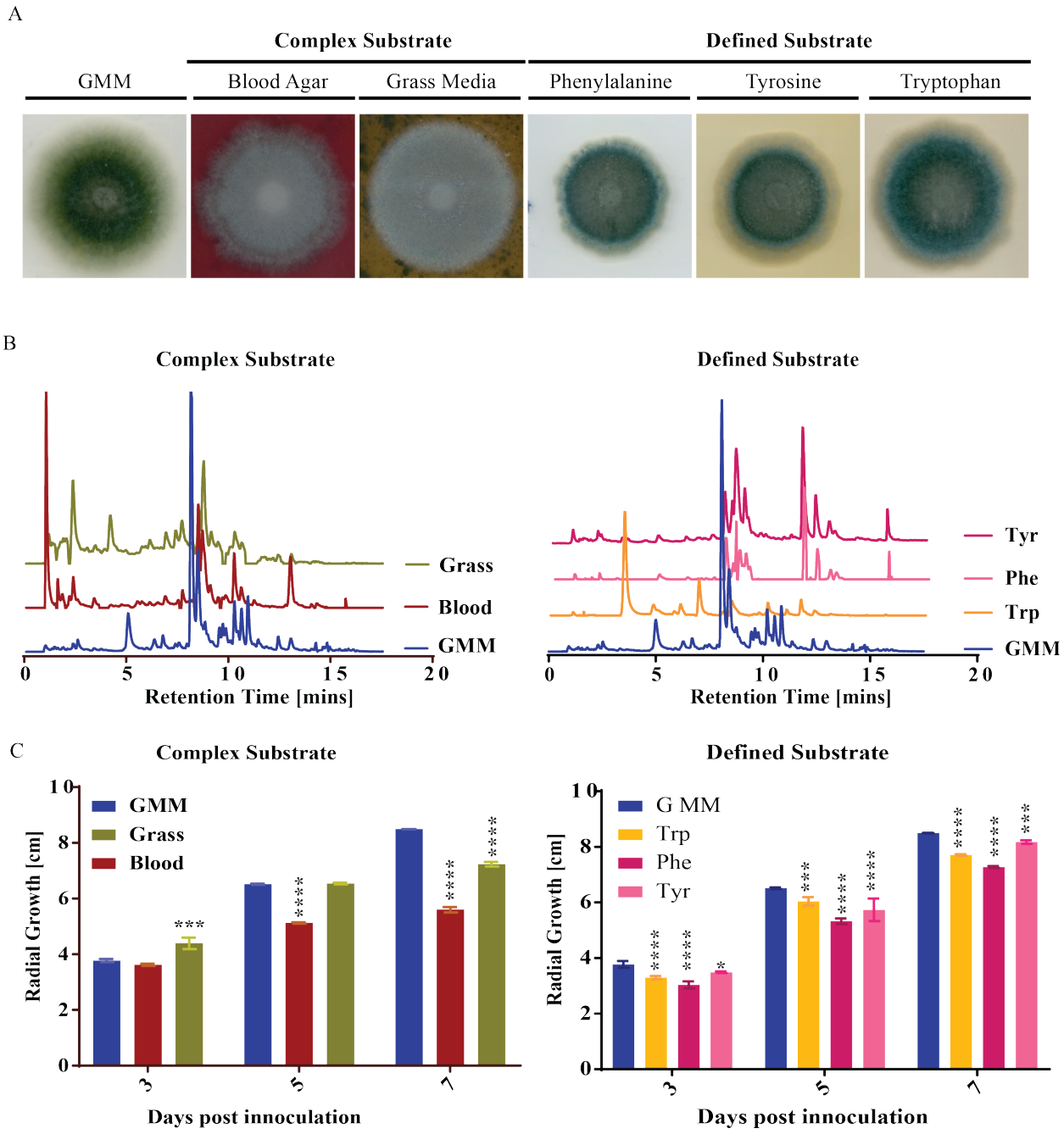

Figure 1. Heterogeneous growth substrates show phenotypic difference and yield differences in spore metabolic profile.

Radial growth (A) of *A. fumigatus* WT grown on indicated complex and defined substrates for 3 days at 37C and quantification (C) at 3, 5, 7 days post inoculation. Secondary metabolite HPLC traces (B) of *A. fumigatus* WT on indicated complex and defined media grown for 7day at 37C. HPLC: High performance liquid chromatography.

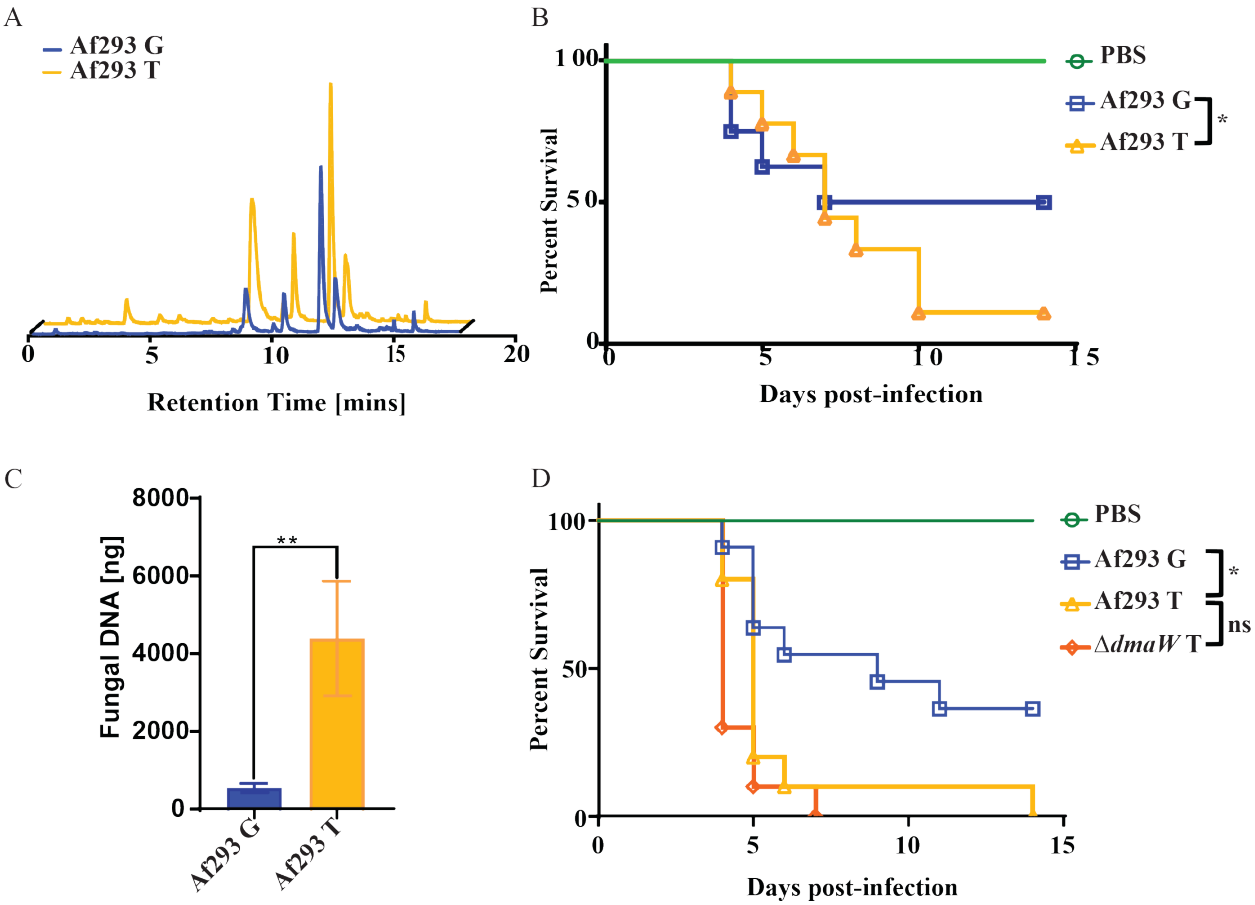

Figure 2. Spores derived from MM+ L-Trp are more virulent than those derived without L-Trp and deletion of fumigaclavine is not responsible.

Increased production of fumigaclavine in metabolite profile of the spore (A). Survival analysis (B) of triamcinolone-treated C57/Bl6 mice (P =0.0255 by log rank test; n= 10 per condition). Total fungal genomic DNA (C) normalized to input DNA in lungs of infected mice 3dpi. Data are represented as Mean ± SEM of triplicate measurements (N = 5 mice for each condition; ** p<0.01). Survival analysis (D) of triamcinolone-treated C57/Bl6 mice infected with WT vs. *dmaW* mutants growth on MM with Trp (n= 10 per condition).

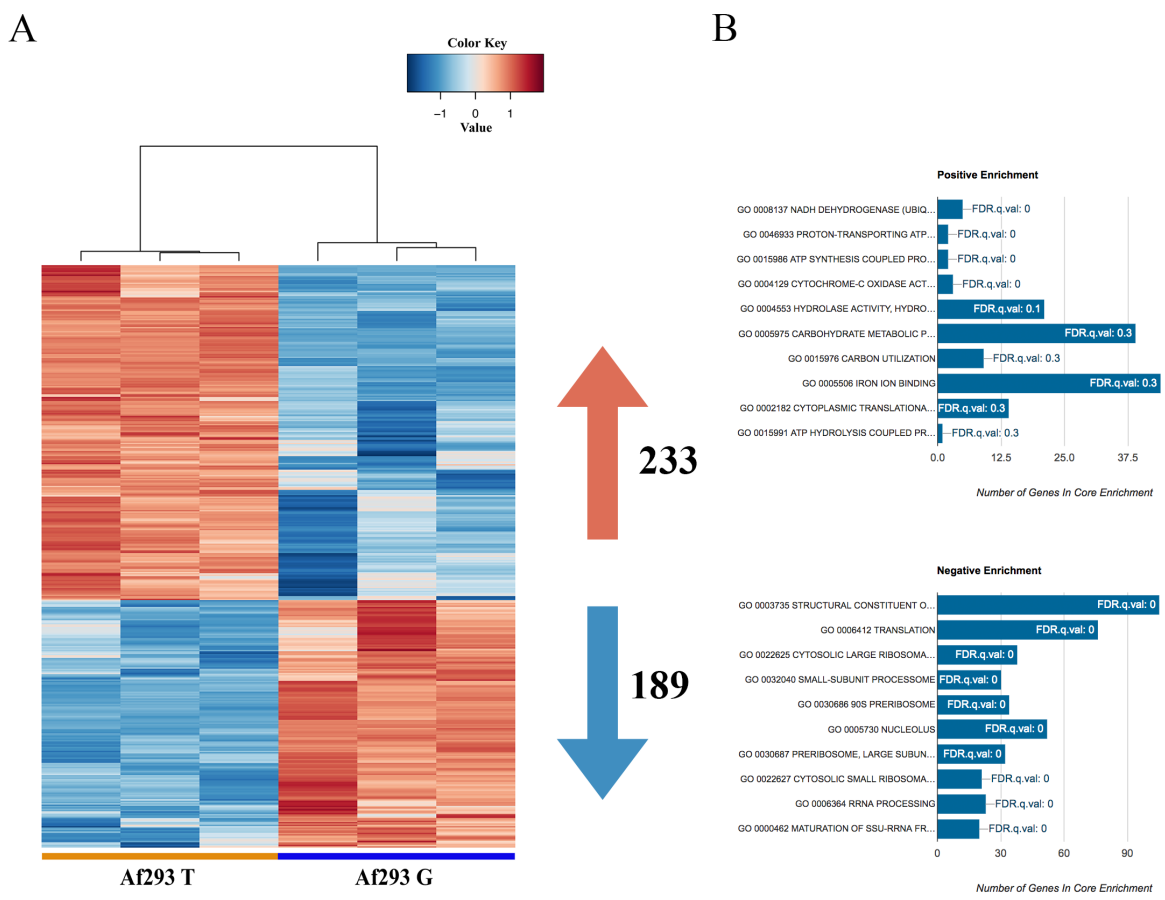

Figure 3. RNA SEQ profiling of the spores derived on MM (+/- L-Trp).

Heatmap of 422 differentially expressed genes (A) in spores derived on MM (+/- L-Trp). Go Category of upregulated and downregulated genes.

A

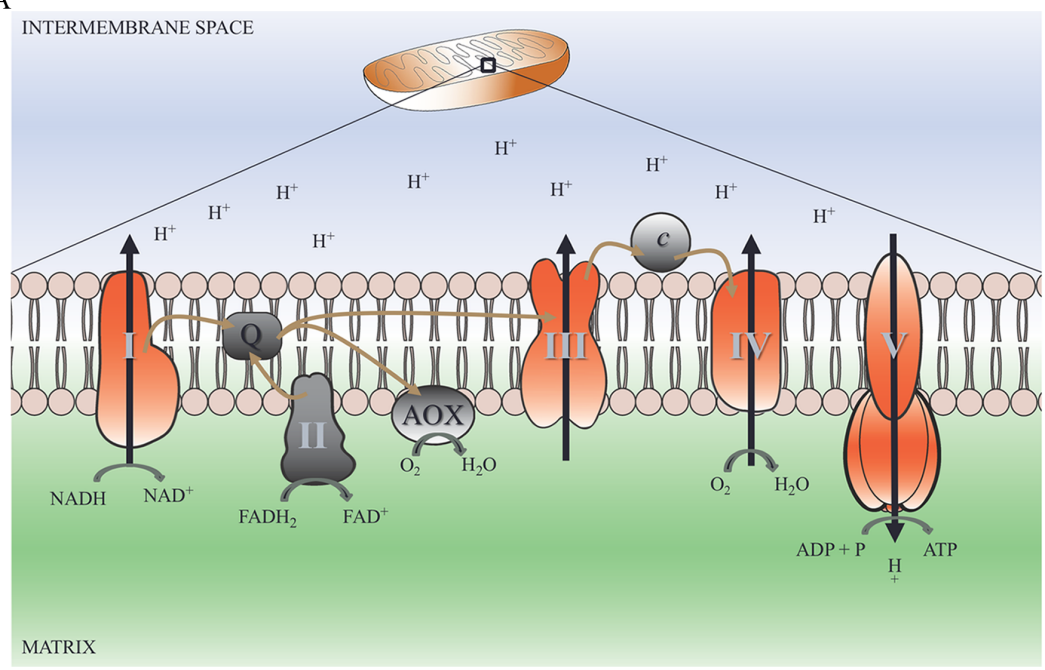
INTERMEMBRANE SPACE
H+
Q
c
I
II
III
IV
V
AOX
NADH
NAD+
FADH2
FAD+
O2
H2O
ADP + P
ATP
MATRIX

B

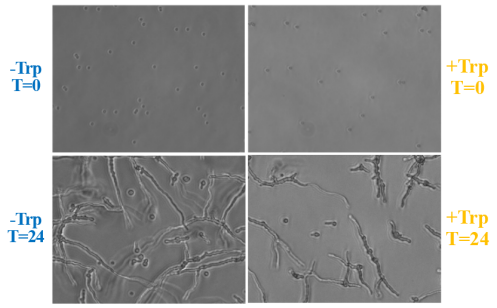
-Trp T=0
+Trp T=0
-Trp T=24
+Trp T=24

C

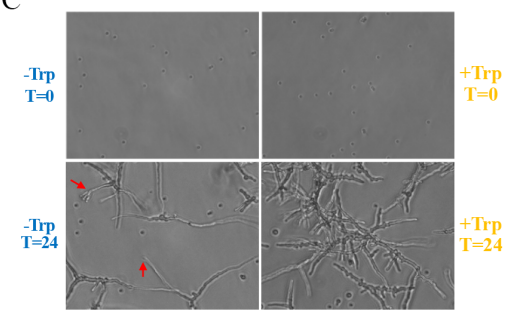
-Trp T=0
+Trp T=0
-Trp T=24
+Trp T=24

D

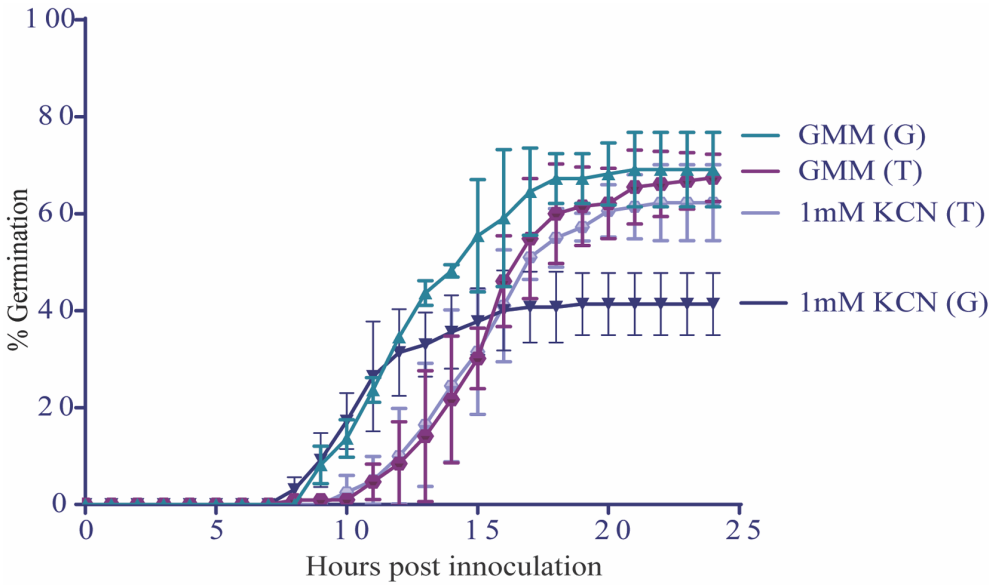
% Germination
Hours post innoculation
GMM (G)
GMM (T)
1mM KCN (T)
1mM KCN (G)

Figure 4. Mitochondrial genes are highly upregulated in spores derived from L-Trp and these spores are more tolerant of ETC inhibitors.

Cartoon depiction of *A. fumigatus* mitochondria (A) and ETC complex upregulated in RNA Seq dataset (red-upregulated; grey- not differentially expressed; brown arrows denote flow of electrons). Germination of spores derived from MM media with and without Trp in the absence (B) and presence of 1mM KCN (C). Red arrows depictf conidiophore development in the spores derived from media without Trp and in the presence of KCN. Quantification of germination of spores derived from MM media with and without Trp.

4.8 Supplemental Figures and Tables

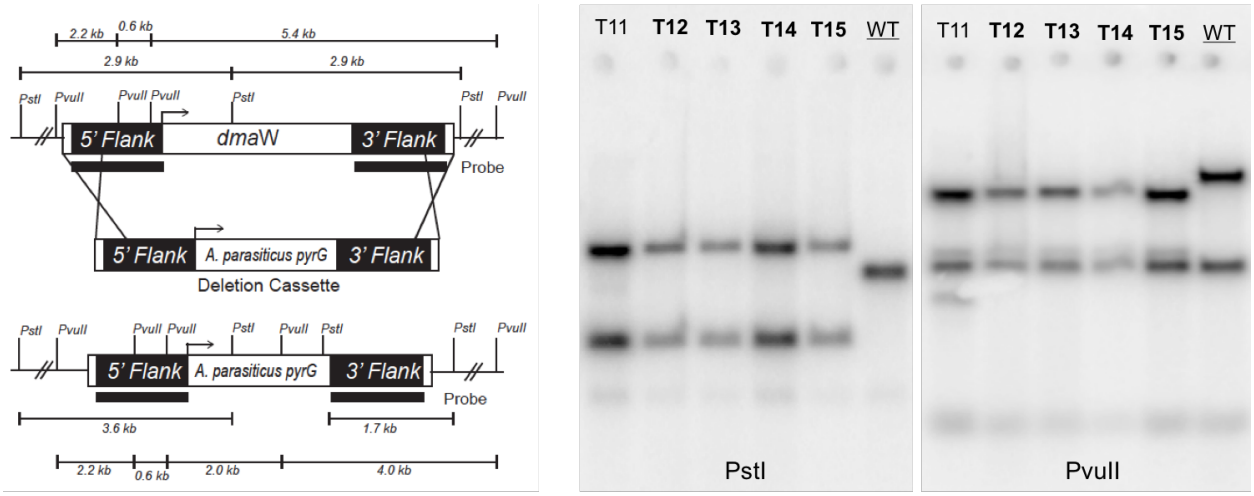

Figure S1. Southern confirmation of *dmaW* deletion.

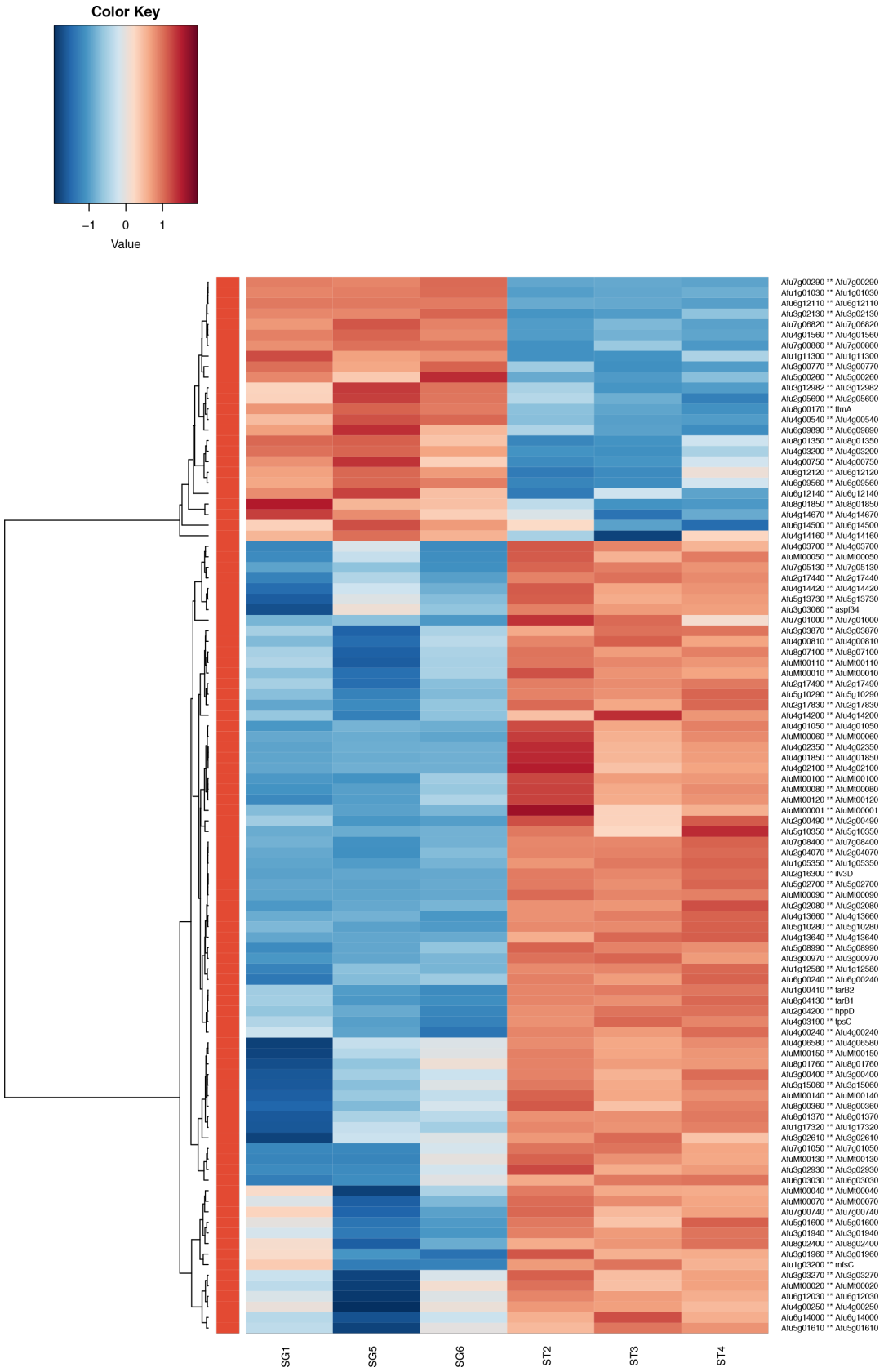

Figure S2. Detailed heatmap of top 100 differentially expressed genes.

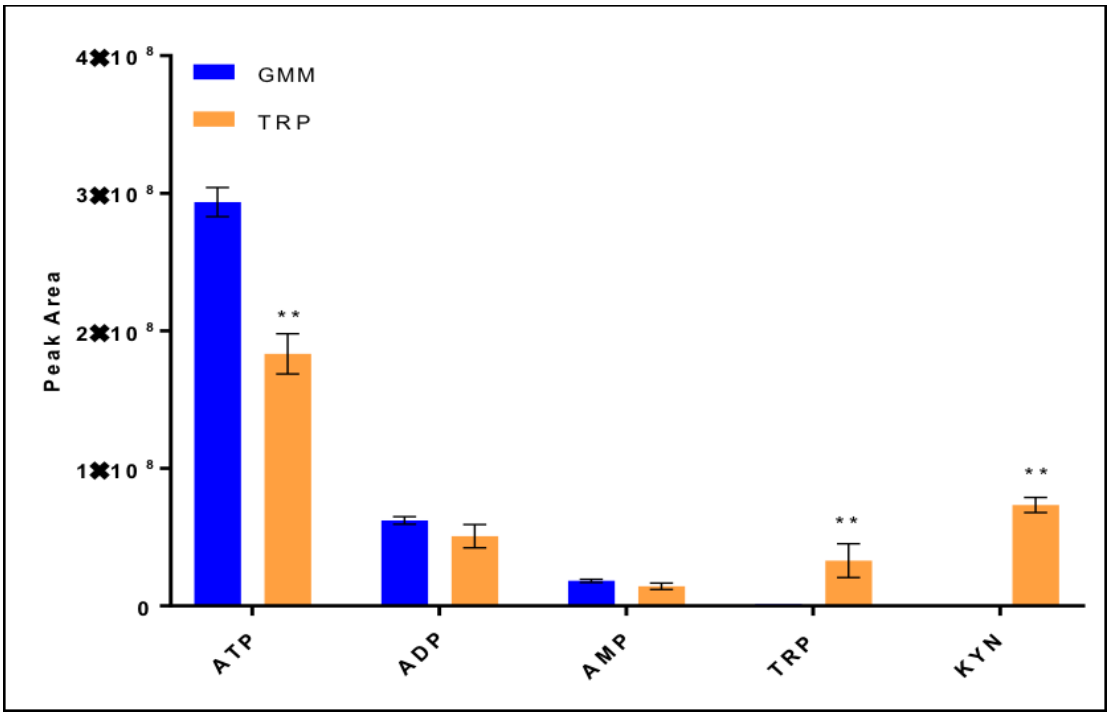

Figure S3. Metabolite measurement for spores grown on GMM vs. Trp.

Table S1. Primers used in this study

Number	Name	Sequence 5'- 3'
TC-1149	TC- DAfu2g18040 F1	TGAAGGGAAGGGTGGTAGATTCG
TC-1150	TC- DAfu2g18040 R1	TATCAAGCTATCGATACCTCGACTCGAGAG TCATCTTGGATAAGGGCATATGC
TC-1151	TC- DAfu2g18040 F2	TCGCTGCAGCCTCTCCGATTGTCGAATTGA ACAGCTCGGGACTTACTTCC
TC-1152	TC- DAfu2g18040 R2	TCGAGATCGGAGTTGTCTTTGG
TC-4	pyrG_prom_F	CGTAATACGACTCACTATAGGG
TC-5	pyrG_term_R	ATTCGACAATCGGAGAGGCTGC
TC-1153	TC-DAfu2g18040 F3	ATCCCTTTTGTCCAGAGCAACG
TC-1154	TC- DAfu2g18040 R3	TGACCCATATACCCACTCAAGG
TC-1155	TC-DAfu2g18040 F4	AGAAGATGTCTGGGTTCTGGTGG
TC-1156	TC-DAfu2g18040 R4	ACGGGCAGCACCTAATATACC

Table S2. Fungal strains used in this study

Name	ID	Parental strain	Genotype	Reference
AF293			Wild-type	(22)
AF293.1		AF293	pyrG1	(22)
Δ*dmaW*	TTC31.15	AF293.1	Δ*dmaW*::*A.parasiticus pyrG*	This study

Table S3. Differentially expressed genes of transcription factors governing fatty acid beta oxidation.

Putative Function	Gene Attributes		ST vs SG			Expression RPKM					
Note	Afu number	Gene	logFC5	P.Value5	adj.P.Val45	SG1	SG5	SG6	ST2	ST3	ST4
Fatty acid beta oxidation	Afu4g03960	*farA*	0.0682	0.3205	0.4558	45.476	43.377	43.161	46.205	46.272	45.172
Fatty acid beta oxidation	Afu8g04130	*farB1*	2.5486	0.0000	0.0002	26.310	16.255	14.594	102.098	97.648	124.840
Fatty acid beta oxidation	Afu1g00410	*farB2*	2.4088	0.0000	0.0002	3.416	2.244	1.945	12.404	13.261	13.836

Table S4. Differentially expressed genes of fumigaclavine biosynthesis

Putative Function	Gene Attributes		ST vs SG			Expression RPKM					
Note	Afu number	Gene	logFC5	P.Value5	adj.P.Val45	SG1	SG5	SG6	ST2	ST3	ST4
Fumigaclavine biosynthesis	Afu2g18040	*dmaW*	1.7994	0.0003	0.0034	13.333	28.207	26.649	93.574	83.461	49.674
Fumigaclavine biosynthesis	Afu2g18060	*fgaMT*	0.9166	0.0181	0.0546	3.830	7.323	7.448	14.637	10.892	7.364
Fumigaclavine biosynthesis	Afu2g18050	*fgaOx1*	0.9696	0.0106	0.0369	1.640	3.806	2.939	5.710	5.562	3.834
Fumigaclavine biosynthesis	Afu2g18030	*fgaCat*	0.5728	0.0986	0.1906	15.398	37.026	28.267	45.955	39.500	26.069
Fumigaclavine biosynthesis	Afu2g18000	*fgaDH*	0.4686	0.2370	0.3643	53.147	165.472	109.019	184.369	117.197	112.479
Fumigaclavine biosynthesis	Afu2g17960	*fgaOx3*	1.2431	0.0218	0.0626	1.720	5.389	4.516	10.326	9.468	4.448
Fumigaclavine biosynthesis	Afu2g17970	*fgaFS*	1.0104	0.0095	0.0345	6.758	14.621	12.576	26.076	23.328	14.209
Fumigaclavine biosynthesis	Afu2g18020	*fgaAT*	1.0468	0.0124	0.0412	1.549	3.464	2.552	5.740	5.615	3.132
Fumigaclavine biosynthesis	Afu2g17990	*fgaPT1*	0.4218	0.2276	0.3533	24.446	59.996	54.414	75.154	51.088	46.412
Fumigaclavine biosynthesis	Afu2g18010	*easM*	-0.2022	0.1323	0.2371	44.482	58.625	61.031	45.608	45.525	50.223
Fumigaclavine biosynthesis	Afu2g17980	*easK*	1.3249	0.0004	0.0039	1.497	2.020	2.070	4.824	4.786	3.964

Table S5. Differentially expressed genes of mitochondrially-encoded genes

Putative Function	Gene Attributes		ST vs SG			Expression RPKM					
Note	Afu number	Gene	logFC5	P.Value5	adj.P.Val45	SG1	SG5	SG6	ST2	ST3	ST4
ETC CI: NDH1	AfuMt00010	AfuMt00010	5.5430	0.0014	0.0091	0.0318	0.0000	0.0517	2.2283	0.8967	0.7137
ETC CI: NDH2	AfuMt00150	AfuMt00150	4.8765	0.0016	0.0100	0.0000	0.1005	0.2059	1.7884	1.0399	1.3463
ETC CI: NDH3	AfuMt00110	AfuMt00110	5.1777	0.0004	0.0041	0.2073	0.0000	0.1795	4.1026	3.3714	2.7867
ETC CI: NDH4	AfuMt00020	AfuMt00020	4.4778	0.0090	0.0330	0.1383	0.0000	0.4118	2.7411	0.8367	1.3857
ETC CI: NDH4	AfuMt00130	AfuMt00130	4.0733	0.0056	0.0236	0.0000	0.0000	0.2034	1.4252	0.8621	0.6380
ETC CI: NDH5	AfuMt00140	AfuMt00140	4.7318	0.0008	0.0062	0.0256	0.2055	0.3508	5.2393	2.2517	3.0927
ETC CI: NDH6	AfuMt00050	AfuMt00050	4.5804	0.0035	0.0169	0.0000	0.0522	0.0000	0.8571	0.2926	0.5822
ETC CIII: Cytochrome B	AfuMt00001	AfuMt00001	2.9068	0.0090	0.0330	0.5404	0.4105	0.5059	8.7726	1.8092	2.4992
ETC CIV: Cox1	AfuMt00080	AfuMt00080	4.2998	0.0003	0.0035	0.8024	0.9483	1.7591	38.2023	13.1673	18.2513
ETC CIV: Cox2	AfuMt00120	AfuMt00120	4.2256	0.0011	0.0077	0.4217	0.5793	1.4174	24.0624	7.9148	10.5351
ETC CIV: Cox3	AfuMt00060	AfuMt00060	3.5834	0.0005	0.0045	0.7934	0.8384	0.7684	16.2945	5.9828	8.5497
ETC CV: ATP6	AfuMt00040	AfuMt00040	4.9120	0.0045	0.0199	1.2236	0.0000	0.2602	7.0596	3.5270	3.2940
ETC CV: ATP9	AfuMt00100	AfuMt00100	4.0310	0.0001	0.0017	1.2644	1.1993	2.7622	42.3461	18.9991	19.7555
Endonuclease	AfuMt00090	AfuMt00090	5.3380	0.0006	0.0052	0.0000	0.0000	0.0000	0.4612	0.3382	0.3540
Ribosomal protein S5	AfuMt00070	AfuMt00070	5.9201	0.0010	0.0073	0.2469	0.0000	0.0445	3.9790	2.4543	1.6207

4.9 References

1. Tuite NL, Lacey K. Overview of invasive fungal infections. Methods Mol Biol. 2013;968:1-23.
2. Carmona EM, Limper AH. Overview of Treatment Approaches for Fungal Infections. Clin Chest Med. 2017;38(3):393-402.
3. Boral H, Metin B, Dogen A, Seyedmousavi S, Ilkit M. Overview of selected virulence attributes in Aspergillus fumigatus, Candida albicans, Cryptococcus neoformans, Trichophyton rubrum, and Exophiala dermatitidis. Fungal genetics and biology : FG & B. 2018;111:92-107.
4. Dagenais TR, Keller NP. Pathogenesis of *Aspergillus fumigatus* in invasive aspergillosis. Clin Microbiol Rev. 2009;22(3):447-65.
5. Gregg KS, Kauffman CA. Invasive Aspergillosis: Epidemiology, Clinical Aspects, and Treatment. Seminars in respiratory and critical care medicine. 2015;36(5):662-72.
6. Alanio A, Desnos-Ollivier M, Dromer F. Dynamics of *Cryptococcus neoformans*-macrophage interactions reveal that fungal background influences outcome during cryptococcal meningoencephalitis in humans. MBio. 2011;2(4).
7. Keller NP. Heterogeneity Confounds Establishment of "a" Model Microbial Strain. mBio. 2017;8(1).
8. Kowalski CH, Beattie SR, Fuller KK, McGurk EA, Tang Y-WW, Hohl TM, et al. Heterogeneity among Isolates Reveals that Fitness in Low Oxygen Correlates with Aspergillus fumigatus Virulence. mBio. 2016;7(5).
9. Knox BP, Blachowicz A, Palmer JM, Romsdahl J, Huttenlocher A, Wang CCC, et al. Characterization of Aspergillus fumigatus Isolates from Air and Surfaces of the International Space Station. mSphere. 2016;1(5).
10. Hirakawa MP, Martinez DA, Sakthikumar S, Anderson MZ, Berlin A, Gujja S, et al. Genetic and phenotypic intra-species variation in Candida albicans. Genome Res. 2015;25(3):413-25.
11. Caffrey-Carr AK, Kowalski CH, Beattie SR, Blaseg NA, Upshaw CR, Thammahong A, et al. IL-1α is Critical for Resistance Against Highly Virulent Aspergillus fumigatus Isolates. Infection and immunity. 2017.
12. Rizzetto L, Giovannini G, Bromley M, Bowyer P, Romani L, Cavalieri D. Strain dependent variation of immune responses to A. fumigatus: definition of pathogenic species. PloS one. 2013;8(2).
13. Throckmorton K, Lim FY, Kontoyiannis DP, Zheng W, Keller NP. Redundant synthesis of a conidial polyketide by two distinct secondary metabolite clusters in Aspergillus fumigatus. Environmental microbiology. 2016;18(1):246-59.
14. Kato N, Suzuki H, Okumura H, Takahashi S, Osada H. A Point Mutation in ftmD Blocks the Fumitremorgin Biosynthetic Pathway in Aspergillus fumigatus Strain Af293. Bioscience, Biotechnology and Biochemistry. 2014;77(5):1061-7.
15. Fuller KK, Cramer RA, Zegans ME, Dunlap JC, Loros JJ. Aspergillus fumigatus Photobiology Illuminates the Marked Heterogeneity between Isolates. mBio. 2016;7(5).

16. Grahl N, Dinamarco TM, Willger SD, Goldman GH, Cramer RA. Aspergillus fumigatus mitochondrial electron transport chain mediates oxidative stress homeostasis, hypoxia responses and fungal pathogenesis. Molecular microbiology. 2012;84(2):383-99.
17. Grahl N, Puttikamonkul S, Macdonald JM, Gamcsik MP, Ngo LY, Hohl TM, et al. In vivo hypoxia and a fungal alcohol dehydrogenase influence the pathogenesis of invasive pulmonary aspergillosis. PLoS Pathog. 2011;7(7):e1002145.
18. Grahl N, Shepardson KM, Chung D, Cramer RA. Hypoxia and fungal pathogenesis: to air or not to air? Eukaryot Cell. 2012;11(5):560-70.
19. Barker BM, Kroll K, Vodisch M, Mazurie A, Kniemeyer O, Cramer RA. Transcriptomic and proteomic analyses of the Aspergillus fumigatus hypoxia response using an oxygen-controlled fermenter. BMC Genomics. 2012;13:62.
20. Ortiz-Urquiza A, Fan Y, Garrett T, Keyhani NO. Growth substrates and caleosin-mediated functions affect conidial virulence in the insect pathogenic fungus Beauveria bassiana. Microbiology. 2016;162(11):1913-21.
21. Council NR. Guide for the care and use of laboratory animals. . National Academies Press, Washington, DC1996.
22. Osherov N, Kontoyiannis DP, Romans A, May GS. Resistance to itraconazole in *Aspergillus nidulans* and *Aspergillus fumigatus* is conferred by extra copies of the *A. nidulans* P-450 14α-demethylase gene, *pdmA*. Journal of Antimicrobial Chemotherapy. 2001;48(1):75-81.
23. Shimizu K, Keller NP. Genetic involvement of a cAMP-dependent protein kinase in a G protein signaling pathway regulating morphological and chemical transitions in *Aspergillus nidulans*. Genetics. 2001;157(2):591-600.
24. Sambrook J, Russell D. Molecular cloning: a laboratory manual. Cold Spring Harbor, New York: Cold Spring Harbor Laboratory Press; 2001.
25. Szewczyk E, Nayak T, Oakley CE, Edgerton H, Xiong Y, Taheri-Talesh N, et al. Fusion PCR and gene targeting in *Aspergillus nidulans*. Nature protocols. 2006;1(6):3111-20.
26. Lim FY, Sanchez JF, Wang CC, Keller NP. Toward awakening cryptic secondary metabolite gene clusters in filamentous fungi. Methods in enzymology. 2012;517:303-24.
27. Calvo AM, Bok J, Brooks W, Keller NP. veA is required for toxin and sclerotial production in *Aspergillus parasiticus*. Applied and Environmental Microbiology. 2004;70(8):4733-9.
28. Fischer GJ, Bacon W, Yang J, Palmer JM, Dagenais T, Hammock BD, et al. Lipoxygenase Activity Accelerates Programmed Spore Germination inAspergillus fumigatus. Frontiers in microbiology. 2017;8:831.
29. Wiemann P, Lechner BE, Baccile JA, Velk TA, Yin WB, Bok JW, et al. Perturbations in small molecule synthesis uncovers an iron-responsive secondary metabolite network in *Aspergillus fumigatus*. Front Microbiol [Internet]. 2014 4208449]; 5:[530 p.].
30. Lim FY, Ames B, Walsh CT, Keller NP. Co-ordination between BrlA regulation and secretion of the oxidoreductase FmqD directs selective accumulation of fumiquinazoline C to conidial tissues in Aspergillus fumigatus. Cellular microbiology. 2014;16(8):1267-83.

31. Liao Y, Smyth GK, Shi W. The Subread aligner: fast, accurate and scalable read mapping by seed-and-vote. Nucleic acids research. 2013;41(10):e108.
32. Ritchie ME, Phipson B, Wu D, Hu Y, Law CW, Shi W, et al. limma powers differential expression analyses for RNA-sequencing and microarray studies. Nucleic acids research. 2015;43(7):e47.
33. Choera T, Zelante T, Romani L, Keller NP. A Multifaceted Role of Tryptophan Metabolism and Indoleamine 2,3-Dioxygenase Activity in Aspergillus fumigatus-Host Interactions. Front Immunol. 2017;8:1996.
34. Igarashi Y, Yabuta Y, Sekine A, Fujii K, Harada K, Oikawa T, et al. Directed biosynthesis of fluorinated pseurotin A, synerazol and gliotoxin. J Antibiot (Tokyo). 2004;57(11):748-54.
35. Macdonald JC, Slater GP. Biosynthesis of gliotoxin and mycelianamide. Can J Biochem. 1975;53(4):475-8.
36. Panaccione DG, Arnold SL. Ergot alkaloids contribute to virulence in an insect model of invasive aspergillosis. Sci Rep. 2017;7(1):8930.
37. Khalid S, Baccile JA, Spraker JE, Tannous J, Imran M, Schroeder FC, et al. NRPS-Derived Isoquinolines and Lipopetides Mediate Antagonism between Plant Pathogenic Fungi and Bacteria. ACS chemical biology. 2018;13(1):171-9.
38. Robinson SL, Panaccione DG. Chemotypic and genotypic diversity in the ergot alkaloid pathway of Aspergillus fumigatus. Mycologia. 2012;104(4):804-12.
39. Wang PM, Choera T, Wiemann P, Pisithkul T, Amador-Noguez D, Keller NP. TrpE feedback mutants reveal roadblocks and conduits toward increasing secondary metabolism in Aspergillus fumigatus. Fungal genetics and biology : FG & B. 2016;89:102-13.
40. Al-Bader N, Vanier G, Liu H, Gravelat FN, Urb M, Hoareau CM, et al. Role of trehalose biosynthesis in Aspergillus fumigatus development, stress response, and virulence. Infect Immun. 2010;78(7):3007-18.
41. Fillinger S, Chaveroche MK, van Dijck P, de Vries R, Ruijter G, Thevelein J, et al. Trehalose is required for the acquisition of tolerance to a variety of stresses in the filamentous fungus Aspergillus nidulans. Microbiology. 2001;147(Pt 7):1851-62.
42. Serneels J, Tournu H, Van Dijck P. Tight control of trehalose content is required for efficient heat-induced cell elongation in Candida albicans. J Biol Chem. 2012;287(44):36873-82.
43. Ohashi K, Kawai S, Murata K. Secretion of quinolinic acid, an intermediate in the kynurenine pathway, for utilization in NAD+ biosynthesis in the yeast *Saccharomyces cerevisiae*. Eukaryot Cell. 2013;12(5):648-53.

CONCLUDING REMARKS AND FUTURE DIRECTIONS

This thesis set out to investigate the role of one of the essential amino acids (tryptophan) in the opportunistic pathogen, *A. fumigatus* addressing both metabolism and virulence. I have provided strong evidence that metabolites of the tryptophan pathway can influence fungal physiology, metabolism, as well as the outcome of disease in the context of invasive aspergillosis.

In Chapter 2 I described how altering the tryptophan biosynthetic pathway changes the flux of this essential amino acid that can be redirected into secondary metabolism as Trp is often a precursor feeding into NRPS derived metabolites. Some interesting observations from the work in Chapter 2 opens room for future explorations. The deletion of the TrpE as shown in Chapter 2 is a Trp auxotroph in-vitro; in parallel, the work from Sasse et al.(2016) demonstrates that this auxotrophy remains in vivo with this fungal strain demonstrating an avirulent phenotype *in vivo* (1). These results provide many avenues for exploring therapeutics targeting enzymes involved in essential amino acid biosynthesis. The existing classes of antifungal target either the cell wall or ergosterol biosynthesis and with the rise in many antifungal resistance strains (2, 3), another approach for antifungal development is direly needed. Another avenue the work from this chapter leads to is in investigating the role of the isochorismate synthase (*icsA)*. IcsA had previously been encoded as a putative anthranilate synthase, which the experiments in Chapter 2 proved is not involved in the synthesis of anthranilate or tryptophan. However, the overexpression and the deletion of the *icsA* gene demonstrated the functionality of this protein, as the deletion and overexpression strains drew away from the chorismite pool and other metabolites of the shikimate pathway in the opposing direction. IcsA by sequence alignment is a homolog to isochorismate synthase of another pulmonary pathogen *Mycobacterium tuberculosis* (4). In *Mycobacterium tuberculosis*, isochorismate is the precursor to either salicylate or the siderophore Mycobactin T (5, 6). This is another desired pathway for either drug development or for understanding pathogenicity;

therefore, is worth investigating further in *A. fumigatus*. In the conclusion of Chapter 2, we observed that excess tryptophan is really driven into degradation so removing this arm in the TrpE mutant would be ideal in trying to increase the intracellular tryptophan to be driven into secondary metabolism.

In Chapter 3, I presented the crosstalk between *A. fumigatus* and the mammalian's shared tryptophan (Trp) catabolites, that not only influenced fungal development, but also influenced the balance between tolerance/inflammation and controlling infection in host-pathogen interactions. The deletion of fungal indoleamine 2, 3 dioxygenases (Ido) led to an immune exacerbation phenotype *in vivo.* The results of this study suggested that the inflammatory responses and uncontrolled infection was either due to the loss of the Ido metabolites or the increase of the Aro metabolites or both. The reduction of fungal burden and pathophysiology observed in the *A. fumigatus* Aro mutants' infections suggested that this arm is involved in inflammation and fungal control. To explore the mechanism further, future studies should be aimed at looking at the immune responses from purified Trp catabolites to tease which metabolite is leading to the heightened immune responses. Furthermore, to address the role of these metabolites in infection, a co-infection of metabolites primed prior to WT spores may reveal the importance of these metabolites in infection control. Another approach is to overexpress the *ido* genes in *A. fumigatus* and compare against the deletion *ido* mutants. Gaining this knowledge may reveal a new mechanism of host- fungi interactions and may open door into designing therapeutic for chronic or allergenic responses.

One aspect of the virulence study conducted in Chapter 3 is that the infection was performed on immunocompetent mice. Hence, a follow up virulence study with an immunosuppressed murine model would be desired to reflect what an immunocompromised host might encounter.

In Chapter 4, I presented yet another branch of tryptophan metabolism by using tryptophan as a growth substrate. As a proof of concept to display that different growth substrates display variable growth patterns and metabolic profile, I measured secondary metabolite and showed that both complex and defined substrates displayed differences in growth and metabolite production. This opened up the question about the infectivity of the spore depending on the substrate it is derived from. I followed through with one of the substrate (i.e growth on Trp) and showed that the same WT strain is more infectious, when the spore is derived from media containing Trp. The secondary metabolite profile suggested that the increased virulence may be due to fumigaclavine as previous studies demonstrated fumigaclavine to be a virulence factor in an insect model (7); however, the deletion of the fumigaclavine gene cluster concluded that this cluster did not impact the increase virulence observed with Trp derived spores. Instead, the transcriptomics data displayed heightened mitochondrial gene expression and utilizing KCN as an inhibitor of the final step of the electron transport chain deemed the Trp derived spores more resistant. In fact, the Trp derived spores in the presence of KCN grew in dense filament which could be a fitness trait desired in the context of invasive disease. There are many future directions resulting from this study. First, as the mitochondria is source of energy in the form of ATP (8), measuring ATP and respiration in the form of oxygen consumption would be ideal. As the working hypothesis is that spores derived from Trp are more fit to survive in the host, a competition assay comparing the spores derived from the two conditions utilizing the flare assay (9) would confirm this hypothesis. Briefly, this assay would take a WT spores that are fluorescently labeled opposing colors (either GFP spores derived from media with Trp and RFP spores derived from media without Trp or vice versa) and look for survival of spores in vivo utilizing flow cytometry (9). Lastly, in the transcriptomics data, there were putative transcription factors that are upregulated, so future experiments to

characterize these transcription factors by generating mutants of these transcription factors and conducting screening experiments testing mitochondrial activity either through inhibiting the various complexes of the electron transport chain or measuring respiration may reveal if there is a global regulator of mitochondrial activity. The results of Chapter 4 also highlight the prepackaged resources of the ubiquitous asexual spore, as the data presented display that the spore is metabolically active depending on the environment it is derived from. This is not a surprising finding as these small hydrophobic airborne propagules are the main dispersal form, existing in very contrasting ecosystems such as brewing compost heap, the depths of the ocean, the alveoli of human lung, or even on space stations (10) yet have the ability to form new fungal colonies through germination.

Overall, this thesis has explored many branches of tryptophan metabolism in the opportunist fungal pathogen *A. fumigatus*, while opening many new questions. One such question open question in the balance between pathogen/commensal. Our interactions with microbial commensal/pathogens will continue to exist, therefore it is critical that we understand what drives pathogenicity/commensalism and understanding Trp metabolism is a step toward understanding this balance/imbalance.

References

1. Sasse A, Hamer SN, Amich J, Binder J, Krappmann S. Mutant characterization and *in vivo* conditional repression identify aromatic amino acid biosynthesis to be essential for *Aspergillus fumigatus* virulence. Virulence. 2016;7(1):56-62.
2. Perlin DS, Shor E, Zhao Y. Update on Antifungal Drug Resistance. Current clinical microbiology reports. 2015;2(2):84-95.
3. Sanglard D. Emerging threats in antifungal-resistant fungal pathogens. Front Med (Lausanne). 2016;3:11.
4. Wang PM, Choera T, Wiemann P, Pisithkul T, Amador-Noguez D, Keller NP. TrpE feedback mutants reveal roadblocks and conduits toward increasing secondary metabolism in *Aspergillus fumigatus*. Fungal genetics and biology : FG & B. 2016;89:102-13.
5. Nagachar N, Ratledge C. Roles of trpE2, entC and entD in salicylic acid biosynthesis in Mycobacterium smegmatis. FEMS Microbiol Lett. 2010;308(2):159-65.
6. Zwahlen J, Kolappan S, Zhou R, Kisker C, Tonge PJ. Structure and mechanism of MbtI, the salicylate synthase from Mycobacterium tuberculosis. Biochemistry. 2007;46(4):954-64.
7. Panaccione DG, Arnold SL. Ergot alkaloids contribute to virulence in an insect model of invasive aspergillosis. Sci Rep. 2017;7(1):8930.
8. Grahl N, Dinamarco TM, Willger SD, Goldman GH, Cramer RA. *Aspergillus fumigatus* mitochondrial electron transport chain mediates oxidative stress homeostasis, hypoxia responses and fungal pathogenesis. Molecular microbiology. 2012;84(2):383-99.
9. Jhingran A, Kasahara S, Hohl TM. Flow Cytometry of Lung and Bronchoalveolar Lavage Fluid Cells from Mice Challenged with Fluorescent *Aspergillus* Reporter (FLARE) Conidia. Bio Protoc. 2016;6(18).
10. Keller NP. Heterogeneity Confounds Establishment of "a" Model Microbial Strain. mBio. 2017;8(1).

APPENDIX

List of publications not included in this thesis produced from work performed at the University of Wisconsin-Madison

1. **Revitalization of a forward genetic screen identifies three new regulators of fungal secondary metabolism in the genus Aspergillus.**

   Pfannenstiel BT, Zhao X, Wortman J, Wiemann P, Throckmorton K, Spraker JE, Soukup AA, Luo X, Lindner DL, Lim FY, Knox BP, Haas B, Fischer GJ, **Choera** T, Butchko RAE, Bok JW, Affeldt KJ, Keller NP, Palmer JM. **MBio.** 2017 Sep 5;8(5).

2. ***Aspergillus fumigatus*** **copper export machinery and reactive oxygen intermediate defense counter host copper-mediated oxidative antimicrobial offense.**

   Wiemann P, Perevitsky A, Lim FY, Shadkchan Y, Knox BP, Landero Figueora JA, **Choera** T, Niu M, Steinberger AJ, Wüthrich M, Idol RA, Klein BS, Dinauer MC, Huttenlocher A, Osherov N, Keller NP. **Cell Rep.** 2017 Jun 6;19(10):2174-2176.

3. **FleA expression in *Aspergillus fumigatus* is recognized by fucosylated structures on mucins and macrophages to prevent lung infection.**

   Kerr SC, Fischer GJ, Sinha M, McCabe O, Palmer JM, **Choera** T, Lim FY, Wimmerova M, Carrington SD, Yuan S, Lowell CA, Oscarson S, Keller NP, Fahy JV. **PLoS Pathog**. 2016 Apr 8;12(4):e1005555.